Simulation of ship manoeuvring performance in calm water and waves

Ship Science report n°138

School of Engineering Sciences,
Ship Science

L. Letki and D.A. Hudson

July 2005

University
of Southampton

Abstract

Traditional manoeuvring and seakeeping theories do not usually include any study of the interaction of the manoeuvring and seakeeping performances of a ship. A unified mathematical model, which brings together both aspects of ship manoeuvring in a seaway, has been proposed by Bailey, 1999 [9] and a time simulation has been developed on this basis.

This study summarises the principles of the unified mathematical model and the verification of software, in which preliminary results for a *Mariner* vessel are presented. Then it extends the use of the model for another ship, the *British Bombardier* tanker, in order to further the validation process. The influence of parameters of the model, such as the mesh or the viscous ramp used at low frequencies, is investigated. Then, the predictions of circle manoeuvres and zigzag manoeuvres are compared with full-scale trials results. The comparisons are detailed and it shows that, although non linear effects have to be considered, the software predicts good tendencies in the evolution of ship manoeuvring characteristics, when some parameters such as rudder angle change. The investigation finally includes a preliminary study of the effect of waves on the ship's manoeuvring characteristics, for following and head seas.

Contents

Introduction

The mathematical models developed to describe the manoeuvring and seakeeping of a rigid vessel have evolved from different standpoints. No mathematical model existed in which both aspects - manoeuvring and seakeeping - were considered. The manoeuvring characteristics were usually studied in calm water and the seakeeping characteristics studied for a ship with a constant straight course. But, from the viewpoint of operations and safety of a vessel, it is also necessary to investigate the manoeuvring of a ship in a seaway. Few theories have been developed on this subject and they never considered the interactions between all the motions, usually being restricted to yaw and sway motions.

A unified mathematical model has been proposed by Bailey, 1999 [9] to describe the motions of a ship manoeuvring in a seaway. Then, it has been implemented in a software called *Simulat*. Some preliminary results of a *Mariner* vessel performing circle and zigzag manoeuvres in calm water and in waves were obtained. But the validation process was not further investigated.

This report presents briefly the principles of the unified mathematical model and the principles of the time simulation and its implementation. Then, the software has been verified, using the predictions for the *Mariner* vessel. It has then been extended to another vessel, the *British Bombardier* tanker, in order to further the validation process, comparing the predictions with experimental data and investigating briefly the effects of waves on the ship manoeuvring performance.

1 A unified mathematical model describing the manoeuvring of a ship travelling in a seaway

Two different mathematical models have been developed independently to describe the motions of a ship. Manoeuvring theory is usually associated with calm water, whereas in a seakeeping analysis the vessel operates at a specific speed and heading in a regular or irregular seaway. A unified mathematical model describing the manoeuvring of a ship travelling in a seaway has been developed by Bailey, 1999 [9].

1.1 Principles

The principles of this unified theory are the following :

- The equations of motions are expressed in a body fixed axis system and use **impulse response functions** and convolutions to express the fluid actions.
- The impulse response functions are calculated with an **hybrid method** : hydrodynamic coefficients are generated by traditional seakeeping calculations and converted to the body axis system. A viscous ramp may be added in order to correct the values at low frequencies, where viscosity has a major role. This viscous ramp is based on experimental data.

The details concerning this unified mathematical model and its derivation are developed in Appendix A.

1.2 Relations between the unified mathematical theory and traditional theories

The traditional seakeeping and manoeuvring theories can be obtained with the unified theory if some assumptions are made.

The traditional seakeeping equations of motion are derived from the unified equations of motions if it is assumed that :

- the motion is steady-state sinusoidal
- the waves are sinusoidal and encountered at a constant frequency (same as motion frequency).

The traditional manoeuvring equations of motion are derived from the unified equations of motions if it is assumed that :

- the motion is slow in some way. Under these circumstances, the frequency dependent oscillatory derivatives approximate the slow motion derivatives of calm water manoeuvring.
- the water is calm, so that the wave excitation is set to zero.

These relations between the unified theory and the traditional theories will be used in order to **validate the model**. In fact, if the conditions above are satisfied, the unified theory must give the same results as traditional theory in the prediction of the motions of the ship.

1.3 Time simulation

A real time simulation has been developed by Bailey, 1999 [9] to predict the manoeuvring of a vessel in a seaway. The method is based on the unified mathematical model presented above.

Calculation features and assumptions

- Heading of the vessel relative to waves may change substantially with time (e.g. a circle manoeuvre).
- Influence of propeller, wave influences on rudder action and convolution of wave actions are omitted.
- Wave excitation is assumed to be instantaneous and is determined by **integrating pressure of the instantaneous wetted surface to the waterline**.
- The restoring and wave excitations are not necessary linear, but in the limiting case of small motions and waves, the predictions are linear. The linear assumptions adopted in the mathematical model are not violated.
- The instantaneous excitation is evaluated with the ship in the perturbed condition.
- Rudder actions are modelled using rudder slow motion derivatives of traditional manoeuvring theory.
- Spatial position is calculated by integrating component velocities over time.

Implementation (for details, see [10])

To implement a numerical time stepping scheme, the equations of motion are rearranged, such that the second order integro-differential equations of motions could be expressed in terms of a system of first order equations in the form (Runge Kutta scheme): $\dot{\mathbf{X}} = \mathbf{F}(\mathbf{X}, t)$, where $\mathbf{X} =^T [u, v, w, p, q, r, X^*, Y^*, Z^*, \theta, \phi, \psi]$ and $\mathbf{F}$ contains not only the different actions, but also some velocities in the spatial frame.

Simulation The simulation starts with the ship in the calm water equilibrium condition. Thereafter, at each time step and at each step of the Runge Kutta scheme, the necessary convolutions are performed together with calculation of the relevant wave excitations and restoring moment.

2 Description and verification of the software - *Mariner* vessel

The aim of this chapter is to describe the role of each program involved in the time simulation of a ship manoeuvring in waves. In order to understand these roles and **to verify the software**, the same vessel as in Bailey, 1999 [9] is adopted, **a *Mariner* type vessel**, and the objective is to obtain the same predictions as those in Bailey, 1999 [9] and to compare to predictions of traditional manoeuvring theory.

Contents

2.1 Architecture of the software

An overview of the structure of the software, with the different subprograms and their relations, is presented in figure a.

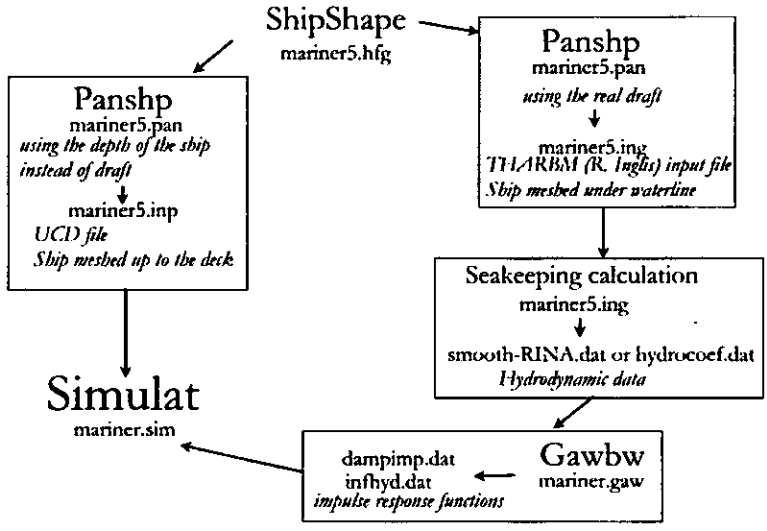

Figure a - Structure of the programs

2.2 *Mariner* vessel

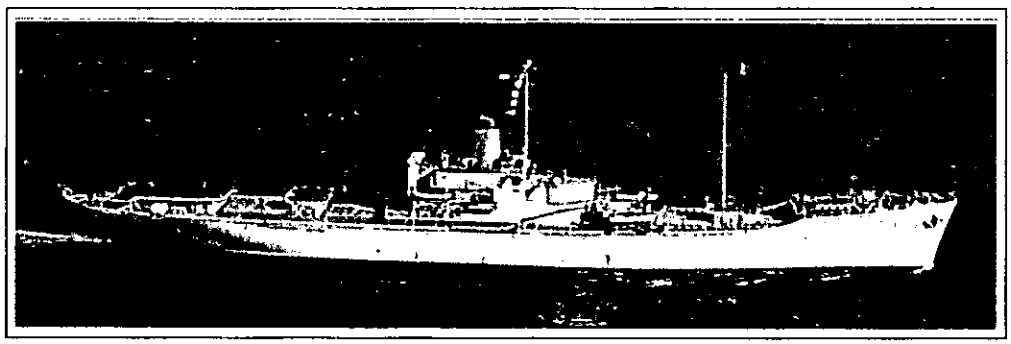

Figure b - *Mariner* type ship : USS Compass Island.

By way of example, the ship used in the simulation (and so in the different programs) is a *Mariner* type vessel, shown in figure b, having dimensions of :

Length L (m)	160.93
Draught (m)	7.47
Displacement (m^2)	16652.4
LCG fwd midships (m)	-3.73
VCG above keel (m)	7.742
I_{44} (kgm^2)	7.368e8
I_{55} (kgm^2)	1.916e10
I_{66} (kgm^2)	1.946e10
I_{46} (kgm^2)	0
Speed (m/s)	7.716
Fn	0.19

2.3 ShipShape

The ship's lines are defined initially using *ShipShape*, developed by the Wolfson Unit.

The initial frame of the *Mariner* ship is defined in a file containing the coordinates of curves describing the ship up to the deck line. The frame is defined with the origin at midship on the keel, with the following axis orientation : x forward, y port, and z up. (Figure 1)

2.4 Panshp program

From this point all the computational work is run with UNIX or LINUX. Bailey, 1999 [9] has implemented the different programs and routines in C programs.

Role The role of this program is to mesh the ship.

Principles of *panshp* program To mesh the ship, *Panshp* favours the aspect ratio of the panels. In fact, in hydrodynamic applications, this ratio has to be close to 1, in order to evaluate correctly the fluid actions. The global number of panels is not a parameter of *Panshp*. When the number of panels increases, the panels description is closer to the hull of the ship but the aspect ratio may not be respected and it may be a bad option.

Panshp makes the mesh section by section, from the extremity to the midships. Starting at the most forward section line, a panel height is calculated by dividing the perimeter of the section line by the specified number of panels around a section. The spatial distance to the next section line is calculated by multiplying this panel height by the aspect ratio. *Panshp* repeats this until midships, and the longitudinal difference between midship and last calculated section line is distributed back over the sections. The quadrilateral panels are formed using panel corners at adjacent section lines.

The same procedure is applied for the aft part of the hull. Calculation of bow and stern panels uses panel corners on the last section line and on the bow or stern line.

Output files *Panshp* program has to be used twice :

- Firstly, to create the mesh for *Simulat* input file, all the ship is meshed (up to the deck) and the origin is at midships on the keel.
- Then, to create the mesh for traditional seakeeping calculation, the ship is meshed under the water-line only and the origin is moved to the water-line.

The mesh used in the following programs is presented in the figure 2.

2.5 Gawbw program

Role The role of this program is to calculate the impulse response functions, with the hybrid method presented in the mathematical model. The viscous ramp added is linear : the values at zero frequency corresponds to the slow motion derivatives and the upper frequency (where the viscous ramp equals zero) is chosen in reference to experimental data.

Input data The program uses, as input file, the frequency dependent hydrodynamic coefficients calculated with a traditional seakeeping theory. Here the file generated and used by Bailey, 1999 [9] is used directly. The seakeeping calculation has not been repeated. These coefficients are translated to the body fixed axis system, and then the viscous ramp is added in reference to experimental data. The data used for the *Mariner* type ship are the data obtained by Van Leeuwen and Glansdorp, 1966 [7]. The slow motion derivatives used at the start of the viscous ramp ($\omega = 0$) are thus the following (non-dimensionalised) and the end of the viscous ramp is fixed at $\omega' = 34$, where all the hydrodynamic coefficients seem to become constant (arbitrary):

$$\left| \begin{array}{c|c} Y'_v & -1010e^{-5} \\ Y'_r & 290e^{-5} \\ N'_v & -349e^{-5} \\ N'_r & -200e^{-5} \end{array} \right|$$

Output files Figures 3, 4 show examples of the oscillatory derivatives obtained both experimentally and theoretically, with or without adding the viscous ramp, and then the corresponding impulse response functions.

For the data presented here, it is evident that better adjustment of the initial size of the viscous ramp could bring the theoretical data in closer agreement with the oscillatory experimental data, but the use of the slow motion derivatives to decide the initial value of the viscous ramp is a good first approximation. The upper limit of the viscous ramp could also be improved, but will depend on the coefficients. For example, the limit needs to be smaller for the coefficient N_r than for the coefficient Y_v. Here the same limit is used for all the coefficients.

2.6 Simulat program

Role *Simulat* is the program which finally predicts the motions of the vessel in a seaway.

Principles The simulation starts with the ship in the calm water equilibrium condition (which is calculated by the *Itequilpos* subroutine) and thereafter, at each time step and at each step of the Runge Kutta scheme, the necessary convolutions are performed together with calculation of the relevant wave excitations and restoring moment (*calcfs* subroutine), in order to solve the equations of motion.

The program uses the impulse response functions calculated by *Gawbw* program, the infinite frequency values of the hydrodynamic data, and obviously the mesh of the ship generated by *Panshp* program.

2.7 First results : Manoeuvring - Steady turn diameter

As an example of the use of *Simulat* program, this section deals with a steady turn motion (circle manoeuvre). These simulations were also performed by Bailey, 1999 [9]. They have two main purposes :

- To compare the results of the unified theory to those of a traditional linear manoeuvring theory. As explained previously, they must be similar in certain conditions.
- To make a preliminary investigation of the effect of waves and of the possibilities offered by *Simulat* in this domain.

The version of *Simulat* used here is the version 6.0.

2.7.1 Calm water predictions

Predictions of traditional linear theory It has been shown [2] that, in a linear theory of manoeuvring, the sway velocity of a ship during a steady turn is, using the slow motion derivatives :

$$v = \frac{-\delta[Y_\delta N_r + (m\overline{U} - Y_r)N_\delta]}{N_r Y_v + N_v(m\overline{U} - Y_r)N_v}$$

and the steady yaw rate is :

$$r = \frac{\delta[Y_\delta N_v - Y_v N_\delta]}{N_r Y_v + N_v(m\overline{U} - Y_r)N_v}$$

The radius of the steady circle can then be written as :

$$R = \frac{\overline{U}}{\cos(\tan^{-1}(v/\overline{U}))}\frac{1}{r}$$

The data concerning the *Mariner* ship and the slow motion derivatives (initialization of the viscous ramp) are those presented in the previous sections. The slow motion derivatives concerning the rudder actions are the following (standard non-dimensionalisation):

Y'_δ	232e-5
N'_δ	-110e-5

If we dimensionalise these data and use the previous expressions, we obtain a prediction of $R = 249m$ for a 5°(0.0873 rad) constant rudder angle (δ).

Simulation For the simulation of a steady turn, surge perturbations are excluded. In order to compare the results with the predictions of linear manoeuvring theory, predictions are made with and without inclusion of roll motion (because it is excluded in the traditional manoeuvring theory). The time step is 0.5 s and the number of time steps is 3000 (25 min).

The rudder application point is taken at the half draft level, and the x position is calculated, using the value of the rudder slow motion derivatives : $Y'_\delta = N'_\delta/(x/L)$ where x represents the position of the application point relative to the centre of gravity.

The magnitude of the rudder action is also calculated with the dimensionalised slow motion derivatives :

$$F = Y'_\delta \frac{1}{2}\rho L^2 \overline{U}^2 \delta$$

The predictions in calm water are presented in figure 5.

Observations

- First at all, it can be seen that the predictions with and without inclusion of roll motion are very similar.
- The steady turn radius, predicted by *Simulat*, is approximatively $R = 255m$, which corresponds to the predictions of traditional linear manoeuvring theory (249 m i.e. 2.5 % error). This confirms that the unified theory produces the same results as traditional linear manoeuvring theory for steady motions and calm water.
- The value of $R = 249m$, which suggests a diameter of only 3L for 5° rudder angle is not realistic. This is due to the use of a linear theory, although it is generally accepted that for such steady turn a non-linear mathematical model is required [9]. These simulations just confirm the comparison between the unified mathematical model and the linear manoeuvring theory.
- Although the predicted radius is not realistic, these simulations can be use for a preliminary investigation of the effect of waves on the ship motions.

2.7.2 Inclusion of waves

Roll motion excluded The parameters are the same as those used for the calm water simulation. The wave amplitude is 1.0m and many simulations are made with different wavelengths ($\lambda/L = 1, 0.5, 0.25, 0.1$). The roll motion is excluded because of the lack of any accurate value for the roll damping. The main step is 0.5 s and the number of time steps is 3000 (25 min). The results obtained for high frequencies could be better with the use of more panels, or if we split the panels, in order to have more precision in the predictions of the forces.

Figures 6, 7, 8, 9, 10 and 11 show the path of the ship in these different seaways and the pitch and heave motions during the turn in waves. We can make some qualitative observations:

- The vessel still performs a turn but it is no longer a strict circle.
- The action of waves on the ship causes an average drift in the direction of wave propagation.
- When the wavelength decreases, this drift is reduced and at high frequencies, we approach the results of calm water simulations.
- The pitch and heave motion change in oscillatory frequency with time.

Roll motion included Figures 12 and 13 present the results obtained when the roll motion is included.

Firstly, no viscous ramp is added to roll damping, and the vessel seems to reach a certain heading relative to waves (about 40 degrees here) and then oscillates about it, but the vessel does not perform a complete turn anymore. This may be caused by the lack of roll damping in the viscous ramp. No data about the roll damping is available. A nominal value at zero frequency is used to determine sensitivity to roll damping ($K'_p = -2.5e^{-6}$). When the viscous ramp is initialized with this value, the magnitude of the roll motion is reduced but the vessel still oscillates about one heading value, so this strange behaviour is not only due to the roll damping.

For the case in which no roll damping is added, we study the influence of wave amplitude on the predicted behaviour of the vessel. We can observe that when the wave amplitude is smaller the vessel performs a circle. The limit between the two sorts of track seems to be around 0.5 m amplitude.

Further investigations have to be performed on the roll damping but also in the yaw-roll coupling terms N_p and I_{xz}, in order to obtain accurate predictions. These predictions have highlighted the sensitivity of predictions to the inclusion of roll.

2.8 Standard manoeuvres

Some standard manoeuvres are defined in the *Standards for ship manoeuvrability* [5], published by the International Maritime Organization (IMO). "They should be used to evaluate the manoeuvring performance of ships and to assist those responsible for the design, construction, repair and operation of ships". That is why these manoeuvres are particularly interesting in this study.

- Firstly the manoeuvring trials performed on full-scale ships are based on these standard manoeuvres. For reasons of comparison, all the model tests are also based on these manoeuvres. Then, the experimental results could be used to compare with the predictions of *Simulat*, and to complete the validation. Note that these tests are normally performed in calm water conditions but the environmental conditions are well recorded and some results in waves may be available.
- Then, the predictions of *Simulat* for these standard manoeuvres could be used by the designer to anticipate the manoeuvring characteristics of the ship. This could be a major application for the software.

For all these reasons, *Simulat* will be tested and used for the manoeuvres defined by the IMO.

2.8.1 Turning tests

A **turning circle manoeuvre** is to be performed for both starboard and port with 35° rudder angle or the maximum design rudder permissible at the test speed. The following information is obtained (Figure 14):

- Tactical diameter
- Advance
- Transfer
- Turning radius

The predictions for a such circle manoeuvre have been useful to validate some aspects of the software as regards a traditional linear manoeuvring theory, but the *Simulat* predictions are dramatically small, for example concerning the steady turn radius, because in such a manoeuvre, a non linear theory has to be used.

Another turning manoeuvre is the **spiral manoeuvre**. It is an orderly sequence of turning circle tests to obtain a steady turning rate versus rudder angle relation.

2.8.2 Zigzag tests

A zigzag test should be initiated to both starboard and port and begins by applying a specified amount of rudder angle to an initially straight approach. The rudder angle is then alternatively shifted to either side after a specified heading from the ship's original heading is reached.

The 10°/10° zigzag test uses rudder angles of 10° and -10° and a heading deviation of 10° from the original course. The following information is obtained (Figure 15):

- Overshoot angles
- Initial turning time to second execute
- Time to check yaw

We have already seen that *Simulat* can predict the results of a circle manoeuvre. The zigzag manoeuvre has also to be predicted, in order that we can use the two main standard manoeuvres in the subsequent analysis.

2.8.3 First predictions of *Simulat* for a 10°/10° zigzag manoeuvre

For the predictions of such a zigzag manoeuvre, the seventh version of *Simulat* has to be used. In fact, in the sixth version, we can only apply a predefined rudder action. In the zigzag manoeuvre, **the rudder action depends on the motions**, since the rudder action is inverted when the heading reaches a certain value. The manoeuvre has thus to be defined, with the rudder action, in the source code.

For the predictions of the zigzag manoeuvre, it was assumed that the rudder action could be applied instantaneously, as a first approximation. Figures 16 and 17 show the path of the ship and the yaw angle, during the manoeuvre in calm water and in waves.

These predictions will be commented in a later chapter.

2.9 Conclusion

The same figures as those detailed in Bailey, 1999 [9] have been obtained.

Thus, it has been shown that all the sub programs involved in the time simulation have been successfully used. **The programs have been verified.** A **User Guide**, explaining all the software process, was written and is included in appendix C.

3 Investigations and extensions for another vessel : British Bombardier

The previous chapter described the first step in studying the simulation program ; it consisted in breaking down each subprogram and reproducing the results of Bailey, 1999 [9] .

The next step is to further the use and validation process. Indeed it has been used so far only for one type of vessel, a *Mariner*. In this chapter, we will **extend the study to the *British Bombardier* tanker.** The results obtained with this new vessel will prove useful in order to better understand the role of several parameters.

All the data about the *British Bombardier* have been provided by J.M.J. Journee, from Delft University of Technology, in a document called : *Experimental Manoeuvring Data of Tanker "British Bombardier"* by J.M.J. Journee and D. Clarke [6].

Contents

3.1 British Bombardier : characteristics and *ShipShape* lines

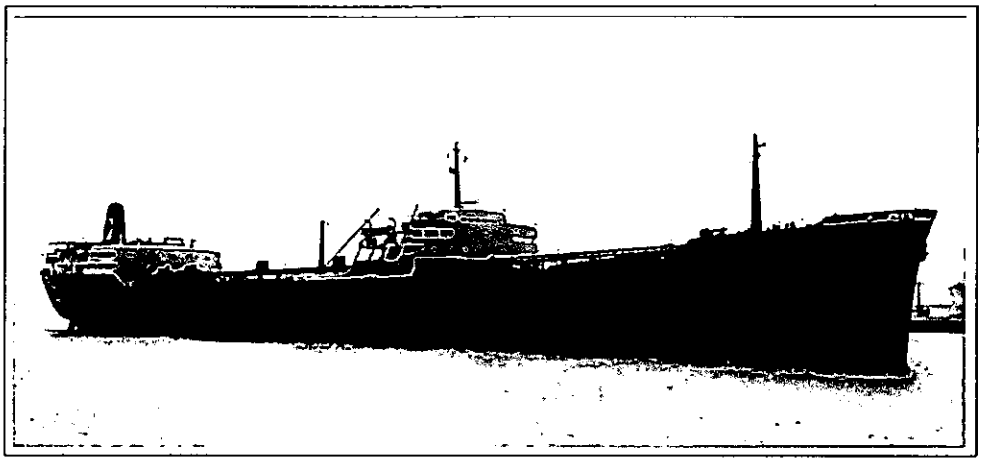

Figure c - British Bombardier's sister ship : British Cavalier.

Here are the main characteristics of the *British Bombardier* (also see figure c) :

Length L (m)	220.98
Beam B (m)	29.566
Draught (m)	12.497
Displacement (m^2)	65089
LCG fwd midships (m)	3.094
VCG above keel (m)	6.49
I_{44} (kgm^2)	8.42e9
I_{55} (kgm^2)	2.04e10
I_{66} (kgm^2)	2.04e10
I_{46} (kgm^2)	0
Speed (m/s)	7.974
Fn	0.17

The inertia moments are based on the radius of gyration $k_{zz} = 0.25L$ and $k_{xx} = 0.38B$ ($I = m * k^2$).

The main curves of the *British Bombardier*, drawn in *ShipShape* are presented in figure 18. See Appendix B for the description of the hull form and the accuracy of the *ShipShape* representation.

This *ShipShape* representation could be improved by using less water-lines and by checking the water-line derivatives at the stern, in order to avoid crossed water-lines.

3.2 Mesh - *Panshp* program

For the mesh used in the seakeeping calculation (only the underwater part is meshed) as well as for the mesh used in *Simulat* program (ship meshed up to deck), two main possibilities are available. The stern could be meshed or not. In the first case, the mesh will be very precise, with small panels at the stern (Figure 19); in the second case, there will be only large panels between the first aft section and the stern section (Figure 20).

Although the first solution leads to a more precise mesh, the second solution was adopted for different reasons :

- Firstly, the more precise mesh had one section on the crossed water-lines just near the stern and, for half of the ship we had some panels with a negative y-coordinate. The second solution avoids this problem, since no section can be defined in this part of the ship.

- Then, although the mesh was less precise, the results (hydrodynamic coefficients and final radius in circle manoeuvres) were not a lot affected; thus, it is preferable to use the mesh with less panels in order to save calculation time.

The number of panels around each section and the aspect ratio can be chosen in order to increase or decrease the number of panels. The sensitivity of the results to the mesh is described in a section below.

Finally, the mesh chosen for the seakeeping calculation has these characteristics (Figure 21):

Number of panels around each section	8
Aspect ratio	0.5
Number of panels for whole ship	2400

The mesh for the *Simulat* program (Figure 22 - up to the deck) has those characteristics :

Number of panels around each section	12
Aspect ratio	1
Number of panels for half ship	876

3.3 Seakeeping calculation - *THARBM* program

The role of this program is to generate the hydrodynamic coefficients for a range of excitation frequencies.

Note : This step has not been run for the Mariner predictions. The output file *hydrocoef*, which had been generated when the programs were written by Bailey, 1999 [9] , has been used directly.

Principles of the program[3] The programs were originally developed by R.B. Inglis and are based on three-dimensional linear potential flow. The fluid is assumed to be ideal (inviscid, homogeneous and the fluid motion irrotational), and the fluid motion may be represented by a velocity potential function, which satisfies the Laplace's equation in the fluid's domain and some boundary conditions.

The Green's theorem is used to reduce the problem to a distribution of velocity potential on the boundaries of the fluid. Then by choosing appropriate singularities, the problem is reduced to the hull surface as the only remaining fluid boundary.

A singularity of unknown strength is attributed to each panel (at its centre) and the condition that there is no flow trough the surface hull gives the strength of these singularities.

Since the velocity potential is now known, the forces, the motions... can be obtained and thus the hydrodynamic coefficients.

The range of values used in order to obtained the *hydrocoef* file, used by the *gawbw* program to calculate the impulse response functions, is finally the following : the first frequency is 0.0008 (s^{-1}), the upper frequency is 2.4 (s^{-1}) and there are 40 frequencies. If the non dimensionalisation is used, we obtained the same range of frequencies as those used for the *Mariner*. The sensitivity to the frequencies is developed in a section below.

Note : THARBM program can be used to determine the values of the restoring moments and the inertia moments, if it is used without any frequency. But the values obtained are not totally accurate.

3.4 Calculation of the impulse response functions and steady turn predictions

The frequency dependent hydrodynamic coefficients calculated by *THARBM* program are used by *Gawbw* program to calculate the impulse response functions. The slow motions derivatives used in the viscous ramp are detailed below. Then, predictions for a steady turn motion have been carried out. (The seventh version of *Simulat* program was used.) In these predictions, surge perturbations have been excluded, as well as roll motion - except in the last section - in order to allow comparisons with traditional linear manoeuvring theory. The time step is 1 s for the 5° rudder angle predictions, and 0.5 s for the 15° rudder angle predictions, and the number of time steps is 3000. By analysing these predictions, the sensitivity of some parameters has been studied, such as the sensitivity to the range of frequencies used in the calculation of hydrodynamic coefficients, the sensitivity to the viscous ramp and the sensitivity to the mesh.

3.4.1 Slow motion derivatives and viscous ramp

The viscous ramp is defined in the same manner as described in the *Mariner* chapter. The report from J.M.J. Journee [6] provides two sets of data for the slow motions derivatives, which have been obtained respectively with PMM tests (see definition in Appendix E) on a 1:55 model and on a 1:100 model. These data are presented here :

	1:100 Model	**1:55 Model**
Y'_v	-1634e-5	-1797e-5
Y'_r	342,6e-5	432,2e-5
N'_v	-472,7e-5	-473,3e-5
N'_r	-199,8e-5	-251,7e-5
Y'_δ	279e-5	313e-5
N'_δ	-125,3e-5	-155,1e-5

Directional stability These slow motion derivatives enable an analysis of the directional stability of the ship, in both cases. In respect of a linear theory, the stability condition is the following [8]:

$$Y'_v N'_r - N'_v(Y'_r - \Delta') > 0$$

where $\Delta' = \frac{\Delta}{\rho/2L^3}$. The data obtained with the 1:100 model leads to an **unstable ship**, although the data obtained with the 1:55 model leads to a **stable ship**.

Note : As a verification, the data used for the *Mariner* leads to a stable ship.

It seems that the simulation program can not predict the motions of an unstable ship : in fact, the predictions of the 5° rudder angle manoeuvre with the slow motion derivatives of the 1:100 Model never leads to a steady turn motion.

Moreover, it is likely that the full scale British Bombardier is a stable ship. In the experimental determination of the slow motions derivatives, there are a lot of **scale effects**, and the results obtained with the larger model seem to be more accurate.

That is why the slow motion derivatives used for the initialisation of the viscous ramp and the calculation of the rudder force are those of the 1:55 Model.

Radius predicted by the traditional linear theory With these values of slow motion derivatives, the radius predicted by the traditional linear manoeuvring theory are : 520 m for 5° rudder angle and 199 m for 15° rudder angle.

A range of predictions has been carried out in order to study the influence of a list of parameters.

3.4.2 Sensitivity to the range of frequency values used in the *THARBM* program

The first parameter to be studied is the range of frequencies for which the seakeeping calculation program generates the hydrodynamic coefficients. The upper frequency and the number of frequencies have not a lot of influence in the predictions but **the lowest frequency seems to be very important.**

Two ranges of values have been tested : 0.0008 to 2.4 (s-1) with 40 values and 0.001 to 2.7 (s^{-1}) with 40 values. For each range of frequencies, the first value has been deleted or not. Then, the *Gawbw* and *Simulat* programs (5° rudder angle, constant) have run. The results are :

Frequencies	Radius (m)
0,0008 to 2,4	518
0,001 to 2,7	519,5
0,0008 to 2,4; **0,0008 deleted**	431,5
0,001 to 2,7; **0,001 deleted**	428

Although the range of frequencies itself is not so important, it is fundamental that the first value of frequency is as close as possible to zero. If it is not the case, the radius obtained is different from the radius predicted by the traditional linear theory.

But, as explained for the *Mariner* example, the results of *Simulat* program in the case of a steady turn motion, must be the same as those predicted by the traditional theory and that has been verified for the *Mariner*.

The reason for this difference is that the initial value of the viscous ramp seems to be added to the first frequency's hydrodynamic coefficient, instead of strictly zero frequency because this is not available. That is why deleting the first frequency value leads to differences only on the impulse response functions in which a viscous ramp has been added. These differences are illustrated in figures 23 and 24, where the hydrodynamic coefficient B_{26} is taken by way of example.

Finally, as some hydrodynamic coefficients tend to infinite value close to zero, we have to find an intermediate for the first value of frequency : not too close to zero because of the tendency to infinity, not too far because of the initialisation of the viscous ramp.

When experimental data are available for the oscillatory derivatives (as for the *Mariner*), to check the data obtained against the experimental data, enables the application of the viscous ramp to be verified.

When there is no experimental data for the oscillatory derivatives available, **the adequacy of the obtained radius with respect to the predicted radius from linear theory is a good test**, since it has been verified that the *Simulat* program is the same as the traditional linear theory for such a manoeuvre.

3.4.3 Sensitivity to the upper frequency value of the viscous ramp (ω)

Concerning the viscous ramp, the sensitivity to the frequency chosen for the end of the viscous ramp (ω) has been studied. The value has been defined for the *Mariner*, in order that the damping coefficients after adding the viscous ramp best correspond to the experimental data. For the *British Bombardier*, for which no such experimental data are available, we have to study the influence of this parameter.

Figures 25 and 26 show, as way of example, the damping coefficient Y_v as function of encounter frequency and the corresponding impulse response function obtained for different values of ω (non-dimensionalized), for the *British Bombardier*. Figure 27 presents the correspondent

tracks of the ship during the 5° rudder angle circle manoeuvre and figure 28 presents the results of same experiences for the *Mariner*. Then figure 29 presents the radius obtained versus ω for both ships.

It can be seen that :

- The sensitivity to this parameter is comparable for both ships. It is more sensitive for small values of ω than for higher values of ω.
- The higher ω is, the larger is the radius.
- If we choose the value of ω just when the hydrodynamic data seems to become constant (around 34 (non-dimensionalised) for both ships), we obtain a good comparison with the predicted radius of the traditional linear manoeuvring theory.

Finally, we can choose **the same value as for the *Mariner*** and expect accurate results. The viscous ramp ends for a non dimensionalised frequency of 34.

3.4.4 Sensitivity to the number of panels in the seakeeping calculation mesh

Finally the sensitivity to the mesh used in the seakeeping calculation was studied. Six different meshes were tested but the results with only two of them are presented here, for clarity. Here are the characteristics of the both meshes (Figures 21 and 30):

	Mesh n°1	Mesh n°2
Number of panels around each section	6	8
Aspect ratio	1	0,5
Number of panels for whole ship	684	2400

Some damping coefficients and impulse response functions obtained for each mesh are presented in figures 31 and 32 .

The main difference is at high frequencies. For the first mesh (684 panels), a resonance frequency is observed, which seems to disappear with the second mesh (2400 panels). The resonance is a **purely numerical problem**. During the seakeeping calculation, there is also fluid in the hull form, although there is no flow through the hull form. This fluid can come in resonance for some high frequency; that is what is observed here. This resonance decreases when the mesh becomes more precise. The frequency of resonance also seems to increase.

That is why the resonance disappears with the mesh n°2. The impulse response functions are also affected as we can see in figure 32. They also are less noisy.

For all these reasons, the second mesh will be used in the further applications of the simulation.

Note : A mesh with even more panels is not used because of the calculation limits of the *THARBM* program.

3.5 Circle manoeuvres in calm water and in waves

3.5.1 Predictions in calm water

Finally, figures 33 and 34 present the predictions by *Simulat* for a circle manoeuvre with 5° rudder angle and 15° rudder angle, with or without roll motion, without any waves. In calm water, the results with and without roll motion are comparable, but not identical. The radius obtained for 5° rudder angle is 221.5 m and for 15° rudder angle, 200 m. The errors in relation to the radius predicted by the traditional manoeuvring linear theory are respectively 0.3 % and 0.5 %.

3.5.2 Predictions in waves

Figure 35 presents the *Simulat* prediction for a 5° rudder angle circle manoeuvre in waves. The roll motion has been excluded. For the highest frequencies, the panels have been split into four to increase the precision.

The same qualitative observations as for the *Mariner* vessel can be made.

If the roll motion is included (Figure 36), the ship still performs a sort of circle but the results are totally different from those excluding the roll motion. It seems to perform more an ellipse than a circle. It has more difficulties to turn when it is approximatively perpendicular to waves. If we have a look at the roll motion, we see that there is a sort of resonance when the ship is perpendicular to waves. It confirms the sensitivity of the simulation to the inclusion of roll.

Although the results are more accurate than for the *Mariner*, further investigations about the roll damping and the coupling inertia moments are required.

3.6 Conclusion

The model has thus been developed and used with another vessel : the *British Bombardier* tanker. **The understanding of the effects of several parameters involved in the model has been improved.** Then, the predictions obtained for *British Bombardier* will prove useful in order to further the validation process.

4 Comparisons with experimental manoeuvring data

Full-scale accelerating, stopping and steering trials with the *British Bombardier* tanker were carried out on 6 and 7 October 1963. These trials were conducted on behalf of the British Ship Research Association by the Experiment Tank Department of Vickers-Armstrong Ltd. David Clarke of the B.S.R.A. had published the experimental results, and they have been provided here by J.M.J Journee [6].

These manoeuvring results will be used here in order **to compare the *Simulat* predictions with experimental data**, both for circle manoeuvres and zigzag manoeuvres.

All the manoeuvres and predictions were performed in **calm water**.

Contents

4.1 Circle manoeuvres

4.1.1 Manoeuvres description and Simulat predictions

Turning circle tests were performed at nominal 100 rpm speed (15.5 kn) for three different rudder angles : -34°, +37° and -19°. The ship's position was obtained from a shipborne Decca Hi-Fix receiver. The propulsion and wind data were also recorded. It is assumed here that the wind had little influence on the manoeuvres.

Predictions for these manoeuvres with the *British Bombardier* were performed using *Simulat 7.0*, at 15.5 kn forward speed, in calm water.

4.1.2 Comparisons between experimental data and *Simulat* predictions

The results of both full scale trials and *Simulat* predictions are presented in figures 37, 38 and 39. We can read the following manoeuvring information :

-19° Circle Manoeuvre			
	Full scale trial	*Simulat* prediction	Error
Advance	984 m	794 m	-19.3 %
Transfer	629 m	462 m	-26.5 %
Tactical diameter	1230 m	783 m	-36.3 %
Turning radius	555 m	170 m (linear prediction : 169 m)	-69.4 %

-34° Circle Manoeuvre			
	Full scale trial	*Simulat* prediction	Error
Advance	723 m	592 m	-18.1 %
Transfer	453 m	337 m	-25.6 %
Tactical diameter	863 m	575 m	-33.4 %
Turning radius	339 m	127 m (linear prediction : 127 m)	-62.5 %

+37° Circle Manoeuvre			
	Full scale trial	*Simulat* prediction	Error
Advance	631 m	568 m	-10 %
Transfer	-419 m	-322 m	-23.1 %
Tactical diameter	-746 m	-550 m	-26.3 %
Turning radius	280 m	124 m (linear prediction : 124 m)	-55.7 %

It can be observed that :

- The more the manoeuvre runs, the more the manoeuvring data predicted by *Simulat* are false : the error increases. There is between 10 % and 25 % error on the transfer and advance, 30 % on the tactical diameter, and more than 55 % on the final turning radius.
- The main reason of these errors are the **non linear effects**, which are not included in the *Simulat* prediction.

  Simulat predicts, for each manoeuvre, the same radius as that predicted by the traditional linear theory.

  In fact, the non linear effects are more important at the end of the manoeuvre, that explained the increase of the error.

  It also comes from the **steady forward speed**. In *Simulat*, this forward speed is constant, although in reality it decreases by more than a half during the circle manoeuvre.

Finally, we have to keep in mind that **the slow motion derivatives** used to initialise the viscous ramp, have been obtained with a model. But it has been seen that there was a large scale effect in the determination of these derivatives. Since the predictions are very sensitive to the viscous ramp, the errors in slow motion derivatives could have a large effect on the predictions too.

- Although the errors on the manoeuvring data are quite important for these circle manoeuvres, we can observe that **the evolution of these data with the rudder angle are predicted correctly by *Simulat*.**

  As an example, let us have a look at the tactical diameter. When the rudder angle increases from -19° to -34°, it decreases by 29.8 % in the full scale trials and by 26.6 % in the *Simulat* predictions.

4.1.3 Conclusion

The manoeuvres predicted by *Simulat* are far from the experimental data. This is as expected, because, as said previously, the *Simulat* predicted radius were not realistic (less than the length of the ship !). In circle manoeuvres, a non linear theory is required. Furthermore, a more accurate description of the forward speed is necessary, in order the surge motion to be better calculated. Some solutions are briefly presented in the "further investigations"chapter. More investigations about the values of slow motions derivatives are also required.

4.2 Zigzag manoeuvres

4.2.1 100 RPM trials

Manoeuvres description

Zigzag trials were run at nominal 100 rpm speed (15.5 kn), with nominal rudder angles 10°, 20° and 30°. The rudder angle was held constant until the ship's heading had swung through 20° or -20°. Then the same amount of opposite rudder angle was applied as quickly and smoothly as possible. The cycle was repeated several times. The ship's heading and rudder angle were recorded during the manoeuvres. Heading was taken from the ship's gyrocompass. Information about wind speed and direction are also available but not exploited here. Since the wind force was around 10 kn, it is assumed that the effect on the ship's behaviour is not too important.

The ship's heading and rudder angle versus time are represented in figure 40, for the three nominal rudder angle manoeuvres.

Experimental manoeuvring results

From these experimental results, we obtain the following manoeuvring information - overshoot angles, initial turning time, times to next execute.

10°/20° Zigzag Manoeuvre			
Initial turning time to second execute		82.9 s	
First overshoot angle	9.2°	Time to third execute	244.1 s
Second overshoot angle	12.4°	Time to fourth execute	221 s
Third overshoot angle	16	Time to fifth execute	
Fourth overshoot angle			
Mean overshoot angle	12.5°	Mean time to next execute	232 s

20°/20° Zigzag Manoeuvre			
Initial turning time to second execute		46.8 s	
First overshoot angle	12.5°	Time to third execute	164.2 s
Second overshoot angle	11.2°	Time to fourth execute	148 s
Third overshoot angle	13.7°	Time to fifth execute	186 s
Fourth overshoot angle	10.7°		
Mean overshoot angle	12.0°	Mean time to next execute	166 s

30°/20° Zigzag Manoeuvre			
Initial turning time to second execute		41.1 s	
First overshoot angle	11.3°	Time to third execute	133 s
Second overshoot angle	14°	Time to fourth execute	136 s
Third overshoot angle	10.3°	Time to fifth execute	146 s
Fourth overshoot angle	12.7°		
Mean overshoot angle	12.1°	Mean time to next execute	138,3 s

It can be seen that :

- For each zigzag test, successive overshoot angles vary a little, although the trend seems to be constant. This variation seems to be linked with the variation of the rudder angle, where, in practice, it is not possible to achieve the desired rudder angle exactly. For the exploitation of the results, in order to erase these little variations, we use the mean overshoot angle.
- The same remark can be done about the time to next execute ; we use the mean time to next execute.
- The initial time to second execute for the 20°/20° test is underestimated, because at the beginning of the manoeuvre, the heading is already negative.

Simulat predictions

Predictions for zigzag manoeuvres for the *British Bombardier* at full speed (15.5 kn) were performed using *Simulat 7.0*. The predictions of the ship's heading is presented in figure 42. The rudder angle were successively 10°, 20° and 30° and the reference heading was 20°, as in the full scale trials presented above. We obtain the following manoeuvring information :

10°/20° Zigzag Manoeuvre			
Initial turning time to second execute		70.6 s	
First overshoot angle	8.3°	Time to third execute	168.4 s
Second overshoot angle	18.6°	Time to fourth execute	208 s
Third overshoot angle	21.9	Time to fifth execute	
Fourth overshoot angle			
Mean overshoot angle	16.2°	Mean time to next execute	188,2 s
Limit overshoot angle	23.6°	Limit time to next execute	222 s

20°/20° Zigzag Manoeuvre			
Initial turning time to second execute		45.5 s	
First overshoot angle	7.7°	Time to third execute	113.5 s
Second overshoot angle	18.8°	Time to fourth execute	143 s
Third overshoot angle	22.9°	Time to fifth execute	153 s
Fourth overshoot angle	25.4°		
Mean overshoot angle	18.7°	Mean time to next execute	136,5 s
Limit overshoot angle	25.4°	Limit time to next execute	158 s

30°/20° Zigzag Manoeuvre			
Initial turning time to second execute		36 s	
First overshoot angle	8.7°	Time to third execute	92 s
Second overshoot angle	19.6°	Time to fourth execute	116 s
Third overshoot angle	22.8°	Time to fifth execute	121 s
Fourth overshoot angle	24.7°		
Mean overshoot angle	12.1°	Mean time to next execute	109,66 s
Limit overshoot angle	25.7°	Limit time to next execute	127 s

It can be seen that :

- During each prediction, the overshoot angle increases with time and seems to reach a constant value after 5 to 6 cycles. In order to compare the results at the beginning of the manoeuvre, we could use a mean value for the four first values. But we have to keep in mind that the variations hidden by the mean are different to those observed in the full-scale trials. Finally, the constant values reached for a long time may be more appropriate.
- The same observation can be made for the times to next execute.

Comparisons between experimental data and *Simulat* predictions

Figure 44 shows the comparison between the full scale trials data and the *Simulat* predictions for the three zigzag manoeuvres. At first glance, these data seem not to correspond to each other. The overshoot angles of *Simulat* predictions are larger, the times to next execute are smaller. The comparisons details are below.

10°/20° Zigzag Manoeuvre				
Full scale trial		Simulat prediction		Error
Initial turning time	82.9 s	Initial turning time	70.6 s	- 14.8 %
Mean overshoot angle	12.5°	Limit overshoot angle	23.6 °	+ 47 %
Mean time to next execute	232 s	Limit time to next execute	222 s	- 4.3 %

20°/20° Zigzag Manoeuvre				
Full scale trial		Simulat prediction		Error
Initial turning time	46.8 s	Initial turning time	45.5 s	- 02.8 %
Mean overshoot angle	12.0°	Limit overshoot angle	25.4 °	+ 53 %
Mean time to next execute	166 s	Limit time to next execute	158 s	- 4.8 %

30°/20° Zigzag Manoeuvre				
Full scale trial		Simulat prediction		Error
Initial turning time	41.1 s	Initial turning time	36 s	- 12.4 %
Mean overshoot angle	12.1°	Limit overshoot angle	25.7 °	+ 53 %
Mean time to next execute	138 s	Limit time to next execute	127 s	- 8.2 %

To summarise, we have an error of approximatively -15 % on the initial turning time (the result for 20°/20° manoeuvre is not good because it was underestimated in the full scale trial), +50 % on the overshoot angles and -5 to -8 % on the times to next execute.

These errors may be due to several reasons :

- The use of a linear theory, hard turns with such rudder angles require a non-linear theory.
- The value of the slow motion derivatives used to initialise the viscous ramp.

- The use of a constant forward speed, speed should decrease during the turns.

In fact, the reasons of the errors are the same as the reasons for which the predictions for circle manoeuvres are not good.

But another comparison could be interesting : since we have three zigzag tests, with increased rudder angle between each test, we could compare the evolution of the manoeuvring characteristics when the rudder angle changes.

Initial turning time Here is presented the evolution of this manoeuvring characteristic :

Initial turning time	10°/20°		20°/20°		30°/20°
Full scale trials	82.9 s	−43.5% →	46.8 s (underestimated)	−12% →	41.1 s
Simulat predictions	70.6 s	−35.5% →	45.5 s	−20.9% →	36 s

Since the second value of the full scale trials is underestimated, we can say that the evolutions of the initial turning time are comparable.

Overshoot angles As regards the overshoot angles, we can observe that, when the rudder angle changes, it does not vary significantly. As well as in the full scale trials, the predicted overshoot angles, compared one after another, do not change significantly either, as well as the limit overshoot angles.

Times to next execute Here is presented the evolution of this manoeuvring characteristic :

Time to next execute	10°/20°		20°/20°		30°/20°
Full scale trials	232 s	−28.4% →	166 s	−16.7% →	138 s
Simulat predictions	222 s	−28.8% →	158 s	−19.6% →	127 s

One more time, the evolutions in the full scale trials and in the predictions are similar.

4.2.2 85 RPM trials

The same zigzag trials were also carried out at 85 rpm nominal speed, which corresponds to a speed of 6.602 m/s (12.5 kn). The same analysis as for the 100 rpm trials is made here, in order to compare the results.

The ship's heading and rudder angle versus time are represented in figure 41, for the three nominal rudder angle manoeuvres.

Experimental manoeuvring results

From these experimental results, the following manoeuvring information are obtained - overshoot angles, initial turning time, times to next execute.

10°/20° Zigzag Manoeuvre			
Initial turning time to second execute		75.3 s	
First overshoot angle	13.6°	Time to third execute	288.8 s
Second overshoot angle	10.7°	Time to fourth execute	235 s
Third overshoot angle	17.4°	Time to fifth execute	283 s
Fourth overshoot angle	10.1°		
Mean overshoot angle	12.9°	Mean time to next execute	269 s

20°/20° Zigzag Manoeuvre			
Initial turning time to second execute		67.8 s	
First overshoot angle	12.2°	Time to third execute	187.2 s
Second overshoot angle	8.7°	Time to fourth execute	162 s
Third overshoot angle	13.5°	Time to fifth execute	209 s
Fourth overshoot angle	8.2°		
Mean overshoot angle	10.7°	Mean time to next execute	186 s

30°/20° Zigzag Manoeuvre			
Initial turning time to second execute		46.6 s	
First overshoot angle	14.5°	Time to third execute	159.4 s
Second overshoot angle	10°	Time to fourth execute	140 s
Third overshoot angle	13.4°	Time to fifth execute	178 s
Fourth overshoot angle	9.4°		
Mean overshoot angle	11.8°	Mean time to next execute	159 s

The same observation about the variations, linked with the small variations of the rudder angle and maybe the wind, can be done, that is why, once again, time mean values will be used.

Simulat predictions

Predictions for zigzag manoeuvres for the *British Bombardier* at this other speed (12.5 kn) were performed using *Simulat 7.0.*

Note : All the programs have been used with the new speed value and prediction for a circle manoeuvre (5° rudder angle) was performed to verify the results. The radius obtained was 534 m instead of 520 m predicted by the traditional linear theory, i.e. 2.6 % error.

The predictions of the ship's heading is presented in figure 43. The rudder angle was successively 10°, 20° and 30° and the reference heading was 20°, as in the full scale trials presented above. The following manoeuvring information are obtained:

10°/20° Zigzag Manoeuvre			
Initial turning time to second execute		84.7 s	
First overshoot angle	8.2°	Time to third execute	206.3 s
Second overshoot angle	18.6°	Time to fourth execute	252 s
Third overshoot angle	22.1°	Time to fifth execute	265 s
Fourth overshoot angle	23.3°		
Limit overshoot angle	24.0°	Limit time to next execute	270 s

20°/20° Zigzag Manoeuvre			
Initial turning time to second execute		56.2 s	
First overshoot angle	8.5°	Time to third execute	140.8 s
Second overshoot angle	19.1°	Time to fourth execute	175 s
Third overshoot angle	23.3°	Time to fifth execute	186 s
Fourth overshoot angle	24.5°		
Limit overshoot angle	25.2°	Limit time to next execute	190 s

30°/20° Zigzag Manoeuvre			
Initial turning time to second execute		44 s	
First overshoot angle	8.5°	Time to third execute	112.1 s
Second overshoot angle	19.1°	Time to fourth execute	139 s
Third overshoot angle	22.6°	Time to fifth execute	148 s
Fourth overshoot angle	24.1°		
Limit overshoot angle	25.6°	Limit time to next execute	154 s

As in the previous section, the limit value of overshoot angles and times to next execute are used for the further comparisons.

Comparisons between experimental data and *Simulat* predictions

Figure 45 shows the comparison between the full scale trials data and the *Simulat* predictions for the three zigzag manoeuvres. As for the 100 rpm case, at first glance, these data seems not to correspond to each other. The overshoot angles of *Simulat* predictions are larger, but the times to next execute are similar. The comparisons details are below.

10°/20° Zigzag Manoeuvre				
Full scale trial		Simulat prediction		Error
Initial turning time	75.3 s	Initial turning time	84.7 s	+ 11.1 %
Mean overshoot angle	12.9°	Limit overshoot angle	24.0°	+ 46.2 %
Mean time to next execute	269 s	Limit time to next execute	270 s	+ 0.4 %

20°/20° Zigzag Manoeuvre				
Full scale trial		Simulat prediction		Error
Initial turning time	67.8 s	Initial turning time	56.2 s	- 17.1 %
Mean overshoot angle	10.7°	Limit overshoot angle	25.2 °	+ 57.5 %
Mean time to next execute	186 s	Limit time to next execute	190 s	+ 2.1 %

30°/20° Zigzag Manoeuvre				
Full scale trial		Simulat prediction		Error
Initial turning time	46.6 s	Initial turning time	44 s	- 5.6 %
Mean overshoot angle	11.8°	Limit overshoot angle	25.6 °	+ 54 %
Mean time to next execute	159 s	Limit time to next execute	154 s	- 3.1 %

To summarise, we have an error of - 17 % to + 15 % on the initial turning time, +50 % on the overshoot angle and 0 to 3 % on the times to next execute.

These errors are similar to those observed on the 100 rpm trials but the times to next execute seems to be better. In the case of this lower speed, *Simulat* program predicts well these times between each action of the rudder.

We compare now the evolution of the manoeuvring characteristics when the rudder angle changes.

Initial turning time Here is presented the evolution of this manoeuvring characteristic :

Initial turning time	10°/20°		20°/20°		30°/20°
Full scale trials	75.3 s	−10% →	67.8 s	−31.3% →	46.6 s
Simulat predictions	84,7 s	−33.7% →	56.2 s	−21.7% →	44 s

Although this is less clear than with the 100 rpm trials, we can say that the general trends of evolution of the initial turning time are comparable. The comparison of the initial turning time are very difficult because it is very sensitive to the initial conditions, which is not known exactly for the full scale trials.

Overshoot angles As well as in the 100 rpm trials, we can observe that, when the rudder angle changes, overshoot angles do not vary significantly. As well as in the full scale trials, the predicted overshoot angles, compared each after each other, do not change significantly either, as well as the limit overshoot angles.

Times to next execute Here is presented the evolution of this manoeuvring characteristic :

Time to next execute	10°/20°		20°/20°		30°/20°
Full scale trials	269 s	−30.8% →	186 s	−14.5% →	159 s
Simulat predictions	270 s	−29.6% →	190 s	−18.9% →	154 s

One more time, the evolutions in the full scale trials and in the predictions are similar.

4.2.3 Conclusion

As a conclusion, it can be said that:

- As regards the initial turning time, the experimental results do not correspond to the predictions very well, and although **the general evolution when the rudder angle change is respected**, the errors remain important. But, if we keep in mind that the measures of initial turning time are not precise because of the dependence of initial conditions, errors less than 20 % are not too bad.
- As regards the overshoot angles, the *Simulat* predictions are more than a half higher, but **it respects the fact that these angles do not vary** when the speed or the nominal rudder angle change.
  Simulat predicts that the overshoot angle increases with time during the zigzag manoeuvre, that can not be observed in the full scale trials.
- As regards the times to next execute, ***Simulat* predictions are good.** The evolutions with the nominal rudder angle and the values are close to the experimental values, particularly at lower speed.

4.3 Conclusion

As a conclusion, it can be said that, although the predictions are not totally accurate, the general evolutions of manoeuvring characteristics as functions of certain parameters - for example, the rudder angle - are well predicted. So **the program has been partly validated with experimental data.**

We need to add that the waves representation had also been validated in [9], but is not developed here.

To further the validation process, some improvements to the model are required. The main domains of further investigation are developed in the corresponding chapter.

5 Investigation of the influence of waves on ship manoeuvrability

Since the software has been partly validated, the model can be used for a first investigation of the influence of waves on ship manoeuvring performance. As for the rudder angle, we can expect *Simulat* to predict well the evolutions of manoeuvring characteristics when the waves vary.

Note : in all the simulations, the roll motion has been excluded, since it has been seen that further investigation is required to predict it correctly.

Contents

5.1 Circle manoeuvres

5.1.1 Following seas

Simulat predictions have been carried out for circle manoeuvres of the *British Bombardier* in following seas. The amplitude of waves was 1.0 m. Several rudder angles (5°, 10°, 15°) and several wave lengths ($\lambda/L = 1, 0.75, 0.5, 0.35, 0.25, 0.1$) have been tested.

The results are presented in figures 46 and 47, for rudder angles of 5° and 10°. The ship performs circles but **a drift in the direction of the wave propagation** is observed. This deviation of the turning trajectory from that in calm water is studied in figure 48, which shows the drifting distance as a function of wave length for different rudder angles. The drifting distance is defined as the quantity of the deviation of the turning trajectory during one complete (360°) turn.

It can be seen that :

- The drifting distance tends to become larger as the rudder angle becomes smaller.
- The drifting distance also tends to become larger as the wavelength becomes larger. The evolution seems to be quasi-linear. (For 5° rudder angle, this behaviour is observed if we do not include the high values obtained around $\lambda/L = 0.8$.)
- For 5° rudder angle, a special behaviour is observed : for around $\lambda/L = 0.8$, the drifting distance increases a lot (double). This may be a resonance frequency for the ship. But it would be useful to investigate this behaviour, in order to explain why it is observed only for the smallest rudder angle.

5.1.2 Head seas

The same simulations have been carried out for head seas. The results are presented in figure 49 for a 5° rudder angle, and the drifting distance is shown as a function of wave length for different rudder angles in figure 49.

It can be observed that :

- The drifting distance has exactly the same evolution and the same values as for the following seas.
- Concerning the resonance observed for 5° rudder angle, it can be seen in figure 49 that the ship seems to have difficulties to make the first turn. Once again, further investigation would be useful to explain this behaviour.

Comparisons with the predictions for the *Mariner* vessel The conclusions concerning the effects of the waves on the manoeuvring performances, in circle manoeuvres, for the British Bombardier are the same as the preliminary comments, which have been made for the Mariner. Furthermore, a similar behaviour as previously has also been observed for the 5° rudder circle manoeuvre of the Mariner. There seems to be a resonance phenomena around $\lambda/L = 0.8$.

5.2 Zigzag manoeuvres

Some predictions have also been carried out for 10°/20° zigzag manoeuvres in waves, for the *British Bombardier*. The amplitude of waves was 1m. Several wave lengths ($\lambda/L = 1, 0.75, 0.6, 0.5$) have been tested, for following and head seas.

The results are presented in figures 50 (track of the ship) and 51 (yaw angle versus time). It can be observed that :

- There is a drift in the direction of the waves, so that in following waves the track is extended, and in head seas it is the contrary.
- The longer the wave length is, the larger is the drift.
- Concerning the yaw angle, the overshoot angles seems to remain constant whatever the waves. But, for following seas, the times to next rudder execute become larger, when the wave length becomes larger. In head seas, it is the contrary : they become smaller when the wave length is longer.

Comparisons with the predictions for the *Mariner* vessel From figures 16 and 17, it can be seen that, for the *Mariner* vessel, the waves have the same effects on the zigzag manoeuvres as for the *British Bombardier*. The difference is that the overshoot angles seem to increase in waves. This is certainly due to the smaller directional stability of the *Mariner* vessel.

5.3 Conclusion

The previous simulations thus present preliminary qualitative results about the effect of waves on the ship manoeuvring performances. In order to further the investigation, these results have to be compared with experimental data. But, for the moment, no such data is available, for the ships studied here.

To summarise, the main effects of the wave are :

- The deviation of the trajectory in regular waves from that in calm water has the tendency to **become larger as the wave length become longer, or when the rudder angle becomes smaller.**
- The effects of head seas or following seas are similar. **The drift is in the direction of the wave propagation.**
- There may exist a wave frequency for which the ship performance is more affected (resonance frequency). But this appears only for small rudder angles.

6 Conclusion and further investigations

As a conclusion, the *Simulat* software, based on the unified theory of a ship travelling in a seaway, has been verified for the *Mariner* vessel and extended to another ship : the *British Bombardier* tanker. It has lead to a better understanding of the parameters of the model, such as the viscous ramp or the mesh used to calculate the impulse response functions. Due to these investigations, the software could now be used for any ship if experimental data for the slow motion derivatives are available.

The comparison of *Simulat* predictions to experimental manoeuvring data for the *British Bombardier* has enabled the partial validation of the software. In fact, it predicts the evolution of the manoeuvring characteristics as functions as the manoeuvring conditions well, but the model requires some improvements in order to predict effectively the track of the manoeuvring ship.

Finally, a preliminary study concerning the effects of waves on the ship's manoeuvring characteristics has been carried out and shows that the manoeuvrability is affected by the wave length and by the wave direction of propagation.

Further Investigations

The aim of the following sections is to present the future investigations which could be undertaken to improve the time simulations and obtain results in better comparison to experimental data.

It just defines the major subjects of the proposed future studies and it does not pretend to be complete and precise. More important work is needed to elaborate and complete those improvements.

Contents

6.1 Introduction of non-linear terms

In the previous chapters we have seen that the most important problem in the simulation was the use of a linear theory.

- The predictions for circle manoeuvres are not accurate, because such a manoeuvre requires a non linear theory.
- The predictions for the zigzag manoeuvres are not accurate either. Because of the large rudder angles generally used, non-linear theory is required to described the turns.

The time simulation could thus be considerably improved if non linear terms are included.

In the current description, using convolution integrals to describe the forces, only linear convolutions have been considered. The non-linear contributions could be added through **non-linear convolution integrals**, corresponding to the higher order terms in the Volterra series expansion. The Volterra series expansion is identical to a Taylor's series in which the constant derivative terms are replaced by convolution integrals, introducing a "memory effect".

The sway force Y due to the sway motion v(t) may be expressed in the form :

$$Y[v(t)] = Y_0 + \int_{-\infty}^{\infty} y_v(\tau_1)v(t-\tau_1)d\tau_1 + \int_{-\infty}^{\infty}\int_{-\infty}^{\infty} y_{vv}(\tau_1,\tau_2)v(t-\tau_1)v(t-\tau_2)d\tau_1 d\tau_2 + \int_{-\infty}^{\infty}\int_{-\infty}^{\infty}\int_{-\infty}^{\infty} y_{vvv}(\tau_1,\tau_2,\tau_3)v(t-\tau_1)v(t-\tau_2)v(t-\tau_3)d\tau_1 d\tau_2 d\tau_3 + ...$$

For the antisymmetric motion (for example, sway motion or yaw motion) one has to add the third order terms, the second orders are zero. For the symmetric motion (for example, surge motion) one add the second order terms. One also must not forget some cross terms (for example impulse response functions such as y_{vrr} or y_{rvv}).

Non-linear terms concerning the rudder action have also to be introduced.

$$Y[\delta(t)] = Y_\delta\delta + Y_{\delta\delta}\delta^2 + Y_{\delta\delta\delta}\delta^3 + crossterms + ...$$

The cross terms are terms including rudder action and motions, such as for example $Y_{r\delta\delta}r\delta^2$.... For the rudder action, no convolution integrals are used, i.e. no memory effect is considered. Slow motion derivatives are used.

For the exact description of the equations using the non linear terms, one could refer to the equations presented in [6]. In these equations, no convolution integrals are used but it gives the non linear terms which have to be used for each force.

The main problem with the introduction of the non-linear convolutions would be the calculation of the impulse response functions, because no experimental frequency-dependent data are available and because the seakeeping calculation may not be able to calculate such non linear coefficients.

In order to avoid this problem, in a first approach, we could introduce the linear terms with a memory effect, and the non-linear without any memory effect. **Although the linear terms are introduced as in the linear theory presented in this report, the non linear terms could be introduced with slow motion derivatives only, using the zero frequency value.**

The data for the higher order of slow motion derivatives may be easier to find. For the *British Bombardier*, they are available in [6].

6.2 Modelling of the propulsion

The second main problem in the simulation concerns the surge motion. In the previous model, a **constant forward speed** is imposed. During the circle manoeuvre this forward speed remains constant, although in the full scale trial it can be seen that it decreases for more than the half. In the zigzag manoeuvre, there is the same problem: the forward speed remains constant during the turns, although in reality it would decrease.

In order to solve this problem the propulsion would have to be defined differently. Instead of defining a speed, a **propulsion force** could be defined. In order to do that properly **the propeller and the rudder** and their interactions have to be studied precisely.

Furthermore, in the current model we use the forward speed to dimensionalise all the slow motion derivatives (and then the forces), although it must be the **water speed at the rudder**, for the rudder forces.

6.3 Wind forces

In the time simulation, the effect of waves are considered but not the effects of wind. But the wind can have lots of influence on the manoeuvring characteristics of the ship, especially for a ship with large superstructure. Moreover, during full scale trials the wind conditions are always recorded. It could be useful to add the wind forces in the model **to predict wind influence** and to compare with experimental results.

Since the manoeuvring trials are relatively short, one could start with one direction and one speed for the real wind : α_w and V_w. The relative wind could be written as follows : $\overrightarrow{V_{rw}} = \overrightarrow{V_w} + \overrightarrow{U}$ where $\overrightarrow{U}$ is the instantaneous speed of the ship. The direction and the speed of the relative wind (α_{rw} and V_{rw}) are then deduced.

The wind forces acting on the ship can be written as follows :

- $F_X = C_X \rho_{air} V_r^2 A_T/2$ for the longitudinal wind force.
- $F_Y = C_Y \rho_{air} V_r^2 A_L/2$ for the lateral wind force.
- $N = C_N \rho_{air} V_r^2 A_L L_{oa}/2$ for the yawing wind moment.

in which : C_X is the longitudinal force coefficient, C_Y the lateral force coefficient, C_N the yawing moment coefficient, ρ_{air} the density of air, V_r the mean relative wind speed between water level and top of superstructure, A_T the transverse projected area, A_L the lateral projected area, and L_{oa} the length overall.

The wind-related data for the ship (projected wind areas), could be obtained from the ship's lines. The wind resistance coefficients can then be obtained as function of the relative wind angle α_{rw}. For the *British Bombardier* they have been obtained from lines plan and photographs and are presented in [6].

The wind effects could thus be introduced in the model :

- The user enters V_w and α_w.
- The user enters a list of values for the wind resistance coefficients corresponding to intervals of relative wind incidence angles.
- V_{rw} and α_{rw} are calculated in the equilibrium position using ship's speed and heading.

- The corresponding to α_{rw} wind resistance coefficients are selected in the tables entered by the user. Then, the wind forces are calculated.
- The forces are included in the equations of motion which are solved for the equilibrium position.
- At each step of the simulation, the same scheme is used. V_{rw} and α_{rw} are calculated using the ship's speed and heading obtained at the previous step.

The introduction of these wind forces is very simple - since for example it is assumed that the wind is constant ! - but the results could be compared with the experimental results for which the relative wind has been recorded.

6.4 Roll motion

In the previous chapter it has been observed that the predictions were very sensitive to roll motion, particularly when the ship is manoeuvring in waves. If one considers the 5° rudder angle circle manoeuvre in waves (amplitude = 1.0 m and λ/L=1), the predictions obtained for the *Mariner* vessel or the *British Bombardier* tanker are totally different (Figures 12 and 36).

It has been seen that the results obtained with the *Mariner* vessel were sensitive to addition of a roll damping but also to wave height (Figure 13). The results obtained are not satisfactory, because they do not seem to represent the reality.

Considering the roll angle (Figure 52), it can be seen that the roll angle increases very quickly at the beginning to reach more than 15° when the ship is perpendicular to the waves. This value is far too large for such a ship in these conditions of waves but it explains why the ship does not perform a circle anymore in the prediction.

For the *British Bombardier* (Figure 53), the roll angle increases, in the same way as for the *Mariner*, at the beginning but the highest value is less than 10°, which is more realistic - even if the ship may not roll like that in such waves. With such a roll motion, the ship can perform circles. But it can be seen that the roll motion increases when the ship is perpendicular to waves and in these positions the ship turns more slowly.

All these observations underline that when the ship is perpendicular to waves, the roll motion increases and it may reach a sort of resonance. These large roll oscillations prevent the ship from turning efficiently. It is well known that such a behaviour occurs in reality.

But, even if the behaviour predicted for the *British Bombardier* seems to be closer to reality, the values remain far too large for both ships. **This may be due to the lack of roll damping and due to the coupling inertia moments for which no accurate values are known.** Further investigations in this domain may be useful in order to better predict the roll motion and its consequences on the manoeuvring characteristics.

Appendix A : A unified mathematical model

Contents

A-1 Manoeuvring theory

In the manoeuvring theory, we consider a set of axes Cxyz (see figure d), fixed to the rigid body. C is fixed at the centre of mass and C_{xz} is a plane of symmetry. The space fixed system is $OX_0Y_0Z_0$ (see figure e). The ship has six degrees of freedom. The Euler angles describing the position of the body axes system are Ψ (swing or yaw), Θ (pitch) and Φ (roll). It is easy to change the reference axes system in the equations through these angles.

A-1.1 Equations of motion

In the relative frame Cxyz, the velocity of the ship can be written as $\overrightarrow{U} = U\overrightarrow{i} + V\overrightarrow{j} + W\overrightarrow{k}$ and the angular velocity $\overrightarrow{\Omega} = P\overrightarrow{i} + Q\overrightarrow{j} + R\overrightarrow{k}$, where P, Q, R are related to the Euler angles.

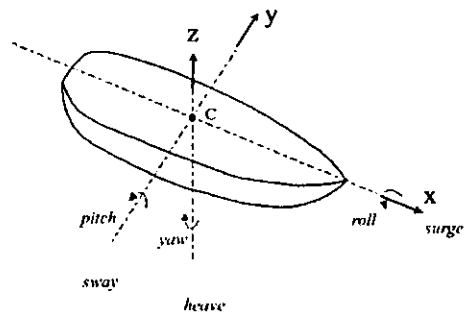

Figure d - Body fixed axis system and degrees of freedom

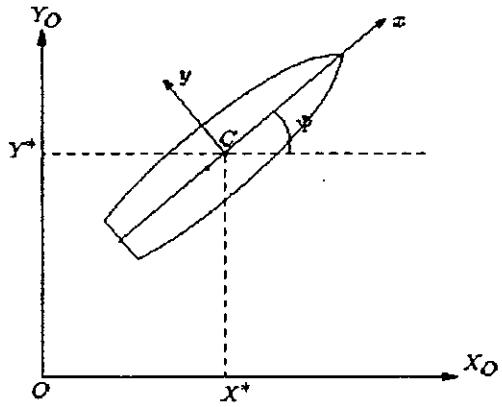

Figure e - Space fixed axes system, Position of the ship [1]

Step 1 : Second Newton's Law

$$\overrightarrow{F} = X\overrightarrow{i} + Y\overrightarrow{j} + Z\overrightarrow{k} = m(\dot{U}\overrightarrow{i} + \dot{V}\overrightarrow{j} + \dot{W}\overrightarrow{k}) + m\overrightarrow{\Omega} \times \overrightarrow{U}$$

$$\overrightarrow{G} = K\overrightarrow{i} + M\overrightarrow{j} + N\overrightarrow{k} = \mathcal{I}(\dot{P}\overrightarrow{i} + \dot{Q}\overrightarrow{j} + \dot{R}\overrightarrow{k}) + \overrightarrow{\Omega} \times \mathcal{I}\overrightarrow{\Omega}$$

Step 2 : Linearisation The hypotheses adopted in this study are :

- Steady reference motion ($\overrightarrow{U} = \overline{U}\overrightarrow{i}$)
- Small perturbations to the reference motion
- Linear mathematical model

Furthermore, due to symmetry, $I_{xy} = I_{yx} = I_{xz} = I_{zx} = 0$

As a consequence of the linearisation procedure, the forces and the moment in a plane of symmetry depend only on the symmetric motion variables (and the equivalent for the perpendicular actions and the antisymmetric motion variables).

Step 3 : Equations of motion Therefore the equations of motion can be written as.

For the symmetric motions :

$$\begin{aligned} m\dot{u} &= \Delta X(t) \\ m\dot{w} - m\overline{U}q &= \Delta Z(t) \\ I_{yy}\dot{q} &= \Delta M(t) \end{aligned} \qquad \text{(Eq 1)}$$

For the antisymmetric motions :

$$\begin{aligned} m\dot{v} + m\overline{U}r &= \Delta Y(t) \\ I_{xx}\dot{p} - I_{xz}\dot{r} &= \Delta K(t) \\ -I_{zx}\dot{p} + I_{zz}\dot{r} &= \Delta N(t) \end{aligned} \qquad \text{(Eq 2)}$$

Position of the ship The position of the ship is meaningless in the relative frame of reference. It is obtained by integrating the velocity between an initial time and time t in the space fixed frame.

$$X^* = \int_0^t (\overline{U} + u)dt$$
$$y^* = \int_0^t (v + \Psi\overline{U})dt$$
$$z^* = \int_0^t (w - \theta\overline{U})dt$$

A-1.2 Forces and moments acting on a ship

The forces and moments acting on the ship must be expressed i order to complete the equations of motions.

These actions are a summation of weight, hydrostatic actions, hydrodynamic actions and other actions specific to the problem (for example a rudder action).

Hydrostatic and hydrodynamic actions are exerted on the ship by the surrounding fluid through two mechanisms : skin friction and pressure, both mechanisms depend directly on the shape of the wetted surface.

For this study, in the case of small displacements, the buoyancy force (integration of pressure on the wetted surface) is expressed as a constant coefficient (restoring coefficient) of the motion displacement.

Since the hydrodynamic forces depend on motion, which in turn will depend on these actions, the hydrodynamic forces may only be expressed in a simplified form if assumptions are made in advance regarding the form of motion and the likely nature of the fluid response.

For a ship manoeuvring slowly in calm water, the hydrodynamic actions are dominated by viscous contributions. To represent these motion dependent hydrodynamic actions, it is usual to use slow motion derivatives. In a linear theory they are assumed to be constant coefficients of the velocity and acceleration perturbation terms. The fluid action represented is instantaneous. No influence of the past motions are included (that is the definition of the "slow"motion.) It will be shown later how these past motions may be considered in a more general case. The contributions to each degree of freedom are then summed, noting the separation between symmetric and antisymmetric actions and motions.

Slow motion derivatives For example, considering the sway motion.

The motion is considered as slow when the following condition is satisfied:

$$\frac{|v|}{|\dot{v}|}, \frac{|\dot{v}|}{|\ddot{v}|}, \ldots \gg \frac{L}{\overline{U}}$$

If the variation of the dynamic motion variables is well behaved mathematically, we can write (first order Taylor series)- the derivatives are evaluated at the reference motion :

$$\Delta Y_{hyd} = v\frac{\partial \Delta Y}{\partial v} + \dot{v}\frac{\partial \Delta Y}{\partial \dot{v}} + \ddot{v}\frac{\partial \Delta Y}{\partial \ddot{v}} + ... + p\frac{\partial \Delta Y}{\partial p} + ... + r\frac{\partial \Delta Y}{\partial r} + ...$$

For a slow motion the higher derivatives are ignored (assumed small).

These derivatives, denoted $Y_v = \frac{\partial \Delta Y}{\partial v}$, are *the slow motion derivatives.* In the present model, they are assumed to be constant.

Equations of motion with the actions and moments For the symmetric motions (X(t), Z(t) and M(t) represent external actions such as wave excitation or the rudder action):

$$\begin{bmatrix} m & 0 & 0 \\ 0 & m & 0 \\ 0 & 0 & I_{yy} \end{bmatrix} \begin{bmatrix} \dot{u} \\ \dot{w} \\ \dot{q} \end{bmatrix} + \begin{bmatrix} 0 & 0 & 0 \\ 0 & 0 & -m\overline{U} \\ 0 & 0 & 0 \end{bmatrix} \begin{bmatrix} u \\ w \\ q \end{bmatrix} =$$
$$\begin{bmatrix} X_{\dot{u}} & X_{\dot{w}} & X_{\dot{q}} \\ Z_{\dot{u}} & Z_{\dot{w}} & Z_{\dot{q}} \\ M_{\dot{u}} & M_{\dot{w}} & M_{\dot{q}} \end{bmatrix} \begin{bmatrix} \dot{u} \\ \dot{w} \\ \dot{q} \end{bmatrix} + \begin{bmatrix} X_u & X_w & X_q \\ Z_u & Z_w & Z_q \\ M_u & M_w & M_q \end{bmatrix} \begin{bmatrix} u \\ w \\ q \end{bmatrix} +$$
$$\begin{bmatrix} 0 & 0 & 0 \\ 0 & Z_{z*} & Z_\theta \\ 0 & M_{z*} & M_\theta \end{bmatrix} \begin{bmatrix} x* \\ z* \\ \theta \end{bmatrix} + \begin{bmatrix} X(t) \\ Z(t) \\ M(t) \end{bmatrix} \qquad \text{(Eq 3)}$$

For the antisymmetric motions (Y(t), K(t) and N(t) represent external actions such as the wave excitation or the rudder action):

$$\begin{bmatrix} m & 0 & 0 \\ 0 & I_{xx} & -I_{xz} \\ 0 & -I_{zx} & I_{zz} \end{bmatrix} \begin{bmatrix} \dot{v} \\ \dot{p} \\ \dot{r} \end{bmatrix} + \begin{bmatrix} 0 & 0 & m\overline{U} \\ 0 & 0 & 0 \\ 0 & 0 & 0 \end{bmatrix} \begin{bmatrix} v \\ p \\ r \end{bmatrix} =$$
$$\begin{bmatrix} Y_{\dot{v}} & Y_{\dot{p}} & Y_{\dot{r}} \\ K_{\dot{v}} & K_{\dot{p}} & K_{\dot{r}} \\ N_{\dot{v}} & N_{\dot{p}} & N_{\dot{r}} \end{bmatrix} \begin{bmatrix} \dot{v} \\ \dot{p} \\ \dot{r} \end{bmatrix} + \begin{bmatrix} Y_v & Y_p & Y_r \\ K_v & K_p & K_r \\ N_v & N_p & N_r \end{bmatrix} \begin{bmatrix} v \\ p \\ r \end{bmatrix} +$$
$$\begin{bmatrix} 0 & 0 & 0 \\ 0 & K_\varphi & 0 \\ 0 & 0 & 0 \end{bmatrix} \begin{bmatrix} y* \\ \varphi \\ \psi \end{bmatrix} + \begin{bmatrix} Y(t) \\ K(t) \\ N(t) \end{bmatrix} \qquad \text{(Eq 4)}$$

Oscillatory derivatives In the case of a steady state sinusoidal motion (of a linear system), the motion and the action have the same frequency but differ in phase and amplitude. The hydrodynamic actions can be written in the same way as previously but the derivatives depend on the frequency ω_e and are denoted $\widetilde{Y}_v(\omega_e)$. They are referred to as *oscillatory derivatives.*

The equation of motion remain the same with the slow motion derivatives being replaced by the oscillatory derivatives.

A-2 Seakeeping theory

In the manoeuvring theory, a set of axes $A\xi\eta\zeta$ is considered : the equilibrium axes system. A is placed in the calm water surface with C, centre of mass, at a distance $\overline{\zeta}$ below A in a vertical plane. The space fixed system is $OX_0Y_0Z_0$. The axes systems are parallel to one another. The distance OA is such that at time t, $OA = \overline{U}t$.

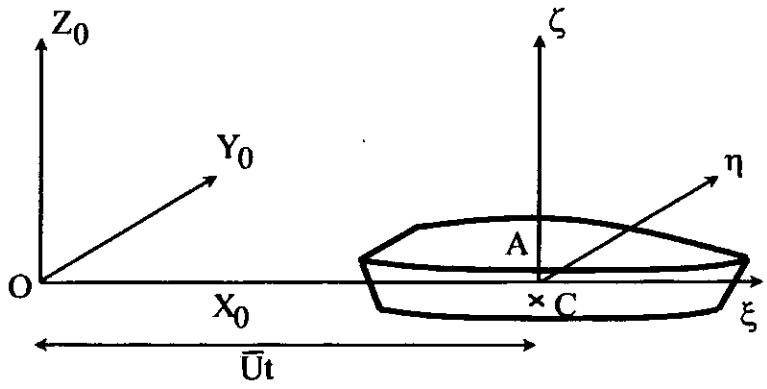

Figure f - Equilibrium axes system

A-2.1 Equations of motion

The motions are *small* translations : $\eta_1(t)$, $\eta_2(t)$ and $\eta_3(t)$ parallel to the axes $A\xi$, $A\eta$ and $A\zeta$; and *small* rotations : $\eta_4(t)$, $\eta_5(t)$ and $\eta_6(t)$ about the axes $A\xi$, $A\eta$ and $A\zeta$.

The steps to obtain the equations of motion are the same as those used for the manoeuvring theory.

A-2.2 Forces and moments acting on a ship

For the seakeeping theory, we consider the case where the excitation is sinusoidal (wave excitation) and the response of the ship is at the same frequency (linear behaviour).

For a wave frequency ω, and for a forward speed $\overline{U}$, the frequency of the excitation (and thus the frequency of response) is the encounter frequency, given by :

$$\omega_e = \omega - \frac{\overline{U}\omega^2}{g} cos\chi_0$$

where χ_0 is the heading to waves.

Hydrodynamic coefficients Just as for the manoeuvring theory, oscillatory derivatives and restoring moments may be used to express the hydrodynamic actions.

In seakeeping theory, the coefficient of the acceleration term, A_{ij}, is the *hydrodynamic added mass* and the coefficient of the velocity, B_{ij} is the *hydrodynamic damping.* These coefficients depend on the encounter frequency.

Equations of motion with the actions and moments For the symmetric motions (where $H_1(t), H_2(t), H_3(t)$ are the components of the wave excitation i.e. $H_j(t) = H_j e^{-i\omega_e t}$:

$$\begin{bmatrix} m & 0 & -m\overline{\zeta} \\ 0 & m & 0 \\ -m\overline{\zeta} & 0 & I_{yy} + m\overline{\zeta}^2 \end{bmatrix} \begin{bmatrix} \ddot{\eta}_1 \\ \ddot{\eta}_3 \\ \ddot{\eta}_5 \end{bmatrix} =$$

$$- \begin{bmatrix} A_{11} & A_{13} & A_{15} \\ A_{31} & A_{33} & A_{35} \\ A_{51} & A_{53} & A_{55} \end{bmatrix} \begin{bmatrix} \ddot{\eta}_1 \\ \ddot{\eta}_3 \\ \ddot{\eta}_5 \end{bmatrix} - \begin{bmatrix} B_{11} & B_{13} & B_{15} \\ B_{31} & B_{33} & B_{35} \\ B_{51} & B_{53} & B_{55} \end{bmatrix} \begin{bmatrix} \dot{\eta}_1 \\ \dot{\eta}_3 \\ \dot{\eta}_5 \end{bmatrix} -$$

$$\begin{bmatrix} 0 & 0 & 0 \\ 0 & C_{33} & C_{35} \\ 0 & C_{53} & C_{55} \end{bmatrix} \cdot \begin{bmatrix} \eta_1 \\ \eta_3 \\ \eta_5 \end{bmatrix} + \begin{bmatrix} H_1(t) \\ H_3(t) \\ H_5(t) \end{bmatrix} \qquad \text{(Eq 5)}$$

For the antisymmetric motions :

$$\begin{bmatrix} m & m\overline{\zeta} & 0 \\ m\overline{\zeta} & I_{xx}+m\overline{\zeta}^2 & -I_{xz} \\ 0 & -I_{zx} & I_{zz} \end{bmatrix} \begin{bmatrix} \ddot{\eta}_2 \\ \ddot{\eta}_4 \\ \ddot{\eta}_6 \end{bmatrix} =$$
$$- \begin{bmatrix} A_{22} & A_{24} & A_{26} \\ A_{42} & A_{44} & A_{46} \\ A_{62} & A_{64} & A_{66} \end{bmatrix} \begin{bmatrix} \ddot{\eta}_2 \\ \ddot{\eta}_4 \\ \ddot{\eta}_6 \end{bmatrix} - \begin{bmatrix} B_{22} & B_{24} & B_{26} \\ B_{42} & B_{44} & B_{46} \\ B_{62} & B_{64} & B_{66} \end{bmatrix} \begin{bmatrix} \dot{\eta}_2 \\ \dot{\eta}_4 \\ \dot{\eta}_6 \end{bmatrix}$$
$$- \begin{bmatrix} 0 & 0 & 0 \\ 0 & C_{44} & 0 \\ 0 & 0 & 0 \end{bmatrix} \begin{bmatrix} \eta_2 \\ \eta_4 \\ \eta_6 \end{bmatrix} + \begin{bmatrix} H_2(t) \\ H_4(t) \\ H_6(t) \end{bmatrix} \qquad \text{(Eq 6)}$$

A-3 Relations between seakeeping and manoeuvring theory

It has been shown that both the body axes system and equilibrium axes system are suitable for describing the equations of motion. We may also obtain simplified relations between the two formulations (manoeuvring theory and seakeeping theory), if it is assumed that the movements of the axes system are small related to each other.

A-3.1 Kinematic conditions

Firstly, relations between the different components of the motion used in each theory may be obtained.

In order to do that, the reference frame must be changed, using the relations between the relative reference frame and the space fixed reference frame, which are known through the definition of the relative reference frame. The matrix, linking the two reference frames, are simplified in the case of small displacements.

For example, the matrix T may be used to relate components of the body fixed and space fixed axis systems. For example : $\overrightarrow{U}_{space} = \underline{\underline{T}}\overrightarrow{U}_{relative}$

$$\underline{\underline{T}} = \begin{bmatrix} 1 & -\psi & \theta \\ \psi & 1 & -\phi \\ -\theta & \phi & 1 \end{bmatrix}$$

If this is done for each representation (manoeuvring theory, then seakeeping theory) then two different expressions of the components of motion in the same space fixed axes system are obtained. Thus, by equating them, we obtain the relationship between motions in the seakeeping and manoeuvring theory.

By rearranging the relations obtained, in the case of sinusoïdal motions, we obtain the following :

$$\begin{cases} \ddot{\eta}_1 = \dot{u} + \overline{\zeta}\dot{q} & \eta_1 = u + \overline{\zeta}q & \eta_1 \equiv x* \\ \ddot{\eta}_3 = \dot{w} - \overline{U}q & \dot{\eta}_3 = w + \dot{q}(\overline{U}/\omega_e^2) & \eta_3 \equiv z* \\ \ddot{\eta}_5 = \dot{q} & \dot{\eta}_5 = q = \dot{\theta} & \eta_5 = \theta \end{cases} \qquad \text{(Eq 7)}$$

$$\begin{cases} \ddot{\eta}_2 = \dot{v} - \overline{\zeta}\dot{p} + \overline{U}r & \dot{\eta}_2 = v - \overline{\zeta}p - \dot{r}(\overline{U}/\omega_e^2) & \eta_2 \equiv y* \\ \ddot{\eta}_4 = \dot{p} & \dot{\eta}_4 = p = \dot{\phi} & \eta_4 = \phi \\ \ddot{\eta}_6 = \dot{r} & \dot{\eta}_6 = r = \dot{\psi} & \eta_6 = \psi \end{cases} \qquad \text{(Eq 8)}$$

A-3.2 Representation of the forces and moments acting on a ship

By using the same method (and the same matrix) relations between the external actions (i.e. between ΔX, ΔY... and ΔH_j) may be obtained. These actions are expressed through the oscillatory derivatives and the hydrodynamic coefficients, related to the components of motion linked to their respective axis system. Thus the previous relations may be used to express these actions with the same components of the motion and finally identify the terms between the different components of motion, since this is true whatever the motion. Therefore a relationship between hydrodynamic coefficients and oscillatory derivatives is obtained.

For example : with the matrix T, we obtain for the sway action $\Delta Y = \Delta H_2$. By using the previous relations :

$$\begin{gathered}\Delta H_2 = -A_{22}\dot{v} - B_{22}v + (\overline{\zeta}A_{22} - A_{24})\dot{p} \\ +(\overline{\zeta}B_{22} - B_{24})p + \{(\overline{U}/\omega_e^2)B_{22} - A_{26}\}\dot{r} \\ -(\overline{U}A_{22} + B_{26})r + H_2(t) = \Delta Y = \\ Y_{\dot{v}}\dot{v} + Y_v v + Y_{\dot{p}}\dot{p} + Y_p v + Y_{\dot{r}}\dot{r} + Y_r r + Y(t)\end{gathered}$$

By identifying the terms, we obtain the followings relations :

$$\begin{cases} Y_{\dot{v}} = -A_{22} & Y_v = -B_{22} \\ Y_{\dot{p}} = \overline{\zeta}A_{22} - A_{24} & Y_p = \overline{\zeta}B_{22} - B_{24} \\ Y_{\dot{r}} = (\overline{U}/\omega_e^2)B_{22} - A_{26} & Y_r = -(\overline{U}A_{22} + B_{26}) \end{cases} \qquad \text{(Eq 9)}$$

These relations are true for both the calm water situation and sinusoidal motions.

It is easy to do the same for all the coefficients. **These relations are very important since they enable a link between manoeuvring theory and seakeeping theory.**

A-4 Impulse response functions

It was noted previously that the representations of the fluid actions consider the actions as instantaneous. In fact, it is known that the past motion of the ship influences the motion dependent hydrodynamic actions. A representation of these actions which includes past motions is therefore needed.

Hydrodynamic coefficients and oscillatory derivatives are specific to sinusoidal motions. The new representation has to be appropriate for arbitrary motions.

A-4.1 Definition

In fact, any fluid action can be expressed, within the bounds of a linear theory, by a convolution integral. for example, for an arbitrary motion v(t) :

$$\int_0^t h(\tau)v(t-\tau)d\tau$$

where the impulse response function is zero for $\tau < 0$ and $\tau > t$. As a consequence, the integral can be extend to a $-\infty, \infty$ integral.

In this convolution formulation, the sway force (for example) can be written :

$$\Delta Y(t) = \int_{-\infty}^{\infty} y_v(\tau)v(t-\tau)d\tau + \int_{-\infty}^{\infty} y_p(\tau)p(t-\tau)d\tau + \int_{-\infty}^{\infty} y_r(\tau)r(t-\tau)d\tau + Y(t)$$

A-4.2 Relation with the oscillatory derivatives and the hydrodynamics coefficients

It was shown [9] that the impulse response functions can be related to the hydrodynamic coefficient, using the Fourier transform and its inverse, in order to link both functional and frequency domains.

In order to explain and illustrate this, lets take an example and consider a Planar Motion Mechanism experiment involving sway motion only : $y(t) = y_0 sin(\omega_e t)$.

The sway action can be expressed in two different manners :

$$\Delta Y(t) = \int_{-\infty}^{\infty} y_v(\tau) v(t-\tau) d\tau = \widetilde{Y}_{\dot{v}}(\omega_e)\dot{v} + \widetilde{Y}_v(\omega_e) v$$

This leads to :

$$\widetilde{Y}_v(\omega_e) = \int_{-\infty}^{\infty} y_v(\tau) cos(\omega_e \tau) d\tau$$

$$\widetilde{Y}_{\dot{v}}(\omega_e) = -\int_{-\infty}^{\infty} \tau y_v(\tau) \frac{sin(\omega_e \tau)}{\omega_e \tau}) d\tau$$

The relations to the hydrodynamic coefficients can be maid trough the previous relations between oscillatory derivatives and those coefficients.

It may be useful to modify the form of this representation, introducing the value of the hydrodynamic coefficients for an infinite frequency [10].

$$\int_{-\infty}^{\infty} y_v(\tau) v(t-\tau) d\tau = -\widetilde{Y}_{\dot{v}}(\infty)\dot{v} + \widetilde{Y}_v(\infty) v + \int_{-\infty}^{\infty} y *_v (\tau) v(t-\tau) d\tau$$

The action appears then as the sum of an instantaneous action and a "memory" of the fluid.

A-4.3 Determination : experimental and theoretical

Planar Motion Mechanism experiments are usually used to measure oscillatory derivatives. These measurements could be used to find the impulse response functions through the inverse transform, as follows :

$$y_v(\tau) = \frac{2}{\pi} \int_0^{\infty} \widetilde{Y}_v(\omega_e) cos(\omega_e \tau) d\omega_e$$

But due to inertial forces exerted on the ship model, the frequency data cannot be measured to high enough frequencies for the previous equation to converge.

On the other hand, the hydrodynamic coefficients may be determined using a three dimensional potential flow panel code. These coefficients may then be related to the oscillatory derivatives, and the impulse response function calculated as above.

However, it is well-known that such a model is deficient, for it cannot account for viscous flow influences. But the viscosity is the most important fluid action in the case of low frequencies. Thus, the results obtained with this model at low frequencies are far from the experimental results. On the contrary, the results obtained at high frequencies are good.

A-4.4 An hybrid method

In order to obtain the best approach of the impulse function, it has been proposed [1] to use an hybrid approach, which uses the potential flow model at high frequencies and the experiments at low frequencies.

Firstly the hydrodynamic coefficients are generated with the potential flow panel code, and they are transformed in oscillatory derivatives through the relations established in the previous section.

Then a viscous "ramp"is added to these results ; the differences between theoretical and experimental data are in fact assumed to be due only to viscous contributions. The values of these viscous "ramp"are adjusted using the experimental data at low frequencies.

With this hybrid method we can then obtain a good approximation of the impulse response functions.

A-5 Representation of wave action

The wave action can be divided into three components. The first one is the direct action of the wave, the second one is the indirect action - in fact, the waves modify the heading of the ship, thus the wave action is modified ; that is why this second term is expressed with the derivatives of the direct action relative to the heading - and finally a rudder action, which tries to oppose the wave excitation.

$$Y(t) = Y_\alpha(\chi_0, t) - \psi(t) Y'_\alpha(\chi_0, t) + Y_\delta(t)$$

A-6 A unified mathematical model describing the manoeuvring of a ship travelling in a seaway

As we have already seen above, the impulse response functions are determined from a combination of the oscillatory data derived from a PMM experiment and the theoretical evaluation of the frequency dependent seakeeping coefficients.

They are then included in the convolution terms of the fluid actions and the following equations of motion can used to describe the manoeuvring of a ship in a seaway (using the body fixed axis system). These equations could easily be translated in the equilibrium axes system used in the seakeeping theory.

Equations of motion For surge motion :

$$\begin{aligned} m\dot{u}(t) = &\int_0^t x_u(\tau) u(t-\tau) d\tau + \int_0^t x_q(\tau) q(t-\tau) d\tau \\ &+ \int_0^t x_w(\tau) w(t-\tau) d\tau + X_\alpha(X^*, Y^*, \psi, \chi_0, \omega, t) + X_\delta(t) + X_0(t) \end{aligned} \qquad \text{(Eq 10)}$$

For heave motion :

$$\begin{aligned} m[\dot{w}(t) - \bar{U} q(t)] = &\int_0^t z_u(\tau) u(t-\tau) d\tau + \int_0^t z_q(\tau) q(t-\tau) d\tau \\ &+ \int_0^t z_w(\tau) w(t-\tau) d\tau + Z_{z^*} z^*(t) \\ &+ Z_\theta \theta(t) + Z_\alpha(X^*, Y^*, \psi, \chi_0, \omega, t) + Z_\delta(t) + Z_0(t) \end{aligned} \qquad \text{(Eq 11)}$$

For pitch motion :

$$\begin{aligned} I_{yy}\dot{q}(t) = &\int_0^t m_u(\tau) u(t-\tau) d\tau + \int_0^t m_q(\tau) q(t-\tau) d\tau \\ &+ \int_0^t m_w(\tau) w(t-\tau) d\tau + M_{z^*} z^*(t) \\ &+ M_\theta \theta(t) + M_\alpha(X^*, Y^*, \psi, \chi_0, \omega, t) + M_\delta(t) + M_0(t) \end{aligned} \qquad \text{(Eq 12)}$$

For sway motion :

$$m[\dot{v}(t) + \bar{U}r(t)] = \int_0^t y_v(\tau)v(t-\tau)d\tau + \int_0^t y_p(\tau)p(t-\tau)d\tau + \int_0^t y_r(\tau)r(t-\tau)d\tau + Y_\alpha(X^*, Y^*, \psi, \chi_0, \omega, t) + Y_\delta(t) + Y_0(t) \quad \text{(Eq 13)}$$

For roll motion :

$$I_{xx}\dot{p}(t) - I_{xz}\dot{r}(t) = \int_0^t k_v(\tau)v(t-\tau)d\tau + \int_0^t k_p(\tau)p(t-\tau)d\tau + \int_0^t k_r(\tau)r(t-\tau)d\tau + K_\phi\phi(t) + K_\alpha(X^*, Y^*, \psi, \chi_0, \omega, t) + K_\delta(t) + K_0(t) \quad \text{(Eq 14)}$$

For yaw motion :

$$-I_{xx}\dot{p}(t) + I_{zz}\dot{r}(t) = \int_0^t n_v(\tau)v(t-\tau)d\tau + \int_0^t n_p(\tau)p(t-\tau)d\tau + \int_0^t n_r(\tau)r(t-\tau)d\tau + N_\alpha(X^*, Y^*, \psi, \chi_0, \omega, t) + N_\delta(t) + N_0(t) \quad \text{(Eq 15)}$$

Appendix B : *British Bombardier* hull form

The aim of this appendix is to describe the main dimensions of the the *British Bombardier* tanker and to compare the real hull form with that drawn with *ShipShape* (see figures g and h).

	British Bombardier tanker	Computed hull form by *Shipshape*
LPB (m)	220.98	220.98
LWL (m)		227.106
B (m)	29.566	29.566
T (m)	12.497	12.497
Δ (m^3)	65089	64337
C_b	0.797	0.788
C_m		0.987
C_p		0.799
C above baseline (m)		6.562
G above baseline (m)	6.49	6.49
M above baseline (m)		12.228

The *ShipShape* calculated displacement is only 1.2 % less than the displacement given for the *British Bombardier* tanker. This is good indication about the accuracy of the representation.

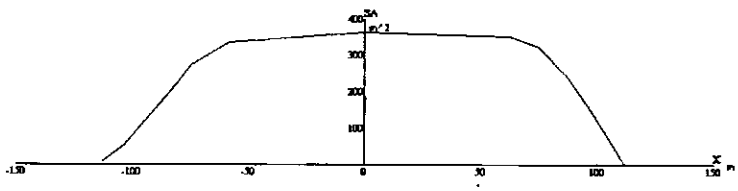

Figure g - Sectional area curve as predicted by *Shipshape* for the *British Bombardier*

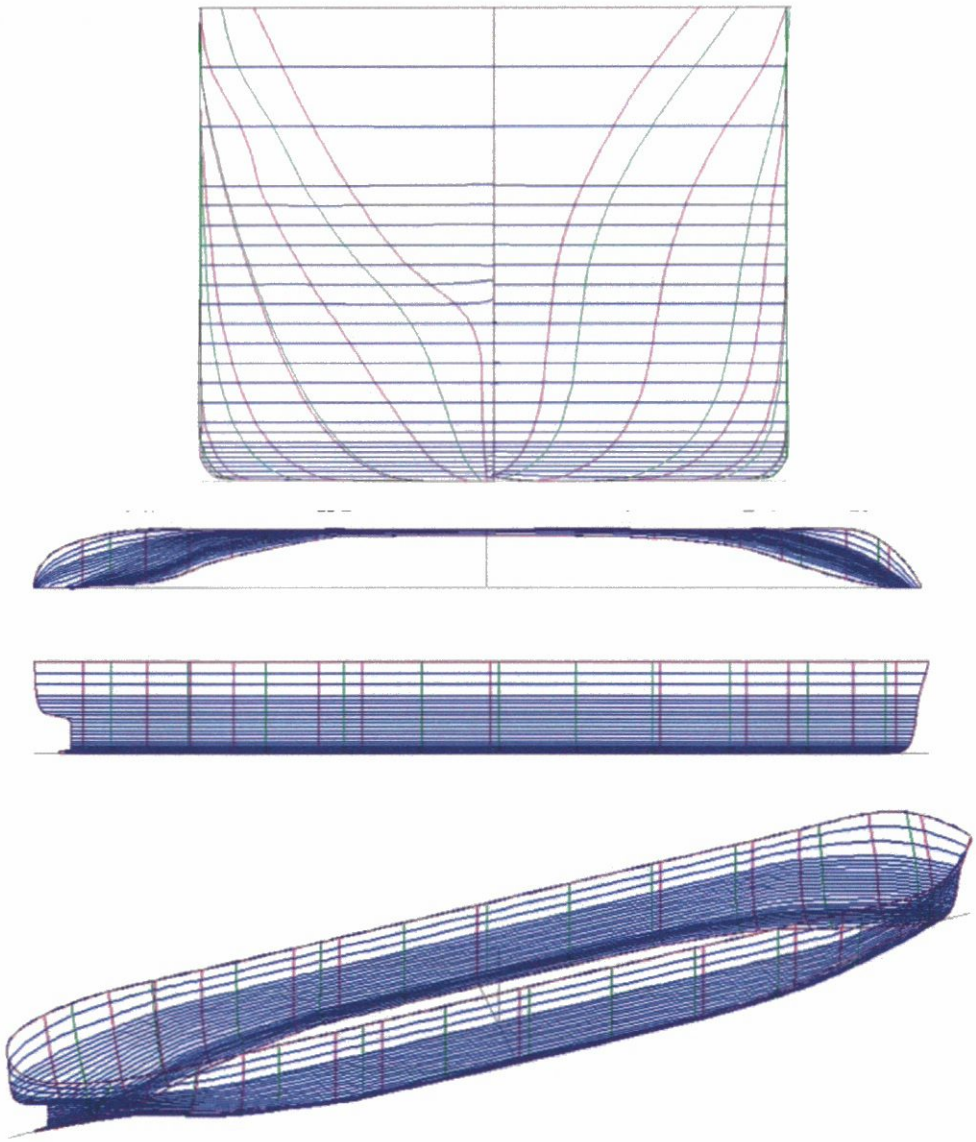

Figure h - Representation of *British Bombardier* by Shipshape.

Appendix C : *Simulat* User Guide

Simulat : Time simulation of ship manoeuvring in waves

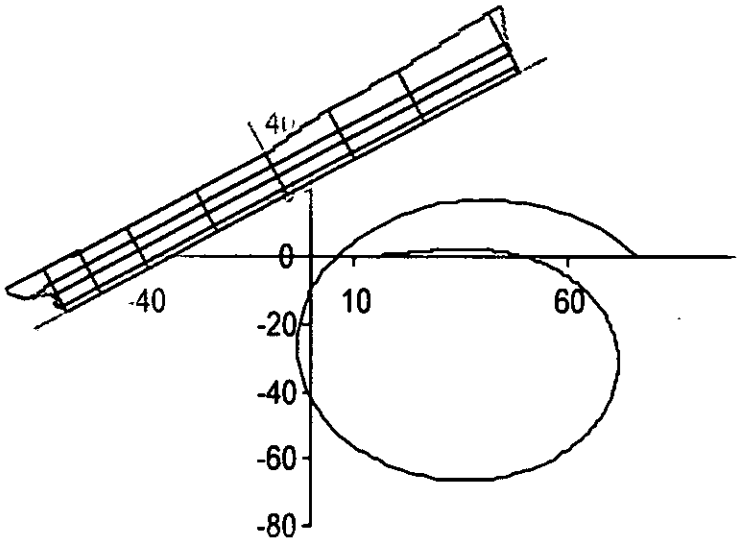

USER GUIDE

School of Engineering Sciences, Ship Science.

Programs developed by P.A. Bailey (1999)
User guide written by L. Letki (2005)

University of Southampton

Contents

1 Introduction

This user guide presents the different programs used in the time simulation of a ship manoeuvring in waves, developed by Bailey, 1999 [9], and the methods to use them. In particular, the input files of each program are detailed and explained when necessary. The ship used as an example is a *Mariner* ship.

Principles and Structure The time simulation uses the unified mathematical model presented in Bailey, 1999 [9][1].

The equations of motions are expressed in a body fixed axis system and use impulse response functions and convolutions to express the fluid actions.

The impulse response functions are calculated with an hybrid method : hydrodynamic coefficients are generated by traditional seakeeping calculations and converted to the body axis system. A viscous ramp may be added in order to correct the values at low frequencies, where viscosity has a major role.

An overview of the structure of the programs is presented in figure 1.1.

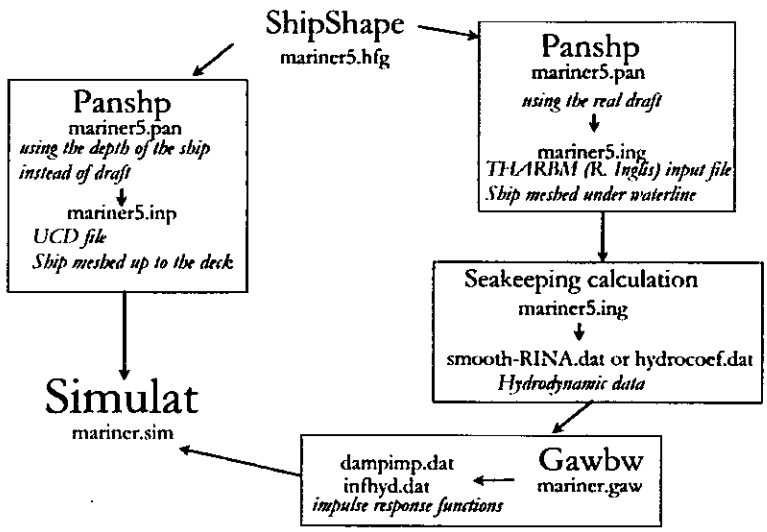

Figure 1.1: Structure of the programs

For the time simulation, different programs are needed before the main program, called *Simulat*. These programs are presented in the Pre-Programs chapter.

You can also find here a description of the global structure of the programs, and their relations.

The principles of the *Simulat* program are presented in the *Simulat* chapter.

2 Pre-programs

2.1 *ShipShape*

Initially ship's curves, sections, length and water lines are designed using a software called *ShipShape*, developed by the Wolfson Unit.

The initial frame of the Mariner ship is defined in a file called mariner5.hfg. It contains the coordinates of curves describing the ship up to the deck line. The frame is defined with the origin at midships on the keel, with the following axis orientation : x forward, y port, and z up.

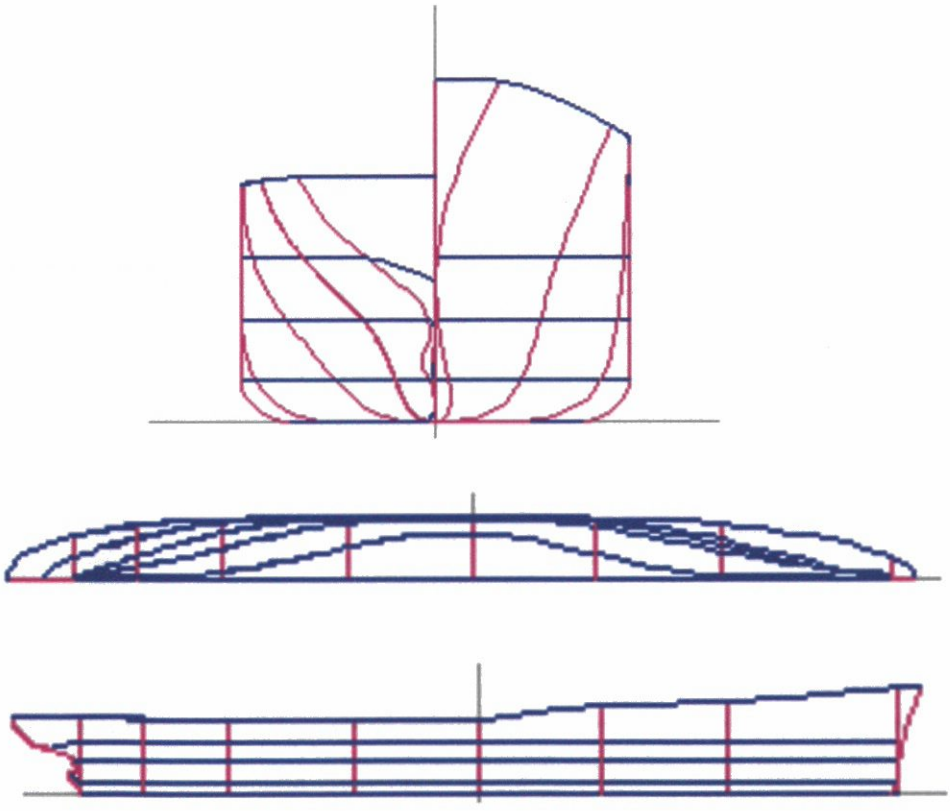

Figure 2.1: Representation of mariner ship by Shipshape, different views

2.2 *Panshp* program

From this point all the computational work is run with UNIX. Bailey, 1999 [9] has implemented the different programs and routines in C programs.

Role The role of this program is to mesh the ship.

Principles of *panshp* program To mesh the ship, *Panshp* favours the aspect ratio of the panels. In fact, in hydrodynamic applications, this ratio should ideally be close to 1, in order to evaluate correctly the fluid actions. The global number of panels is not a parameter of *Panshp*. When the number of panels increases, the panels description is closer to the hull of the ship but the aspect ratio may not be respected and it may be a bad option.

Panshp creates the mesh section by section, from the extremity to the midships. Starting at the most forward section line, a panel height is calculated by dividing the perimeter of the section line by the specified number of panels around a section. The spatial distance to the next section line is calculated by multiplying this panel height by the aspect ratio. *Panshp* repeats this until midships, and the longitudinal difference between midships and the last calculated section line is distributed back over the sections. The quadrilateral panels are formed using panel corners at adjacent section lines.

The same procedure is applied for the aft part of the hull. Calculation of bow and stern panels uses panel corners on the last section line and on the bow or stern line.

Used version The version of the *panshp* program used herein is *panshp14*.

Command ~ philipb/bin/panshp14 mariner.pan

Required files

- mariner5.hfg; *ShipShape* definition of the Mariner ship
- mariner.pan; Input file, described below.

Description of the input file

```
% ***********************************************
% ************ PANSHP14.C INPUT FILE ************
% ***********************************************
% Date written  14/2/98, modified 4/05
% Written by Phil Bailey, modified by Laurence Letki
%
% Numbers entered in the file MUST NOT start at the first character position
% Lines that start with a "%" in the first character position will be ignored
% Filenames and directories must be followed by a space (not a tab!!)
%
%
% Axis system used : x fwd,y to port z up. Origin placed at midhips on the keel.
%
% ***********************************************
%
 //home/lpl104/simulat/panshp   % directory to the data files
 2              % use standard data directory to
%                               find shipshape file (2=yes,1=no)
```

```
mariner5.hfg                % filename of shipshape input filename
2               % add a patch for the keel (1=no, 2=yes)
1               % add a patch for the bow  (1=no, 2 = yes) ;
%       it has been decided that this option is particularly bad ;
%       It is recommend that you put the additionnal
%               patch by hand using ShipShape
```

Don't forget to change the name of the directory to the data files or the name of the ShipShape file, if you work on another ship.

```
%  panfs14.c requires a length which it uses to decide what "big" is
%  This length should usually be the draft, but in some cases a standard length
%  other than the draft is required
 2              % specify draft (1=no,2=yes)
 14.000             % draft or standard length value
%                (If you change draft, or translations here
%                 check ouput routines to make
%                sure that origin translations are still correct)
%         The origin of the coordinate system must be placed at MIDSHIPS
%         and on the KEEL line.
%         The origin used in shipshape may need to be translated.
%         (+ve z up +ve x fwds)
 0.0        % x translation required to put origin at midships
 0.0        % z translation required to put origin on the keel
 0.0        % roll rotation about panshp11 axis (degrees)
 0.0        % pitch rotation about panshp11 axis (degrees)
 0.0        % yaw rotation about panshp11 axis (degrees)
```

If you use Panshp to create the mesh for Simulat input file (UCD output file), enter the depth of the ship instead of the real draft : then, all the ship will be meshed (up to deck).

If you use Panshp to create the mesh for traditional seakeeping calculation (e.g THARBM (Robert Ingliss) output file), enter the real draft of the ship. Only the part of the ship under the water line will be meshed.

```
% ************** Panel height options *************
% Option 1 = express panel height as a fraction of section perimeter
% The number of panels around each section will the same all along the ship
% Option 2 = express panel height as a fraction of draft
% The height of the panels will remain fixed, but the number around
% each section will vary
 1                          % No of Panel height option to use
% Option 1 :
 8                          % Number of panels around each section
% Option 2 :
 2          % Min number of panels to allow around each section
 6                      % Max number of panels to allow around each section
 0.3                    % Panel height as a fraction of height (or std length)
%
% ************** Panel length options *************
% Option 1 = Express panel length as a fraction of draft
%        The length of the panels will remain fixed
% Option 2 = Express panel length using aspect ratio
% All panels in ship will have approx same aspect ratio (panel size varies)
 2                      % No of Panel length option to use
% Option 1:      Express panel length using fraction of draft
 1.0              % Min allowable section spacing as a fraction of draft
% Option 2 :
 1            % Aspect ratio of panels (length/height)
```

```
%
%
 78.5              % x value of first proper bow section on PORT side
 2         % Try and fit bow type section at stern
%                            (Not recomended for transom sterns)
 -74               % x value of first proper stern section on PORT side
 2                 % Add transom (1=no, 2=yes)  PORT side
%
%
 1             % Generate both sides of the ship (1=no,2=yes)
%                    (Note that if the roll or yaw angles are not zero,
%                     both sides of the shipwill automatically be generated)
```

Here above, you can change the parameters of the mesh you want to generate. In fact, as described previously, the global number of panel is not an argument : you can change the **number of panels** around each section and the **aspect ratio** of the panels (which has to be closed to 1 for the hydrodynamic applications).

For *Simulat* program (UCD file), it is not necessary to generate both sides of the ship.

```
%  The following 3 line apply only to cases where other side of ship is entered
 79.0              % x value of first proper bow section on STB side
 2             % Try and fit bow type section at stern
%                            (Not recomended for transom sterns)
 -74               % x value of first proper stern section on STB side
 1                 % Add transom (1=no, 2=yes)  STB side
%%%%%%%%%%%%%%%%%%%%%% end of add other side options %%%%%%%%%%%%%%%%
 1                     % Swap port and starboard sides (1=no,2=yes)
%      (Only use this option if you want to generate half the
%       hull and want the starboard side only)
%
 1.0            % Scale factor for the ship (allows scaling of panel output)
%
%                  ****      OUTPUT CHOICES *****
% ****************  Robert Ingliss file output ****************
%
%   The Robert Ingliss coordinate system Oxyz will have :
%   O at the bow in the still water plane
%   positive x pointing aft
%   positive z pointing down
%       positive y to port
%   When looking along an INWARD pointing panel normal, the panels are
%   entered in a clockwise sense.
%       The mesh should contain only panels below calm water line
%
 2       % write Robert Ingliss output file (2=yes, 1 = no)
 25      % No of lines which describe Robert Ingliss file (excluding comment lines)
%
 2              % Use standard data directory (1=no,2=yes)
 mariner5.ing    % Filename of Robert Ingliss file
 1.0            % speed of ship in m/s
 160.93         % length of ship in m
 83.92          % LCG aft of FP
 0.0            % Height of VCG above waterline
 1660.0         % displacement in m^3
 0.0            % i44
 0.0            % i55
 0.0            % i66
 0.0            % i46
 0.0            % c33
```

```
 0.0            % c44
 0.0            % c55
 0.0            % c34
 0.0            % c35
%   The coordinate system for Robert Ingliss seakeeping
%             needs to be centred at the bow
%             and at the calm water level.
%          Need to know the distance of the bow from midships
%       NOTE : If this is an outrigger then
%       require the x distance from the centre of the outrigger to the
%       bow of the main hull
%
 80             % x translation of origin from midships
 14.000         % z translation of origin from keel ...should be same as draft!!
 4              % Choice of frequency data :
%               1=   Enter wavelength at zero encounter frequency
%                   2=   Enter range of encounter frequencies
%                   3=   Enter range of wavelengths
%                   4=   Enter range of wave frequencies
 1.0            % wave amp (not needed for option 2)
 180.0          % wave heading (180 degrees = head seas) (not needed for option 2)
 200.0          % wavelength (only needed for option 3)
 0.001          % lower frequency (used for options 2 and 4)
 7.0            % upper frequency (used for options 2 and 4)
 30             % number of values (used options 2,3 and 4)
```

The Robert Inglis file is generated. Do not forget to enter the correct draft above, and the correct ship parameters, in order to use the file in seakeeping calculations.

```
% ********************  UCD file output **********************
%
 2    % write UCD output file (2=yes, 1 = no)
 2        % No of lines which describe UCD output file (excluding separators) (>1)
%
 2        % Use standard data directory (1=no,2=yes)
 mariner5.inp   % Filename of UCD file
```

The UCD output file contains the mesh used in the *Simulat* input file (if you have entered the depth of the ship in the draft input above).

```
% ******************  BARR file output ************************
%
 2   % write BARR output file (2=yes, 1 = no)
 3       % No of lines which describe BARR output file (excluding separators) (>1)
%
 2       % Use standard data directory (1=no,2=yes)
 mariner5.bar   % Filename of BARR file
 160.93         % Length of ship in m
```

The file mariner5.bar is created but it is an empty file ?! This file is not needed in the next step.

```
% ******************  postscript file output ************************
 3    % write POSTSCRIPT output file (3=yes and the next, 2=yes, 1 = no)
 7  % No of lines which describe postscript output file (excl comment lines)  (>1)
%
 2        % Use standard data directory (1=no,2=yes)
 ship1.ps  % Filename of Postscript file
 0.0       % yaw rotation  (degrees)
```

```
 0.0      % pitch rotation (degrees)
 0.0      % roll rotation (degrees)
 0.625    % scalefac  (scale to 100 *100)
 1        % automatically scale to 100*100 (1=no 2=yes)
%
% End of required input for panship14.c
```

This part is repeated four times in order to create four PS output files, with different views of the ship. Unfortunately, these files are not created and it is not clear why.

The last message of the execution is : "I don't seem to have any data about draft or baseline of this ship". Since these files (.bar and .ps) are not used after for the time simulation, this problem remains unsolved.

Output files

- mariner5.inp (UCD file); Description of the mesh for one side of the ship (if this option is chosen in the input file) , with the origin at midships of the keel. The points are first listed and counted, then the panels (quad) are listed with the number of each of the four corners of that panel. The file begins with the number of points, and the number of panels.
- mariner5.ing (THARBM (Robert Inglis) file); description of the mesh for both sides of the ship, which can be used by traditional seakeeping calculations (developed by Robert Inglis).

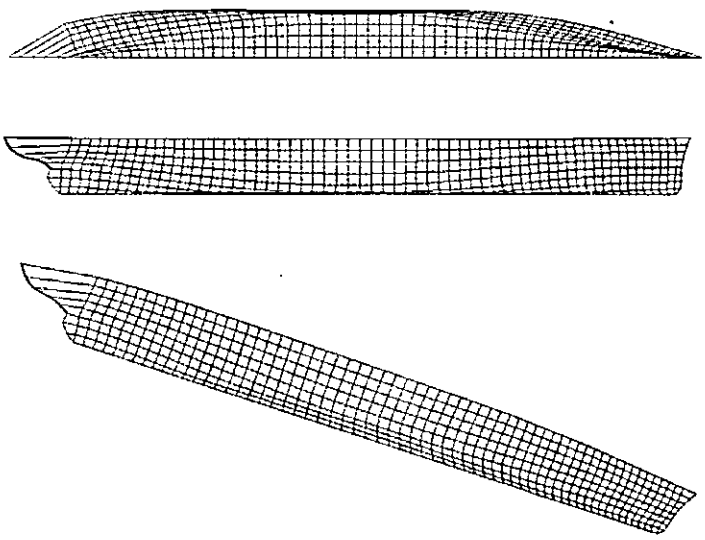

Figure 2.2: Discretisation of one side of Mariner Ship ; number of panels around each section : 8 - Aspect ratio : 1, resulting in 507 panels for one side.

Visualisation In order to see the panels, use *PanVise12*. Firstly, the UCD file mariner.inp has to be modified as follows : add a line just below the first line (with the number of points and panels), with 0000 and add one to the number of points. In fact, points with zero coordinates is added. Then you can open this file with *PanVise12* and see the mesh with different orientations.

Note A *Windows* version of this program has been developed : ***PanelGen***. The parameters are the same but the user interface is easier to use and the visualisation is included.

2.3 Gawbw program

Role The role of this program is to calculate the impulse response functions, with the hybrid method briefly presented in the introduction.

Used version The version of *gawbw* program used herein is *gawbw6*.

Command ~ philipb/bin/gawbw6 vfullbod.gaw

Required files

- hydrocoef.dat; frequency dependent hydrodynamic data, obtained with a traditional seakeeping calculation (and a THARBM (Robert Inglis) file).
- vfullbod.gaw; Input file, described below.

Description of the input file

```
% ********** GAWBW6.C INPUT FILE ************
%
% Numbers entered in the file MUST NOT start at the first character position
% Lines that start with a % in the first character position will be ignored
% Filenames and directories must be followed by a space (not a tab!!)
%
%  This program reads in hydrodynamic data from a number of sources.
%  The first job it does is to undo any non-dimensionalisation
%  that may have been performed
%  on the hydrodynamic data.
%  For this reason it needs to know some information about the full size ship.
%
% The hydrodynamic data that it reads in is assumed to be referenced
% to the Robert Ingliss equilibrium axes.
%
 6                  %version
%
 160.93 % Length between perpendiculars of full scale ship
 -3.73  % LCG of full scale ship fwd of midships
 0.000  % distance of C ABOVE equilibrium axis origin (+ve = UP)
 7.716  % Speed of ship in m/s
%
 .                  % Standard data directory
 2          % Use Standard data directory to read in hydrodynamic data (1=no,2=yes)
 hydrocoef.dat    % Filename of hydrodynamic data file
 1        % Source of hydrodynamic data (1=definebismp.f, 2=all of DOMS versions)
%
%  It is assumed that the data is referenced to upright equilibrium axes
%  with the origin in the flat water plane
%
 2  % Axis system to reference output data to (1=equilbrium axes,
%       2= inverted body axes (z axis pointing up))
%
 0.000     % Distance of new axis system origin fwd of present input
```

```
%          equilibrium origin.
%          For body axes centred at CofG this should be the distance of the CofG
%      fwd of input equilibrium origin (should be zero for rbismp and ndbsafp)
%      For equilibrium axis output it is simply the distance of the output
%      equilibrium axes fwd of the input equilibrium axes
%
 1         % Type of non-dimensionalisation used for output
%       1=no non-dimensionalisation
%       2=Robert Ingliss style non-dimensionalisation
%       3=ITTC non-dimensionalisation
%
 1 % Scale the the hydrodynamic data read from hydrodynamic input file (1=no,2=yes)
```

For Simulat 6, the output data need to be NO non dimensionalised.

```
%  ************** Low Frequency viscous damping data ******************
 2                  % Add a viscous ramp (1=no,2=yes)
%
 3  % Type of non-dimensionalisation used for viscous data
%   (1=none, 2=Robert Ingliss Non-dimensionalisation, 3=Standard)
 34  % upper omega to take viscous ramp to
%     (must be non-dimensionalised according to last option)
%
% IMPORTANT :  The following viscous data MUST be referenced
%              to the OUTPUT AXIS SYSTEM
%   In the case of body axes this will be an INVERTED body axis system
 1       %   add visc (1=no,2=yes)
 0.0     %   visc[0][0]
 1       %   add visc (1=no,2=yes)
 0.0     %   visc[0][1]
 1       %   add visc (1=no,2=yes)
 0.0     %   visc[0][2]
 1       %   add visc (1=no,2=yes)
 0.0     %   visc[0][3]
 1       %   add visc (1=no,2=yes)
 0.0     %   visc[0][4]
 1       %   add visc (1=no,2=yes)
 0.0     %   visc[0][5]
 1       %   add visc (1=no,2=yes)
 0.0     %   visc[1][0]
 2       %   add visc (1=no,2=yes)
-10.1e-3     %   visc[1][1]
 1       %   add visc (1=no,2=yes)
 0.0     %   visc[1][2]
 1       %   add visc (1=no,2=yes)
 0.0     %   visc[1][3]
 1       %   add visc (1=no,2=yes)
 0.0     %   visc[1][4]
 2       %   add visc (1=no,2=yes)
 2.90e-3     %   visc[1][5]
 1       %   add visc (1=no,2=yes)
 0.0     %   visc[2][0]
 1       %   add visc (1=no,2=yes)
 0.0     %   visc[2][1]
 1       %   add visc (1=no,2=yes)
 0.0     %   visc[2][2]
 1       %   add visc (1=no,2=yes)
 0.0     %   visc[2][3]
 1       %   add visc (1=no,2=yes)
 0.0     %   visc[2][4]
 1       %   add visc (1=no,2=yes)
```

```
 0.0      %   visc[2][5]
 1        %   add visc (1=no,2=yes)
 0.0      %   visc[3][0]
 1        %   add visc (1=no,2=yes)
 0.0      %   visc[3][1]
 1        %   add visc (1=no,2=yes)
 0.0      %   visc[3][2]
 1        %   add visc (1=no,2=yes)
 0.0      %   visc[3][3]
 1        %   add visc (1=no,2=yes)
 0.0      %   visc[3][4]
 1        %   add visc (1=no,2=yes)
 0.0      %   visc[3][5]
 1        %   add visc (1=no,2=yes)
 0.0      %   visc[4][0]
 1        %   add visc (1=no,2=yes)
 0.0      %   visc[4][1]
 1        %   add visc (1=no,2=yes)
 0.0      %   visc[4][2]
 1        %   add visc (1=no,2=yes)
 0.0      %   visc[4][3]
 1        %   add visc (1=no,2=yes)
 0.0      %   visc[4][4]
 1        %   add visc (1=no,2=yes)
 0.0      %   visc[4][5]
 1        %   add visc (1=no,2=yes)
 0.0      %   visc[5][0]
 2        %   add visc (1=no,2=yes)
-3.49e-3      %   visc[5][1]
 1        %   add visc (1=no,2=yes)
 0.0      %   visc[5][2]
 1        %   add visc (1=no,2=yes)
 0.0      %   visc[5][3]
 1        %   add visc (1=no,2=yes)
 0.0      %   visc[5][4]
 2        %   add visc (1=no,2=yes)
-2.0e-3      %   visc[5][5]
% ************************************************************
 1     % Invert the output data (multiply all the data by -1) (1=no,2=yes)
```

The part above defines the viscous ramp which may be added to the hydrodynamic data generated by seakeeping calculations, in order that it corresponds to experimental data at low frequencies (where the viscosity is more important). The viscosity coefficients correspond in fact to the slow motion derivatives, obtained experimentally for the ship (zero frequency data).

For Simulat 6, the output data need to be NOT inverted.

```
% ****************** Impulse response function generation *****
%
%   Even if the next option is no, you still need the data lines that follow
%       it otherwise it gets very confused
%
 2       % Generate impulse response functions and other hydro data
%
% NOTE : impulse response functions are calculated using full scale hydro data
%        If the input data was non-dimensionalised gawbw6.c will give it the full
%        scale dimensions before generating impulse response functions
%        Therefore, time steps and intervals for impulse response functions are for
%        full scale ship
```

```
%
 100     % number of frequency values to generate for new hydro data
 40  % upper frequency for new hydro data (output non-dimensionalisation scheme)
%
 2              % Generate h(t) from damping and create new added mass
 2000            % number of time steps for h(t) from damping (FULL SCALE)
 0.15       % time step interval for h(t) from damping (FULL SCALE)
%
 2      % Generate h(t) from added mass  and create new damping
 2000            % number of time steps  for h(t) from added mass (FULL SCALE)
 0.15            % time step interval for h(t) from added mass  (FULL SCALE)
%
% ***************************** Output options ********************************
%All filenames are needed here even though options have been switched off earlier
%
 2              % type of output
 //home/lpl104/simulat/gawbw             % standard output directory
%
 2             % Use standard output directory (1=no,2=yes)
 vdamping.dat   % damping filename
 2             % Use standard output directory (1=no,2=yes)
 vadded.dat     % added mass filename
 2             % Use standard output directory (1=no,2=yes)
 vinfhyd.dat   % Infinite frequency added mass and damping data file
                    %(version 6 and above only)
 2             % Use standard output directory (1=no,2=yes)
 vnewdamp.dat   % damping created from added mass impulse response
                        %function filename
 2             % Use standard output directory (1=no,2=yes)
 vaddimp.dat    % h(t) data from added mass filename
 2             % Use standard output directory (1=no,2=yes)
 vnewadded.dat  % added mass data from damping h(t) filename
 2             % Use standard output directory (1=no,2=yes)
 vdampimp.dat   % h(t) data from damping filename
```

Output files

- vdamping.dat
- vadded.dat
- vnewdamp.dat
- vaddimp.dat
- vnewadded.dat
- vdampimp.dat
- vinfhyd.dat

Only files vdampimp.dat and vinfhyd.dat, and maybe vdamping.dat and vadded.dat are used by Simulat program. They contain respectively the impulse response functions, the value of hydrodynamic data at infinite frequency and the frequency dependent coefficients (damping and added mass).

3 *Simulat* program

3.1 Principles of *Simulat* program

The simulation starts with the ship in the calm water equilibrium condition (which is calculated by the *Itequilpos* subroutine). Thereafter, at each time step and at each step of the Runge Kutta scheme [9][10], the necessary convolutions are performed together with calculation of the relevant wave excitations and restoring moments (*calcfs* subroutine), in order to solve the equations of motion.

Calculation features and assumptions

- Spatial position is calculated by integrating component velocities over time.
- Heading of the vessel relative to waves changes substantially with time (e.g. a circle manoeuvre).
- Wave excitation is assumed to be instantaneous and is taken as that due to the Froude-Kriloff components alone (i.e. diffraction excitation is neglected).
- The restoring and wave excitation are not necessarily linear, but in the limiting case of small ship motions and waves, the predictions of *calcfs* routine are linear. The linear assumptions adopted in the mathematical model are not violated.
- The instantaneous excitation is evaluated with the ship in the perturbed condition.

Two different versions can be used : *Simulat 6*, which runs on a UNIX machine or on a LINUX machine, and *Simulat 7*, which runs on a LINUX machine.

3.2 *Simulat 6*

Command ~ philipb/bin/simulat6 newmesh.sim 160.93 (wavelength)

Required files

- vdampimp.dat; this file contains the impulse response functions, needed to calculate the fluid actions on the ship at each step.
- vinfhyd.dat; this file contains the hydrodynamic data at infinite frequency, also needed to calculate the fluid actions.
- (vdamping.dat)

- (vadded.dat)
- newmesh.sim; Input file, described below.

Description of the input file The file described below is the input file for the simulation, in calm water (no amplitude for the waves), for a constant rudder action of 5° (spiral manoeuvre), with surge perturbations and roll motion excluded.

In Simulat 6, you can, among other things:

- Choose the motions you want to be included or excluded
- Use a constant or a sinusoidal rudder action
- Use different wave amplitudes and wavelengths

```
% ************ SIMULAT6.C INPUT FILE *************
% Numbers entered in the file MUST NOT start at the first character position
% Lines that start with a % in the first character position will be ignored
% Filenames and directories must be followed by a space (not a tab!!)
%
% Axis system used for input : x fwd,y to port z up. Origin
% placed at midships on the keel.
% The program will move the axis system to the center of mass
%
% ***********************************************
    % Standard data directory
%
      160.93     % length of ship in m
   -3.73   % Ship LCG position fwd of midships
   7.742   % Ship VCG position above keel
   16652.4  % Displacement of ship (m^3)
   736790141.95666     % i44
   19160346751.60949    % i55
   19464567513.94932    % i66
   -18292385.51613      % i46
%
  1    % Number of divisions to split each panel into
%
     0.0   % Initial trim (about CG) (Ship entered in untrimmed state) (in degress)
     %Have to be careful with this.  The mesh may
        % already be trimmed.
     7.467  % Initial draft at midships
%
    7.716     % speed of ship in m/s
%
     2         % Find flat water equilibrium orientation at start (1=no, 2=yes)
     1         % Do surge
     2         % Do sway
     2         % Do heave
     1         % Do roll
     2         % Do pitch
     2         % Do yaw
%
     3000       % Number of time steps for run
     0.5       % Time step
% ********************* Wave Excitation ******************************
     160.93    %  Wavelength
     0.000     % Initial heading of waves relative
```

```
              %to ship's initial heading (degrees)
     0.000    % Amplitude of wave (m)
%
     1          % Linear Froude Krylov (up to equil waterline) (1=no,2=yes)
     1          % Put ship in equil position to calculate FK excitation
% ********************* Rudder/Other Excitation ***********************
%   All excitations are referenced the a body fixed axis system
   1           %  Number of excitations to read
%
%  Excitation  number 1:
   0.00        % Magnitude of Force in x direction
   0.1599881e6    % Magnitude of Force in y direction
   0.00        % Magnitude of Force in z direction
   -80.033     % x position of force application point
   %referenced to input axis system (origin at midships on keel)
   0.00        % y position of force application point
   %referenced to input axis system (origin at midships on keel)
   4.04       % z position of force application point
   %referenced to input axis system (origin at midships on keel)
   10.0         % time (s) when force first applied
   30000.0        % Time (s) for which force applied
   0.00        % Frequency of applied force (using cos[w*(t-start time)] )
   0.0         % Time (s) to ramp up force
   0.0         % Time (s) to ramp doen force
%
% ******************* impulse response data ************************
%    Read in impulse data (as output by gawbw6)
%   Impulse data must be referenced to upright body axes
%       Have the viscous ramp included
%       Have no non-dimensionalisation
%       Not be inverted
%
 2             % Use standard data directory (1=no,2=yes)
 vdampimp.dat   % filename of impulse data
%
% ******************* frequency dependent coefficients *************
 1             % Read in  frequency dependent coefficients
 2             % Use standard data directory (1=no,2=yes)
 vadded.dat   % filename of added mass data
 2             % Use standard data directory (1=no,2=yes)
 vdamping.dat   % filename of damping
% ******************* infinite frequency added hydrodynamic data ***
%     File of linee containing infinite frequencyvalues
 2             % Use standard data directory (1=no,2=yes)
 vinfhyd.dat   % filename of impulse data
% ********************** output file **********************************
 2             % Use standard data directory (1=no,2=yes)
 temp.dat   % filename of impulse data
% ********************** panel information ****************************
 507      % number of panels for HALF the ship
    7.85e+01    6.73e-01    1.22e+01
    8.10e+01    3.33e-16    1.23e+01
    8.16e+01    2.22e-16    1.40e+01
    7.85e+01    1.20e+00    1.40e+01
    7.85e+01    3.22e-01    1.05e+01
    8.05e+01    0.00e+00    1.05e+01
    8.10e+01    3.33e-16    1.23e+01
```

The panel information must be the same as in the UCD file, generated by *Panshp*. The origin is at midships on the keel. Check the Z values : they must all be positive. In order

to obtain the description of the panels in three columns, copy the UCD file, mariner5.inp, to Excel and then delete the first column and copy the coordinates of the points into a text file with an empty first column. You can use this file in Unix and copy the panels to the input file of *Simulat*.

Output file

- temp.dat ; The values of the six displacements versus time and the velocities are listed in a big table, each column is decribed at the beginning of the file.
- temp.inp ; This file (UCD file) contains the coordinates of the points of the mesh, numbered by panel.

3.3 *Simulat 7*

Simulat 7 runs on a **LINUX machine.**

Command ~ philipb/bin/linux/simulat7 -n run1 newallruns.sim

Needed files

- vdampimp.dat; this file contains the impulse response functions, needed to calculate the fluid actions on the ship at each step.
- vinfhyd.dat; this file contains the hydrodynamic data at infinite frequency, also needed to calculate the fluid actions.
- (vdamping.dat)
- (vadded.dat)
- newmesh-panels.sim; This file contains the coordinates of the panels of the mesh (in the same format as required by *Simulat 6*)
- newallruns.sim; Input file, described below.

Description of the input file The file described below is the input file for the simulation, for a constant rudder action of 5° (spiral manoeuvre), in different conditions of waves or with different parameters for the ship. In fact, the input file contains many "sub - input files" and with the command you can choose the one you want to run (run1 only, in the example of command above).

In *Simulat 7*, you have the same possibilities of changes as in *Simulat 6*, but you can furthermore generate a **zigzag manoeuvre**, which has been defined in the source code. An extract of the corresponding input file is shown below.

```
%                          SIMULAT7.C INPUT FILE
% Lines that start with a % in the first character position will be ignored
% Axis system used for input : x fwd,y to port z up.
%  Origin placed at midhips on the keel.
%         The program will move the axis system to the centre of mass

\gname{run1}
================================================================================
```

```
Calm water results Check that the method still give the same
answers as Simulat6
\comline{all}{newallruns.sim}
\comline{5deg_rudder}{newallruns.sim}
\motfilename{run1.dat}
\h{0.5}
\i44{736790141.95666 }
\i55{19160346751.60949}
\i66{19464567513.94932 }
\i46{-18292385.51613}
\endplt
=============================================================================
\gname{run2}
=============================================================================
same as run1, but replace all the values with the new interias
(based on radius of gyration =- 0.24 l etc. etc.
\comline{all}{newallruns.sim}
\comline{5deg_rudder}{newallruns.sim}
\motfilename{run2.dat}
\h{0.5}
\endplt
=============================================================================
\gname{run3}
=============================================================================
Same as run2, but put in waves of 1.0m amplitude, lambda/L=1.0
\comline{run2}{newallruns.sim}
\motfilename{run3.dat}
\h{0.5}
\amp{1.0}
\wavelen{160.93}
\endplt
=============================================================================
\gname{multi_w}
=============================================================================
\multi_w{all}{newallruns.sim}{15} {0.139413} {0.208656} {0.27780}
{0.34706} {0.416231} {0.4854452} {0.554639} {0.62386} {0.693030}
{0.762272} {0.831452} {0.900662} {0.969858} {1.039079} {1.108287}
\endplt
=============================================================================
```

Note For run1, you call the parts all and 5deg-rudder, which are described just after and you then only define the parameters which are different from those in these predefined parts. For example, in run1, it has been decided to use different inertias values. Then for the other runs, you can call the previous run and just change some parameters.

```
============================== all ==================================
\gname{all}
principal dimensions
====================
\lbp{ 160.93 }        length between perpendiculars of ship (m)
\lcg{ -3.73 }         lcg of ship forward of midships
\vcg{7.742}vcg above the keel
\disp{ 16652.4} displacement(m^3)
inertias
========
inertias are measured about cofg. These are the old inertias as
used in the thesis i44{ 736790141.95666 } i55{ 19160346751.60949}
i66{ 19464567513.94932 } i46{-18292385.51613 }. Now use the new
inertias, i55 and i66 based on a radius of gyration = 0.241, i44
```

```
based on radius of gyration = 0.3b \i44{ 0.8247e9  }
\i55{2.5462e10 }
\i66{ 2.5462e10  }
\i46{ 0.000  }

initial condition of ship
=========================
\initial_trim{0.0}     initial trim (about cg) (ship entered in
                        untrimmed state) (in degress) have to be careful
                        with this.  the mesh is already trimmed by -0.434
                        degrees (i.e. by the stern)  (degrees)
\initial_draft{7.467 }  initial draft at midships  (m)
\speed{7.716 }         forward speed of ship  (m/s)
\use_itequil{ 2 }       find flat water equilibrium orientation at
                        start (1=no, 2=yes)
simulation setup
================
\divis{1}          number of divisions to split each panel into
\do_mots{1}   do surge motions (1=no, 2=yes)
        {2}   do sway  motions (1=no, 2=yes)
        {2}   do heave motions (1=no, 2=yes)
        {2}   do roll  motions (1=no, 2=yes)
        {2}   do pitch motions (1=no, 2=yes)
        {2}   do yaw   motions (1=no, 2=yes)
\ntime{3000}             number of time steps to use in simulation
\h{0.20}                  time step (s)
wave excitation
===============
\wavelen{160.93}    wavelength (m)  will be overridden
omega{0.1}wave frequency - will be overridden
\headin{0.0}initial
heading of waves relative to ship's initial heading (degrees)
\amp{0.0}         amplitude of wave (m)
\linearfk{1} linear froude
krylov (up to equil waterline) (1=no,2=yes)

have withdrawn the eq_calcfs option as it doen't work
eq_calcfs{1}put ship in equil position to calculate fk excitation

impulse response data
=====================
    read in imuplse data (as output by gawbw6)
        impulse data must be referenced to upright body axes
        have the viscous ramp included
        have no non-dimensionalisation
        not be inverted
\impfilename{vdampimp.dat} filename of impulse data
\infhydfilename{vinfhyd.dat} infinite frequency added mass and
damping

frequency dependent coefficients
================================
use frequency dependent coefficients rather than use convolution
integrals
omega{10.0} freq_coeffs{padded.dat}
            {pdamping.dat}

\comline{panels}{newmesh_panels.sim}
\endplt
=============================================================
```

```
\gname{5deg_rudder} rudder and other excitations
=================================================================
all excitations are referenced the a body fixed axis system.
Rudder angle of 5 degrees : \excite{ 0.00} magnitude of force in x
direction
       { 0.1599881e6 }     magnitude of force in y direction
       {0.00}          magnitude of force in z direction
       {-80.033}       x position of force application point
                        referenced to input axis system
                        (origin at midships on keel)
       {0.00}          y position of force application point
                        referenced to input axis system
                        (origin at midships on keel)
       {3.735}          z position of force application point
                        referenced to input axis system
                        (origin at midships on keel)
       {10.0}          time (s) when force first applied
       {30000.0}       time (s) for which force applied
       {0.00}          frequency of applied force (using cos[w*(t-start time)] )
       {0.0}           time (s) to ramp up force
       {0.0}           time (s) to ramp down force
\endplt
```

Finally, here is an example for a run with a zigzag manoeuvre.

```
=================================================================
\gname{run1}
=================================================================
% Run using simulat7 -n run1 allruns.sim
% Quick test of zig zag manoeuvre
%   Calm water 10-10 zigzag manoeuvre.
\comline{all}{newallruns1.sim}
\motfilename{run1.dat}
\zigzag{1833328.607}   y delta full scale
       {-139888504.3}     n delta full scale
       {15}          time in seconds to start
       {10}     rude ang
       {10}     head ang
\ntime{2000}
\h{0.5}
\endplt
=================================================================
```

Output file

- run.dat ; The values of the six displacements versus time and the velocities are listed in a big table, each column is decribed at the beginning of the file. The output file is the same as in *Simulat 6*.

3.4 Results

In order to use the output files temp.dat or run.dat, generated by *Simulat 6* or *Simulat 7*, open the data file in Excel, defining the columns well. Do not forget to check the cells, in order to verify the format. If there are cells without numbers, but ###, just change the cell format to "scientific".

Then you can, for example, plot the path of the ship, using the graphic tools of Excel (i.e. plot *sway* versus *surge*).

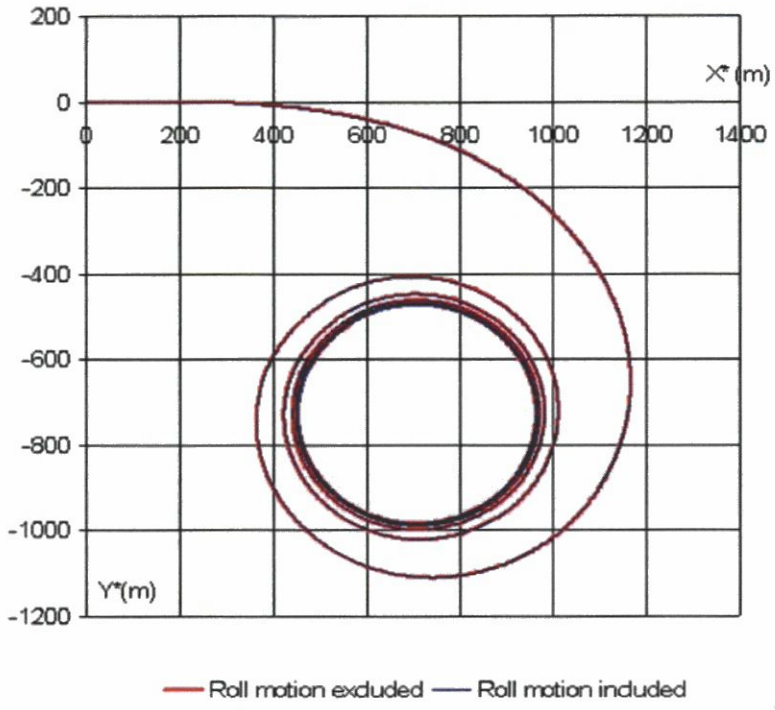

Figure 3.1: Example of a track obtained with the use of two different temp.dat files (*Simulat6*), in Excel.

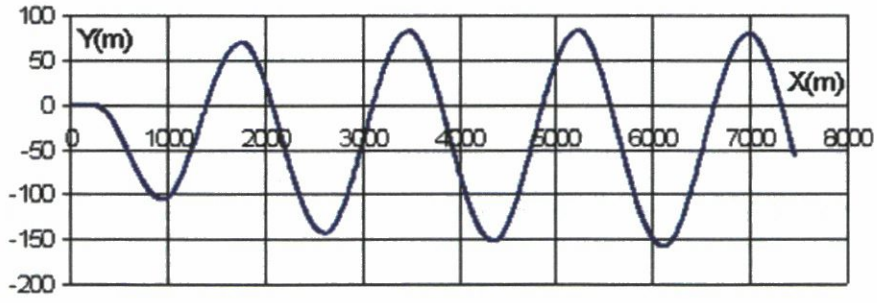

Figure 3.2: Example of a track of a zigzag manoeuvre obtained with the use of a run.dat file (*Simulat7*), in Excel

4 Conclusion

Modifying the parameters of the ship and of the waves, we can thus obtain significant results for the prediction of the manoeuvring of a ship in a seaway in different conditions, and study each of the six degrees of freedom. For more details about the uses of the *Simulat* program, see [9] and relevant papers [10].

In April 2005, these different programs have been used with the same hypothesis and parameters are those used by Bailey, 1999 [9] and the results obtained have been checked against those obtained by Bailey, 1999 [9]. They show short agreement. Thus the programs have been verified.

Figures

Note : In several figures concerning impulse response functions and oscillatory derivatives, the $\widetilde{Y}$ have been omitted, the notation Y has been used instead, when no confusion was possible.

Chapter 2 : Description and verification of the software - *Mariner* vessel

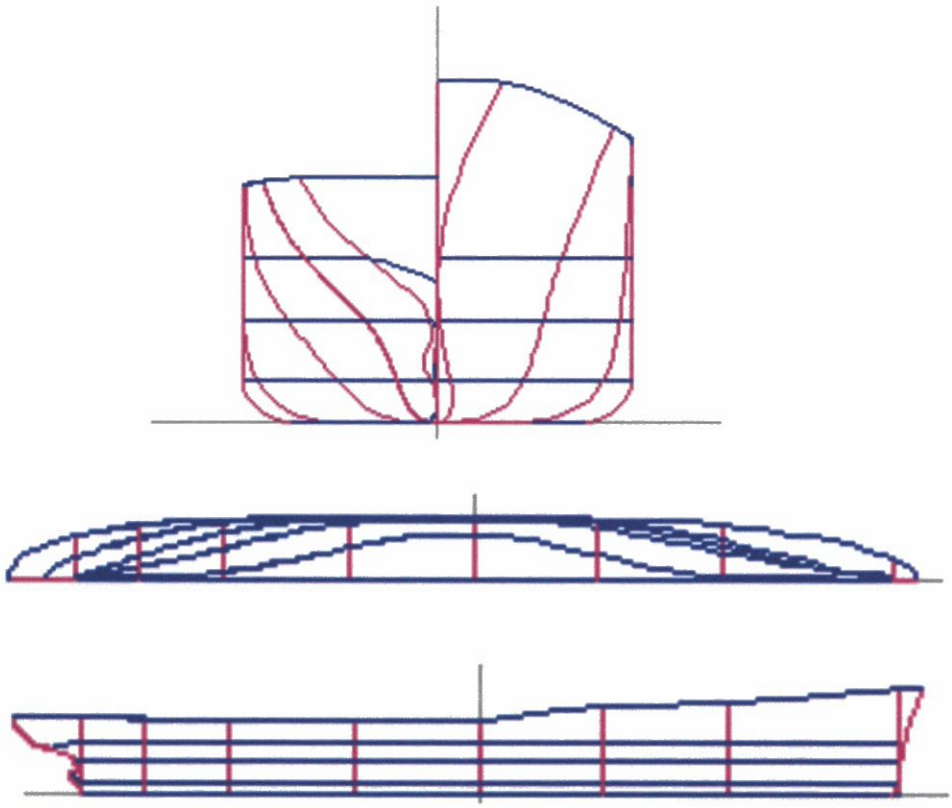

Figure 1: Representation of a *Mariner* ship by *Shipshape*, different views

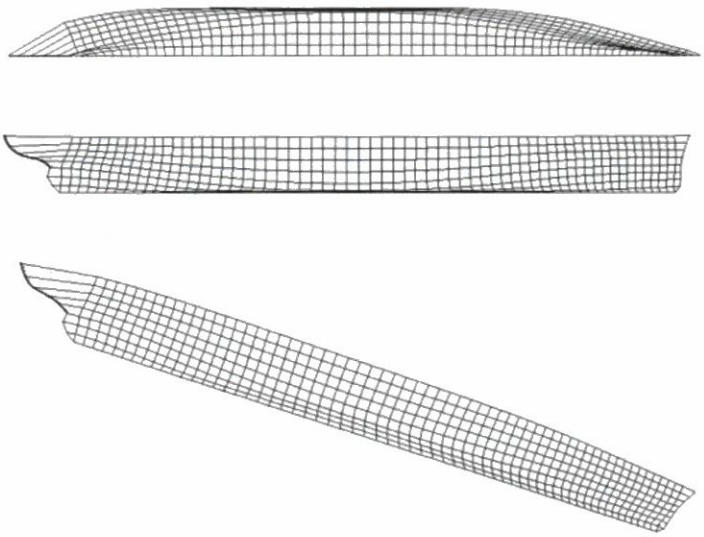

Figure 2: Discretisation of one side of a *Mariner* Ship ; number of panels around each section : 8 - Aspect ratio : 1, resulting in 507 panels for one side

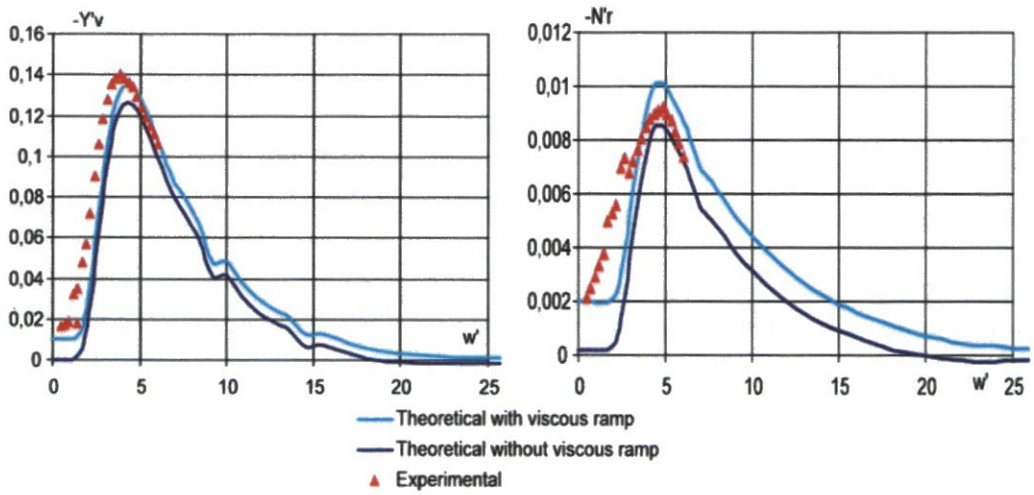

Figure 3: Theoretical and experimental hydrodynamic data for a *Mariner* ship with and without a viscous ramp included in the theoretical prediction of the damping - coefficient $-Y'_v$ and $-N'_r$ versus ω', standard non-dimensionalisation

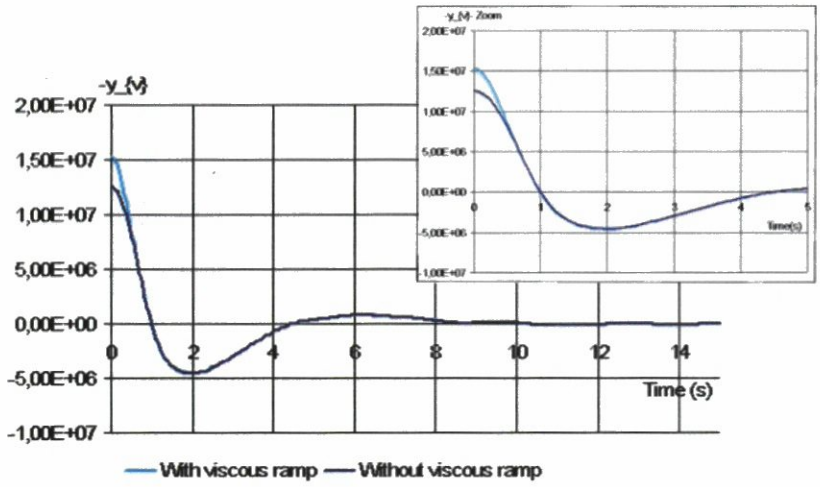

Figure 4: Impulse response function $-y_v(\tau)$ calculated using $\tilde{Y}_v(\omega)$, with and without a viscous ramp added to the frequency data - full scale ; Zoom for τ near 0

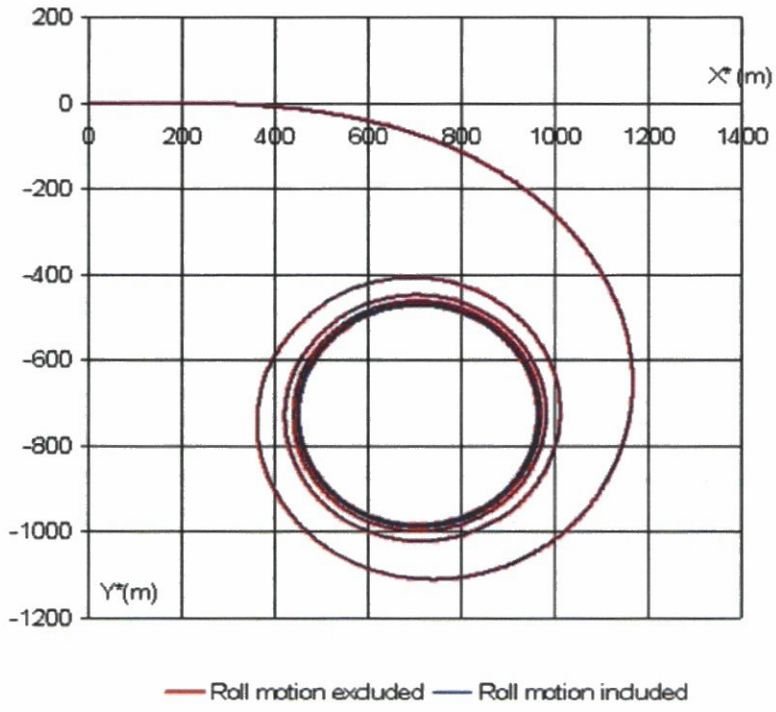

Figure 5: Circle manoeuvre of a *Mariner* ship in calm water - *Simulat* prediction

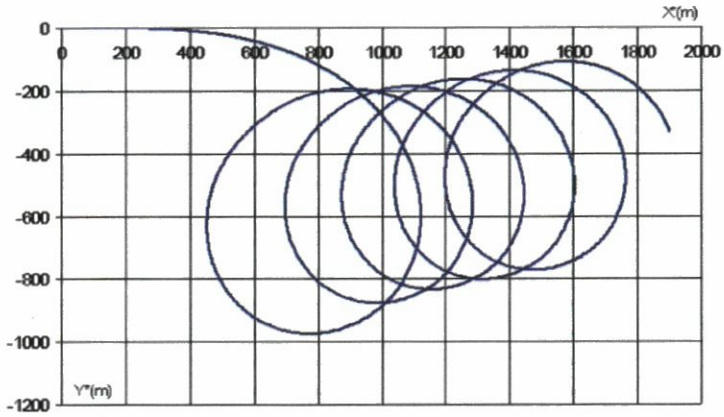

Figure 6: Circle manoeuvre of a *Mariner* ship in waves (1m, $\lambda/L = 1$), roll motion excluded - *Simulat* prediction

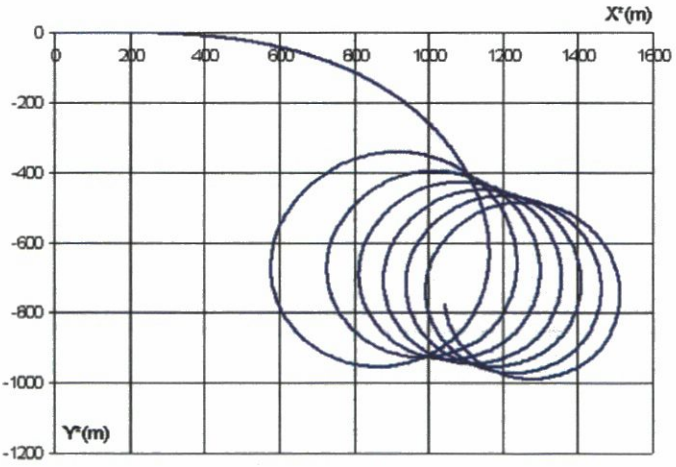

Figure 7: Circle manoeuvre of a Mariner ship in waves (1m, $\lambda/L = 0.5$), roll motion excluded - *Simulat* prediction

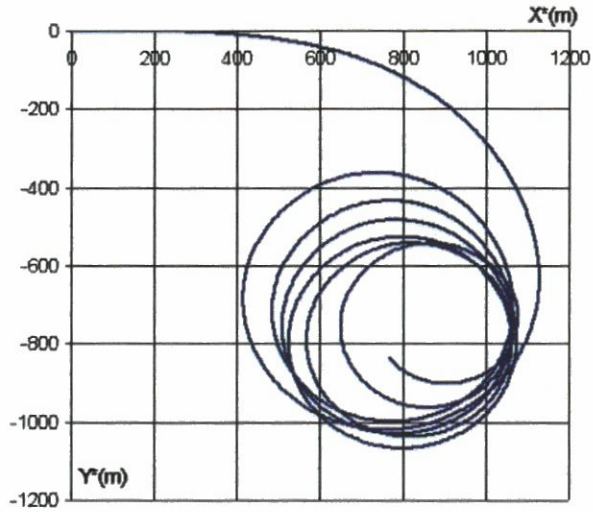

Figure 8: Circle manoeuvre of a *Mariner* ship in waves (1m, $\lambda/L = 0.25$), roll motion excluded - *Simulat* prediction

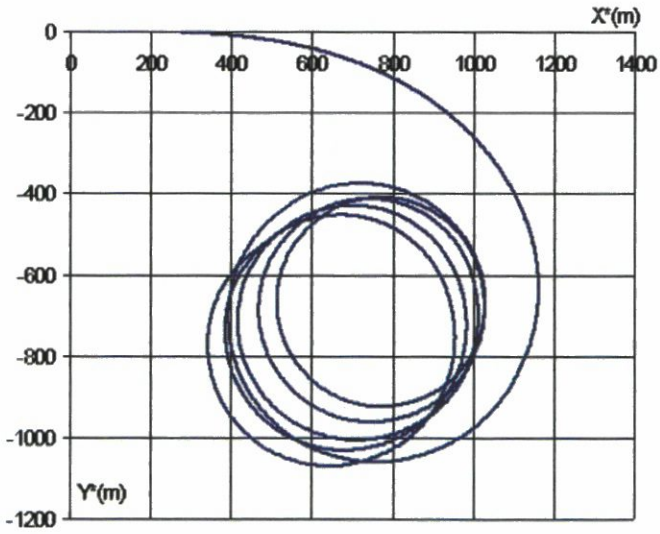

Figure 9: Circle manoeuvre of a *Mariner* ship in waves (1m, $\lambda/L = 0.1$), roll motion excluded - *Simulat* prediction

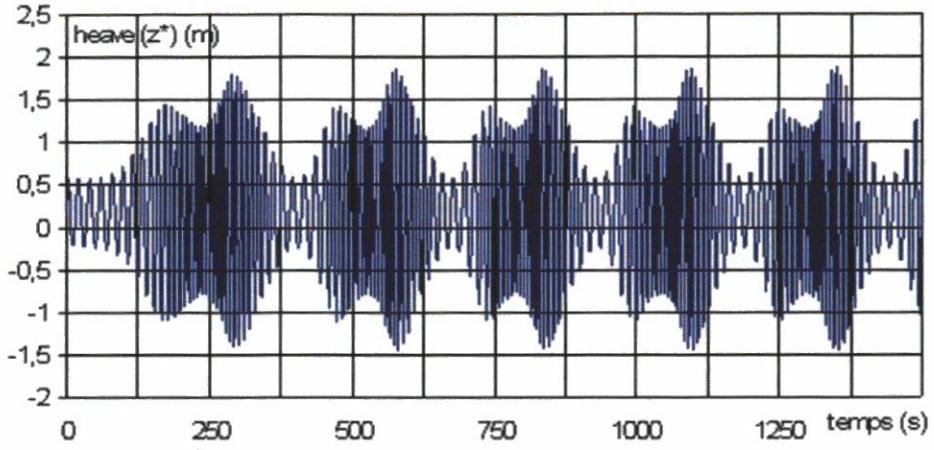

Figure 10: Heave response of a *Mariner* ship during a circle manoeuvre in waves (1m, $\lambda/L = 1$), roll motion excluded - *Simulat* prediction

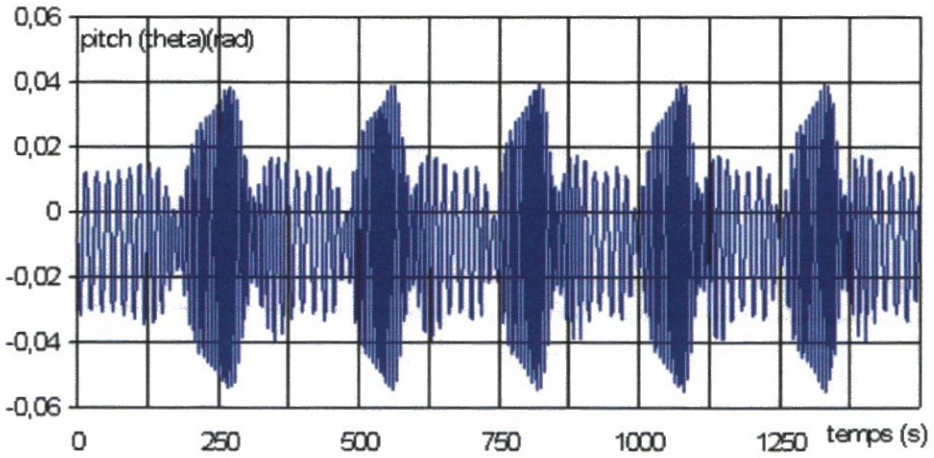

Figure 11: Pitch (degrees) response of a *Mariner* ship during a circle manoeuvre in waves (1m, $\lambda/L = 1$), roll motion excluded - *Simulat* prediction

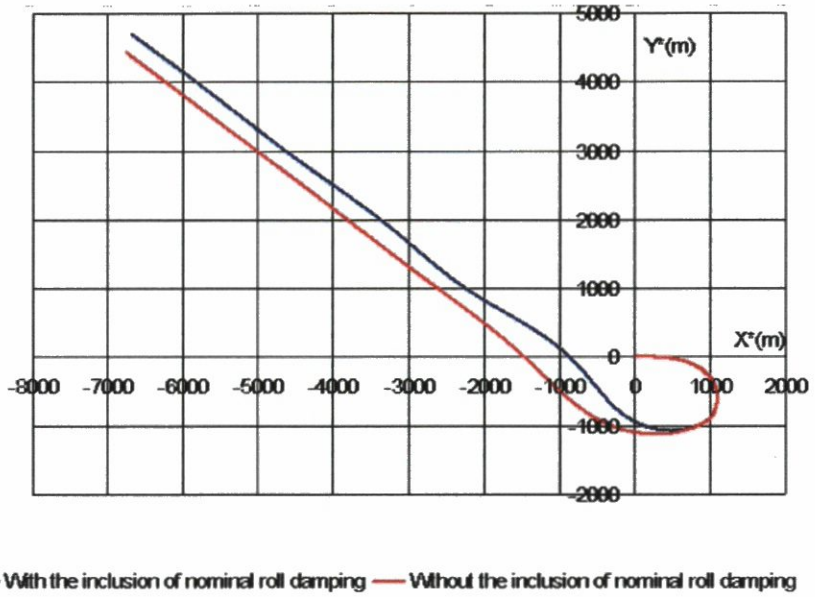

Figure 12: Predicted course of a *Mariner* ship in waves (1m, $\lambda/L = 0.1$), roll motion included, with and without the inclusion of a nominal roll damping - *Simulat* prediction

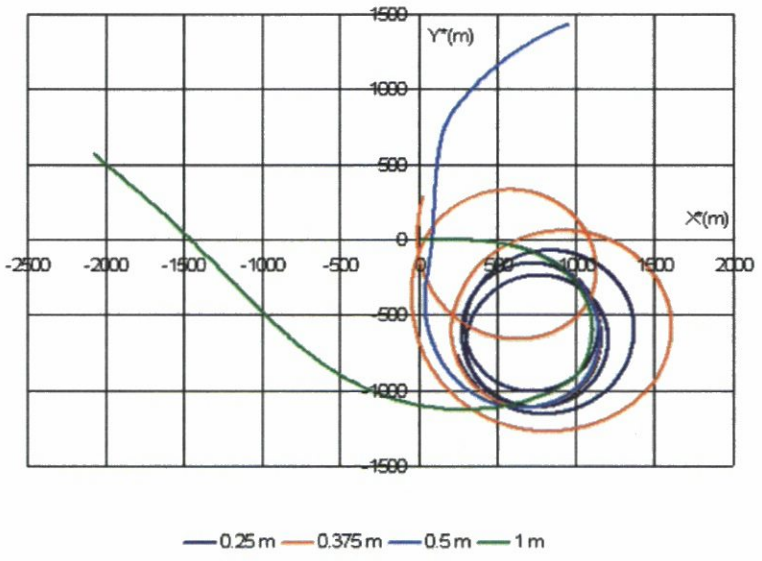

Figure 13: Predicted course of a *Mariner* ship in waves (various wave heights, $\lambda/L = 0.1$), roll motion included, without the inclusion of a nominal roll damping - *Simulat* prediction

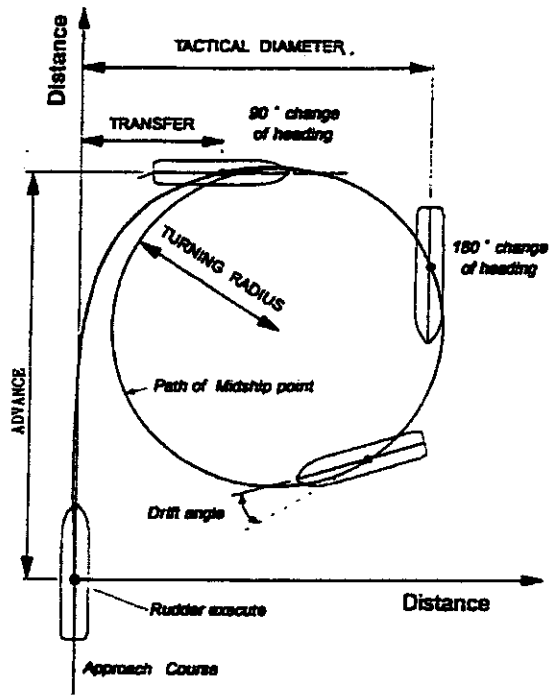

Figure 14: Turning circle test [5]

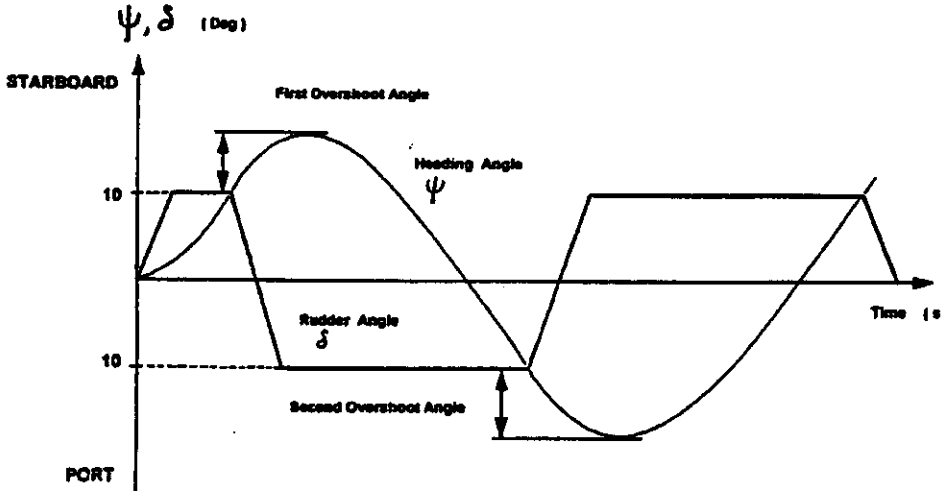

Figure 15: 10°/10° zigzag test [5]

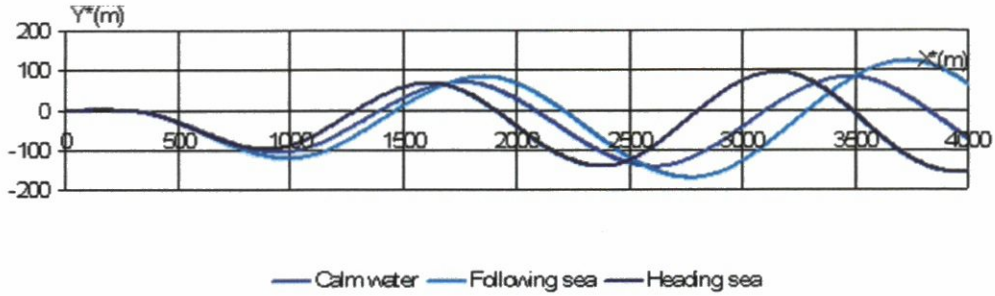

Figure 16: 10°/10° zigzag manoeuvres of a *Mariner* ship in calm water, following seas and head seas (1m, $\lambda/L = 1$), as predicted by *Simulat*.

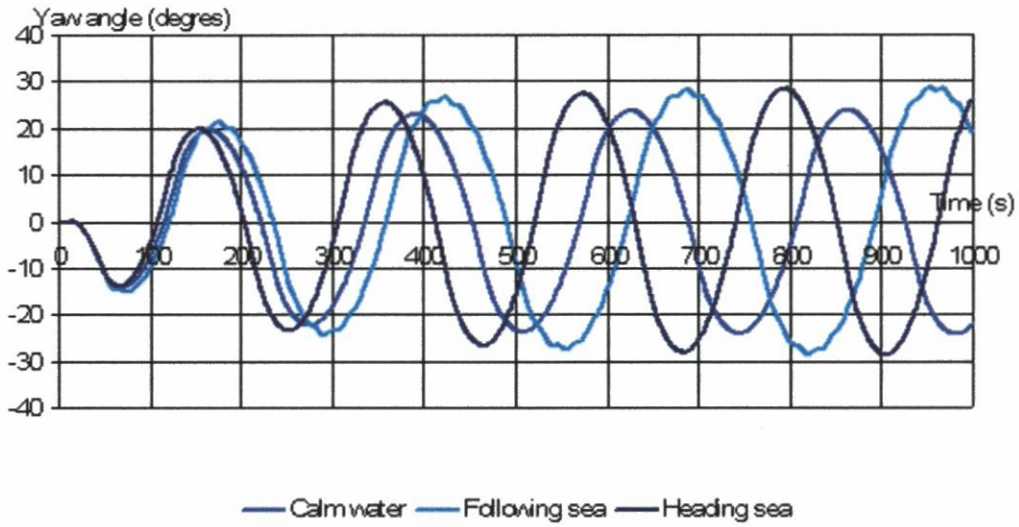

Figure 17: Yaw angle (°) during 10°/10° zigzag manoeuvres of a *Mariner* ship in calm water and in waves, as predicted by *Simulat*

Chapter 3 : First predictions for another vessel : British Bombardier

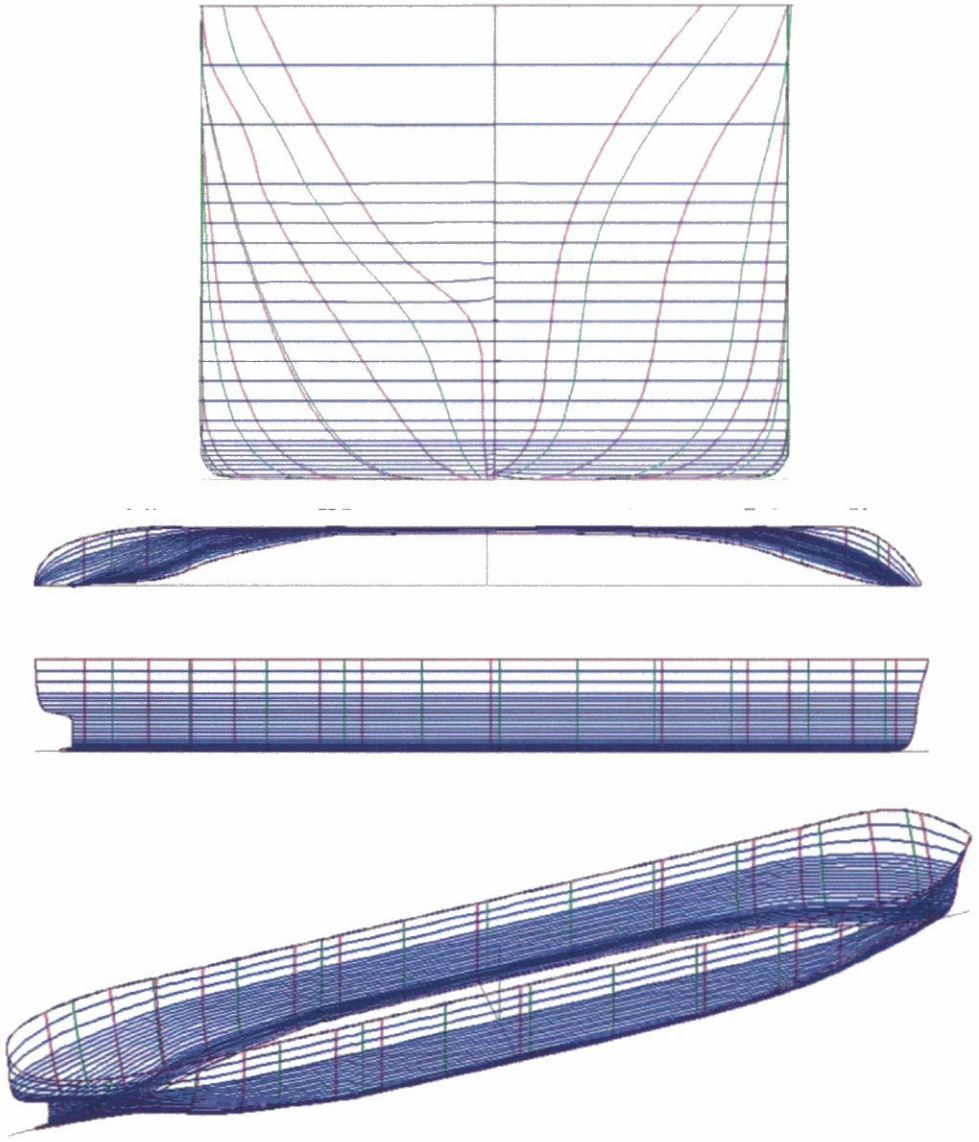

Figure 18: Representation of *British Bombardier* by *Shipshape*, different views

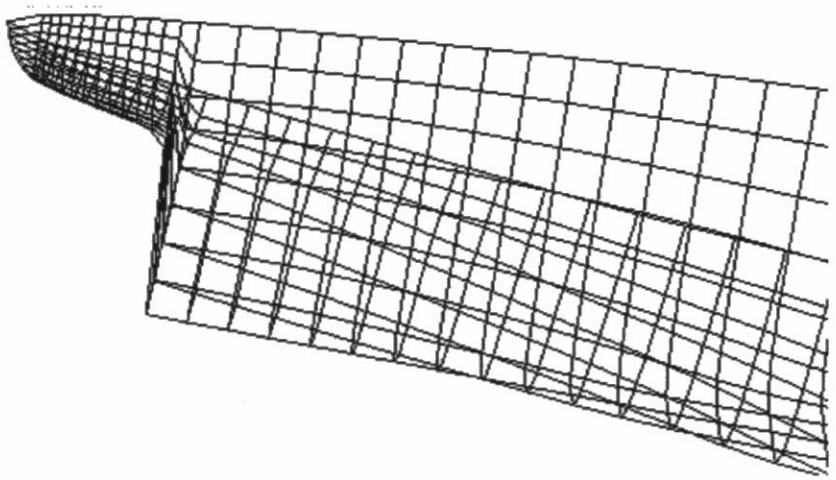

Figure 19: *Panshp* - Discretisation of the stern of the *British Bombardier* up to the water-line, with small panels

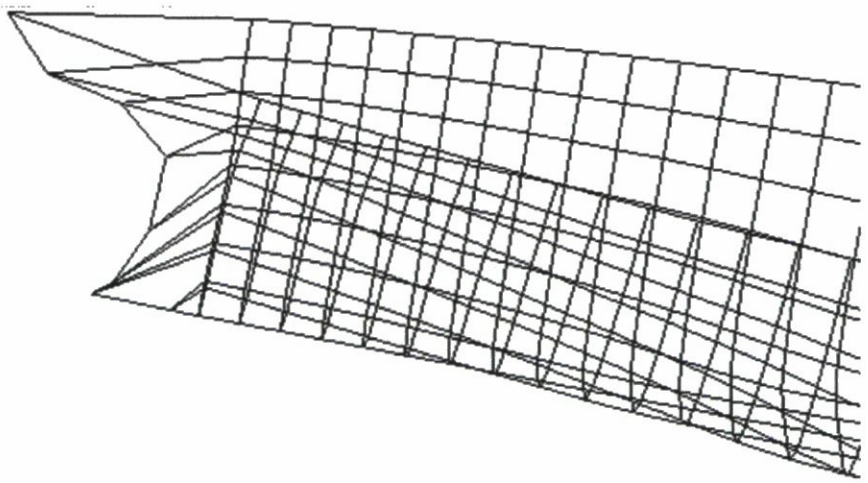

Figure 20: *Panshp* - Discretisation of the stern of the *British Bombardier* up to the water-line, with large panels

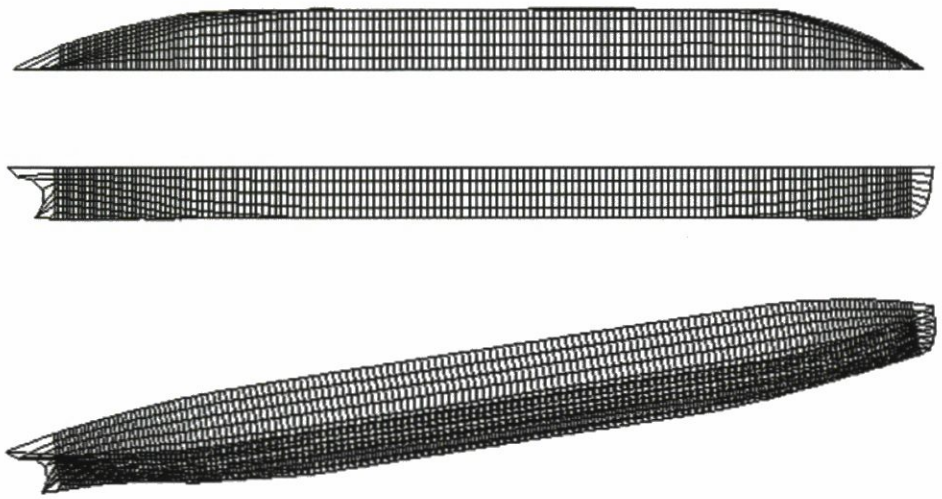

Figure 21: Discretisation of one side of the *British Bombardier* up to the water-line; number of panels around each section : 8 - Aspect ratio : 0,5, resulting in 2400 panels for one side. At bottom, view of the both sides of the discretisation

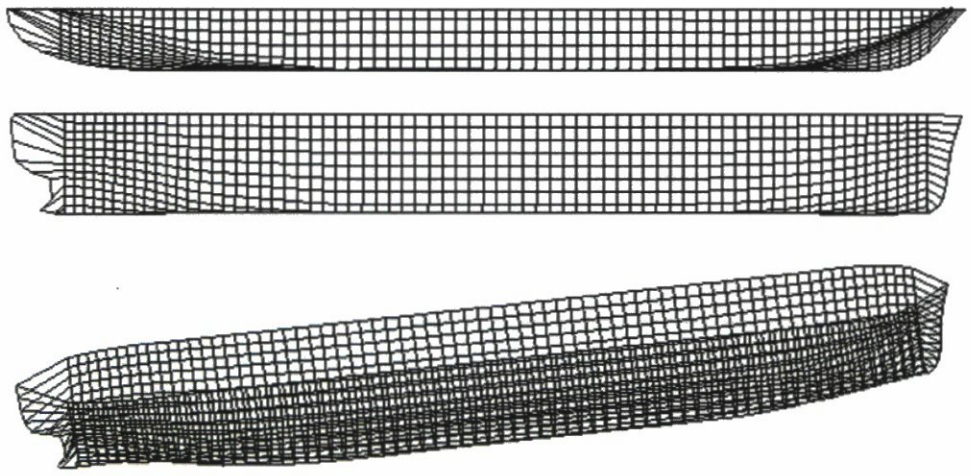

Figure 22: Discretisation of one side of the *British Bombardier* up to the deck; number of panels around each section : 12 - Aspect ratio : 1, resulting in 876 panels for one side. At bottom, view of the both sides of the discretisation

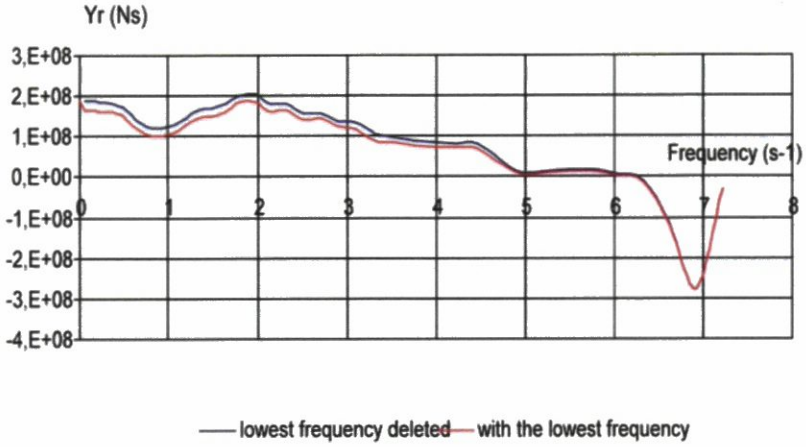

Figure 23: Theoretical hydrodynamical data $\widetilde{Y}_r(\omega)$ for the *British Bombardier* predicted for a range of frequencies between 0,0008 and 2,4 s-1, with and without the lowest frequency - full scale

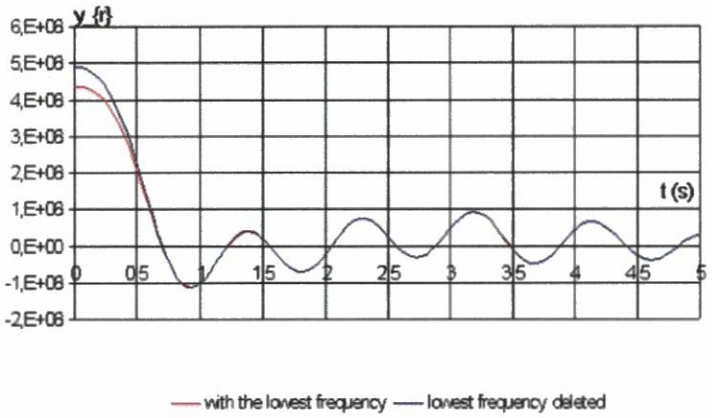

Figure 24: Impulse response function $y_r(\tau)$ calculated using $\tilde{Y}_r(\omega_e)$, with and without the lowest frequency in the calculation of hydrodynamical data - full scale

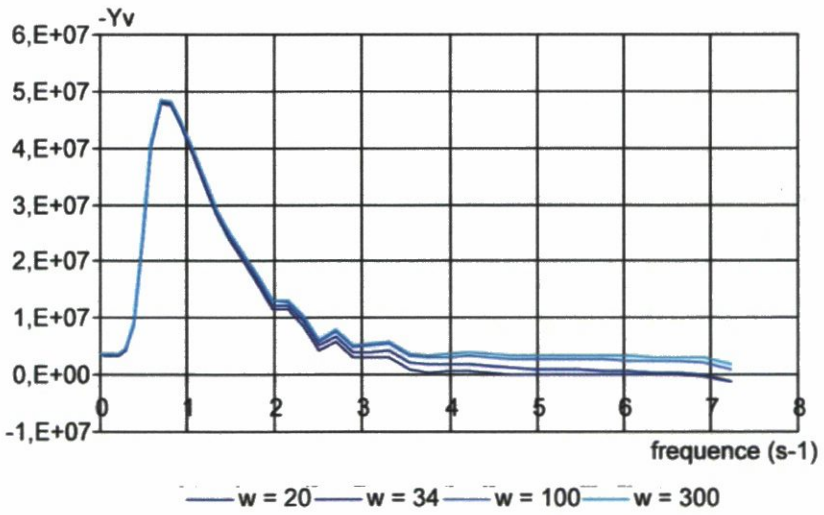

Figure 25: Theoretical hydrodynamical data $-\widetilde{Y}_v(\omega_e)$ for the *British Bombardier* predicted for different values of the non-dimensionalised frequency at which the viscous ramp ends - full scale

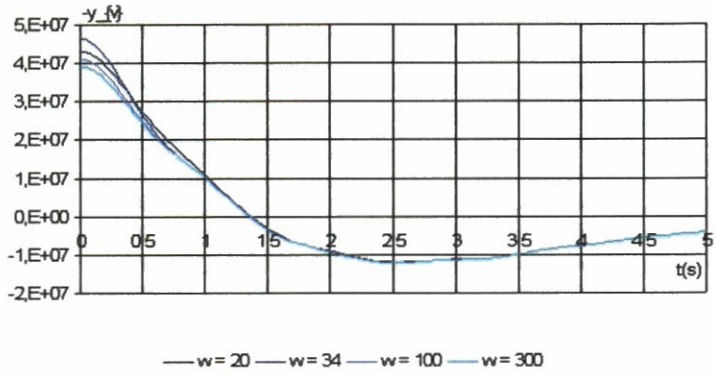

Figure 26: Impulse response function $-y_v(\tau)$ calculated using $\tilde{Y}_v(\omega)$, predicted for different values of the non-dimensionalised frequency at which the viscous ramp ends - full scale

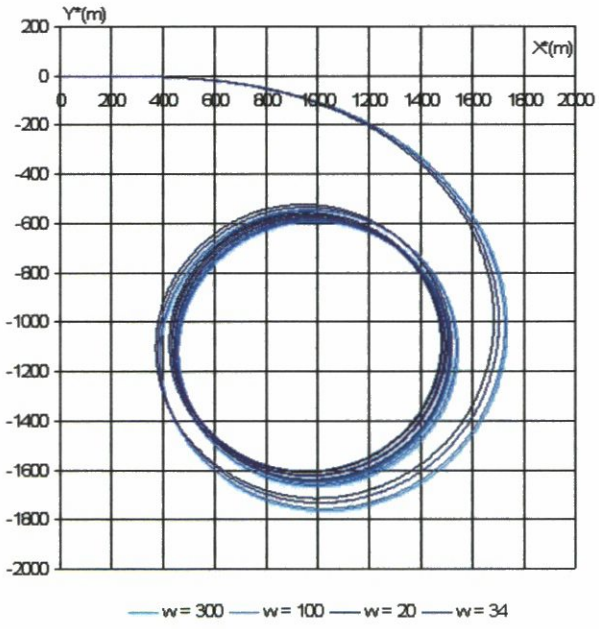

Figure 27: Circle manoeuvre (5° rudder angle) of the *British Bombardier* in calm water for different viscous ramp (different upper frequencies) included in the calculation of the impulse response functions - *Simulat* prediction

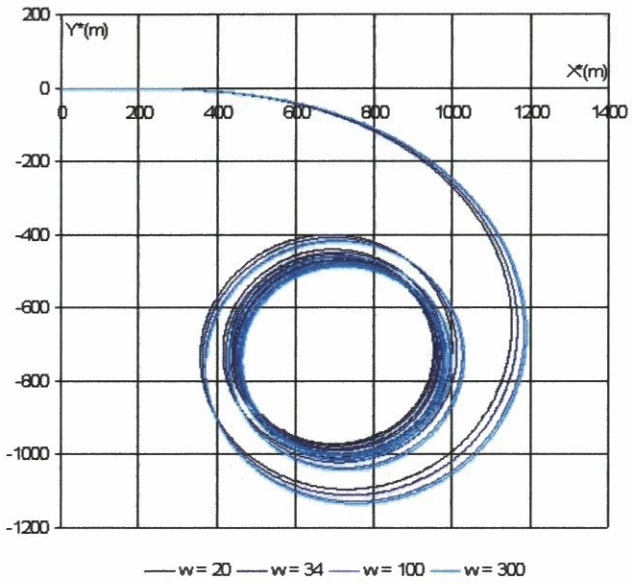

Figure 28: Circle manoeuvre (5° rudder angle) of a *Mariner* ship in calm water for different viscous ramp (different upper frequencies) included in the calculation of the impulse response functions - *Simulat* prediction

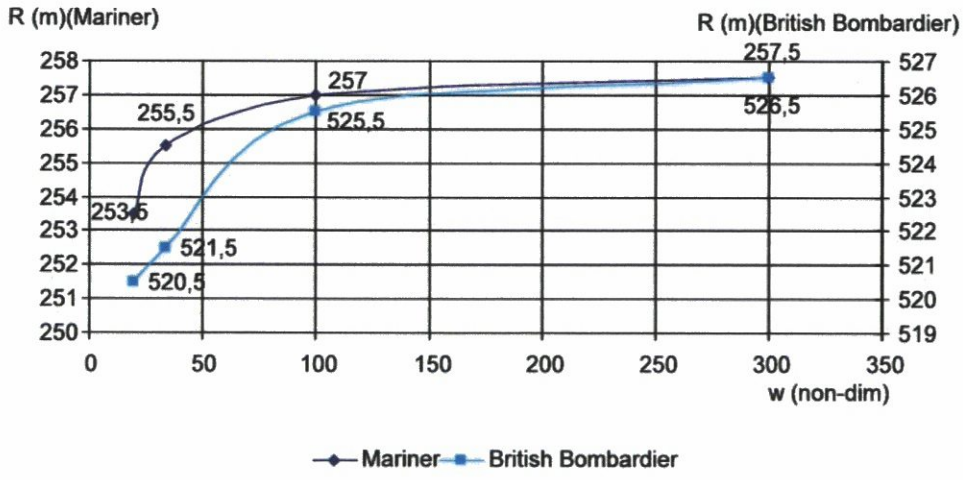

Figure 29: *Simulat* predicted radius of a 5° rudder angle circle manoeuvre versus ω, upper frequency of the viscous ramp, for a *Mariner* and the *British Bombardier*

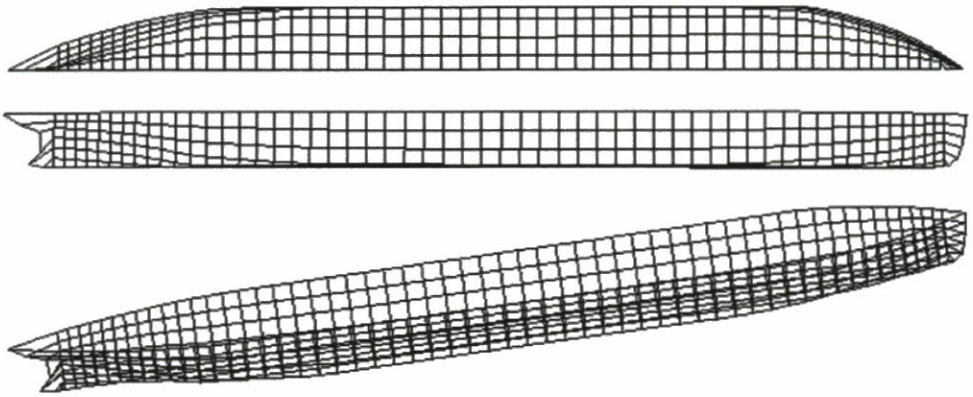

Figure 30: Discretisation of one side of the *British Bombardier* up to the water-line; number of panels around each section : 6 - Aspect ratio : 1, resulting in 684 panels for one side. At bottom, view of the both sides of the discretisation

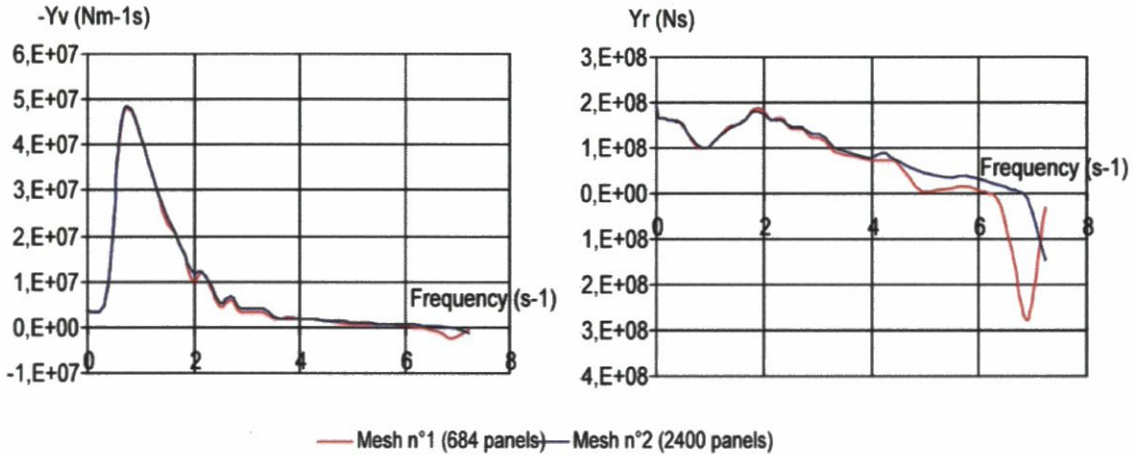

Figure 31: Theoretical hydrodynamical data $-\widetilde{Y}_v(\omega_e)$ and $\widetilde{Y}_r(\omega_e)$ predicted with two different meshes - full scale

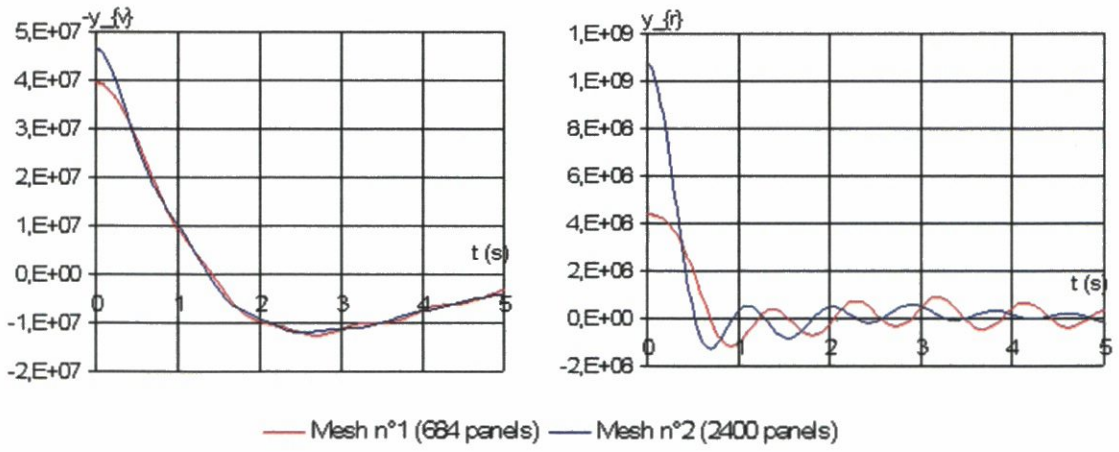

Figure 32: Impulse response function $-y_v(\tau)$ and $y_r(\tau)$ calculated using $\tilde{Y}_v(\omega)$ and $\tilde{Y}_r(\omega)$ predicted with two different meshes - full scale

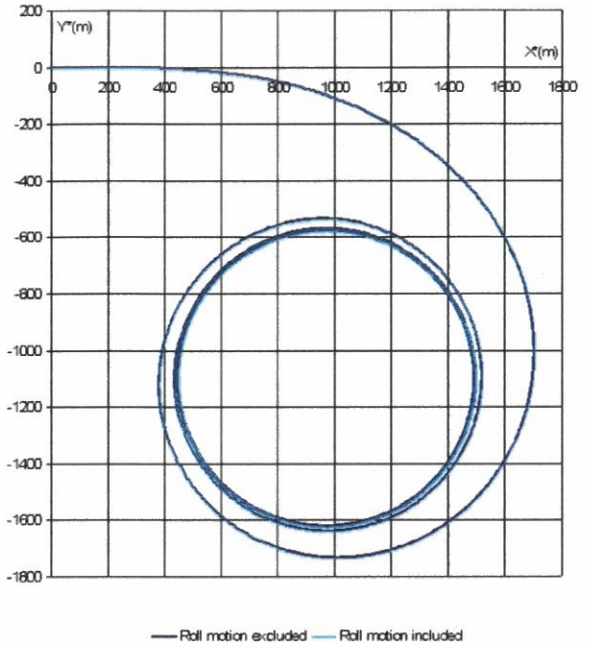

Figure 33: Circle manoeuvre of the *British Bombardier* in calm water for 5° rudder angle - *Simulat* prediction

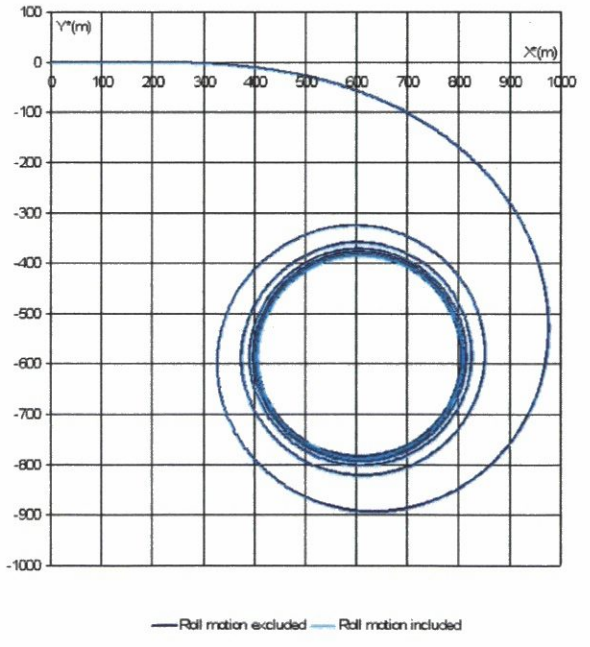

Figure 34: Circle manoeuvre of the *British Bombardier* in calm water for 15° rudder angle - *Simulat* prediction

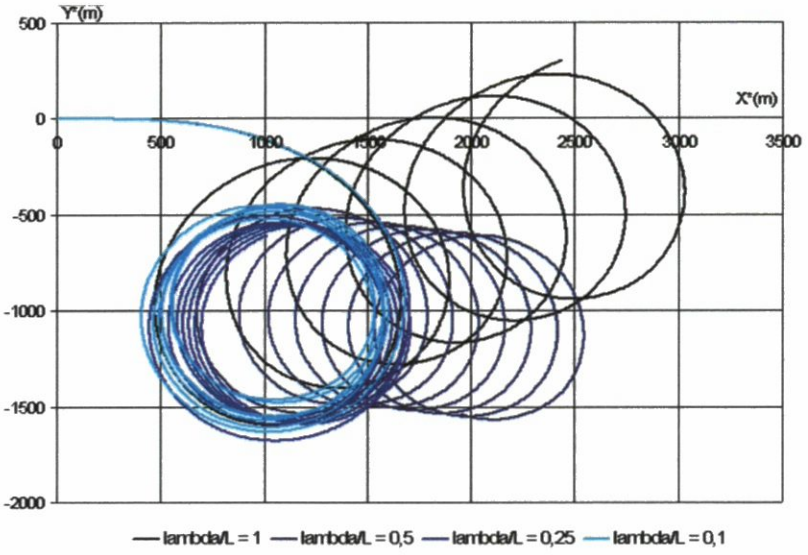

Figure 35: Circle manoeuvres of the *British Bombardier* in following waves (1m, $\lambda/L = 1, 0.5, 0.25, 0.1$), roll motion excluded - *Simulat* prediction

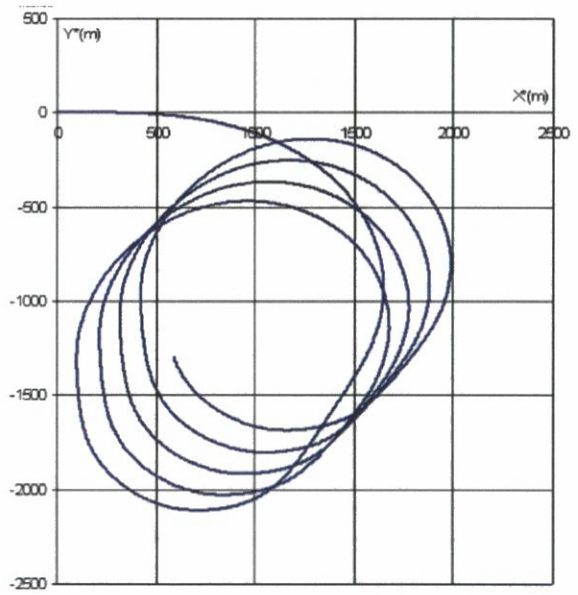

Figure 36: Circle manoeuvre of the *British Bombardier* in following waves (1m, $\lambda/L = 1$), roll motion included - *Simulat* prediction

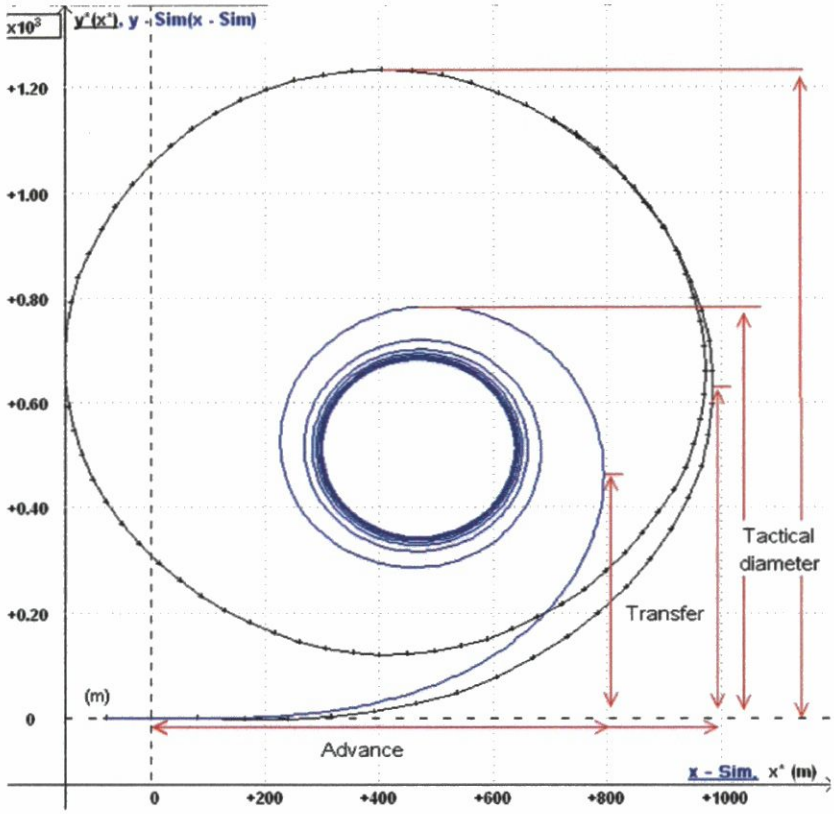

Figure 37: Circle manoeuvre of the *British Bombardier* in calm water for -19° rudder angle - *Simulat* prediction and full manoeuvring trial (taken from [6])

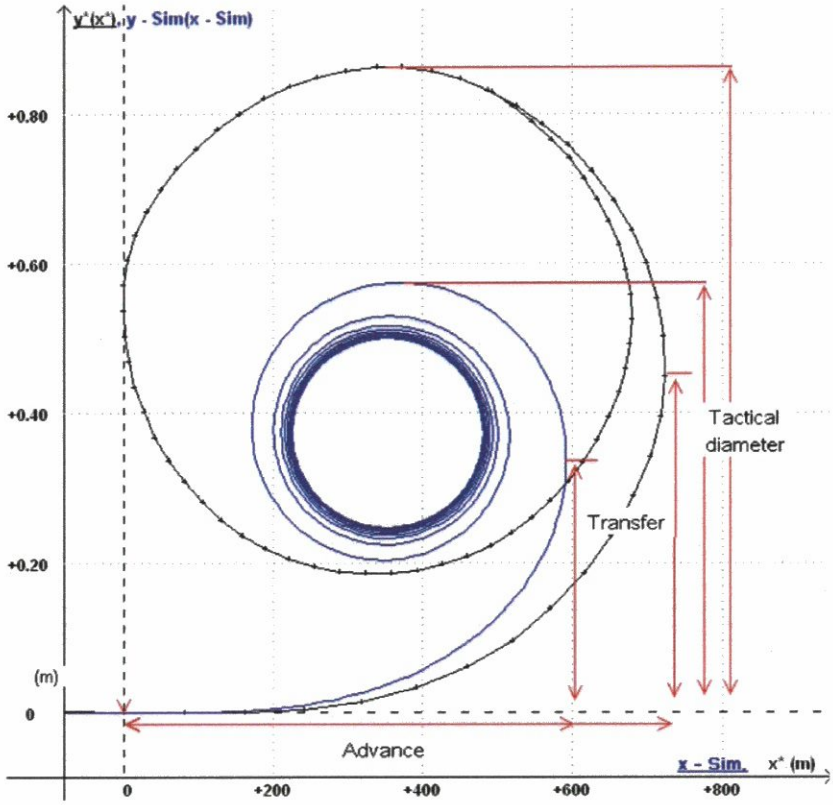

Figure 38: Circle manoeuvre of the *British Bombardier* in calm water for -34° rudder angle - *Simulat* prediction and full-scale manoeuvring trial (taken from [6])

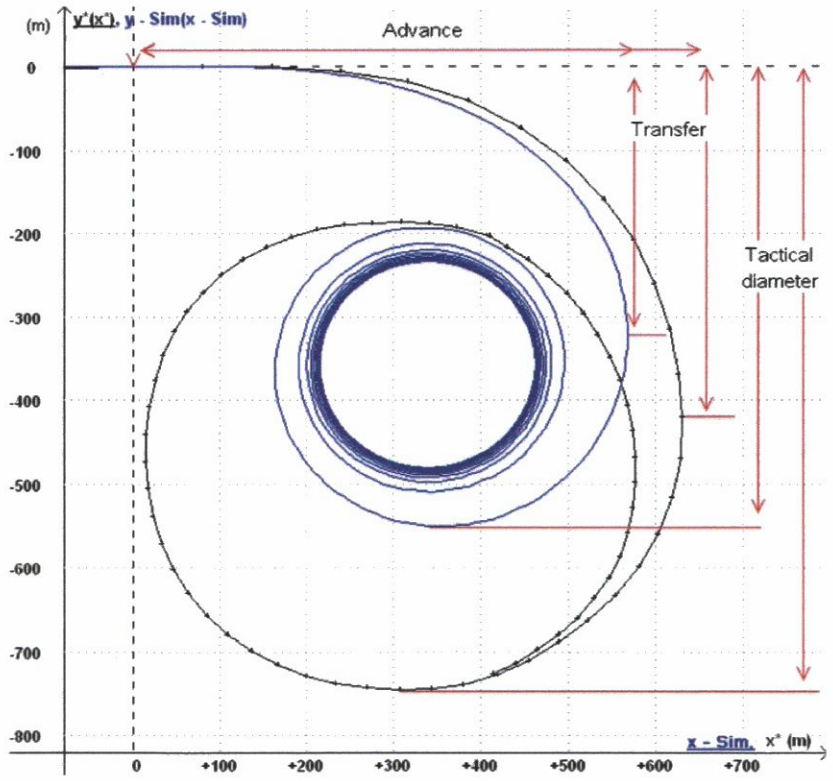

Figure 39: Circle manoeuvre of the *British Bombardier* in calm water for 37° rudder angle - *Simulat* prediction and full-scale manoeuvring trial (taken from [6])

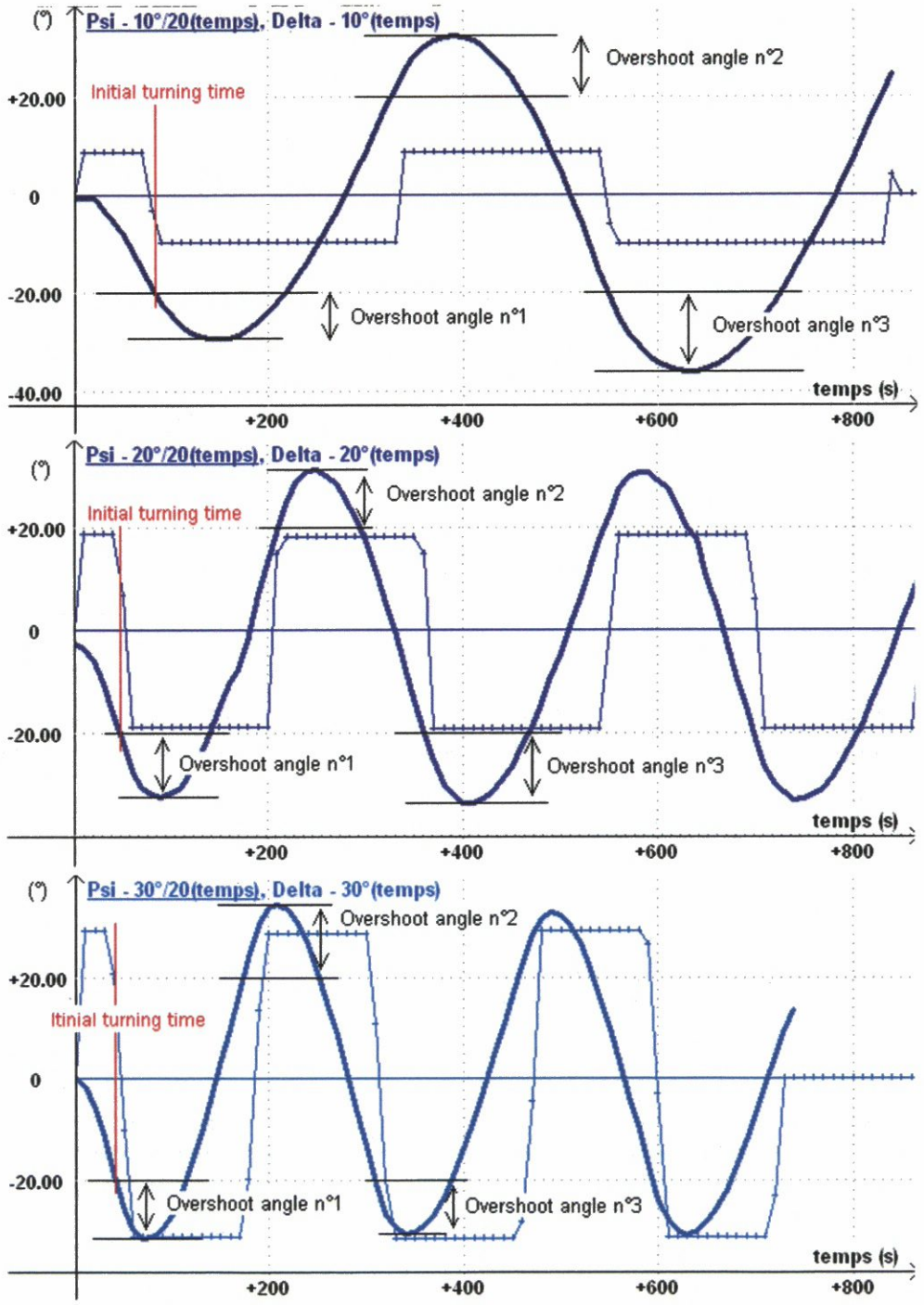

Figure 40: Ship's heading and rudder angle during zigzag manoeuvres of the *British Bombardier* in calm water (10°/20°, 20°/20°, 30°/20°) at 100 rpm - Full-scale manoeuvring trial (taken from [6])

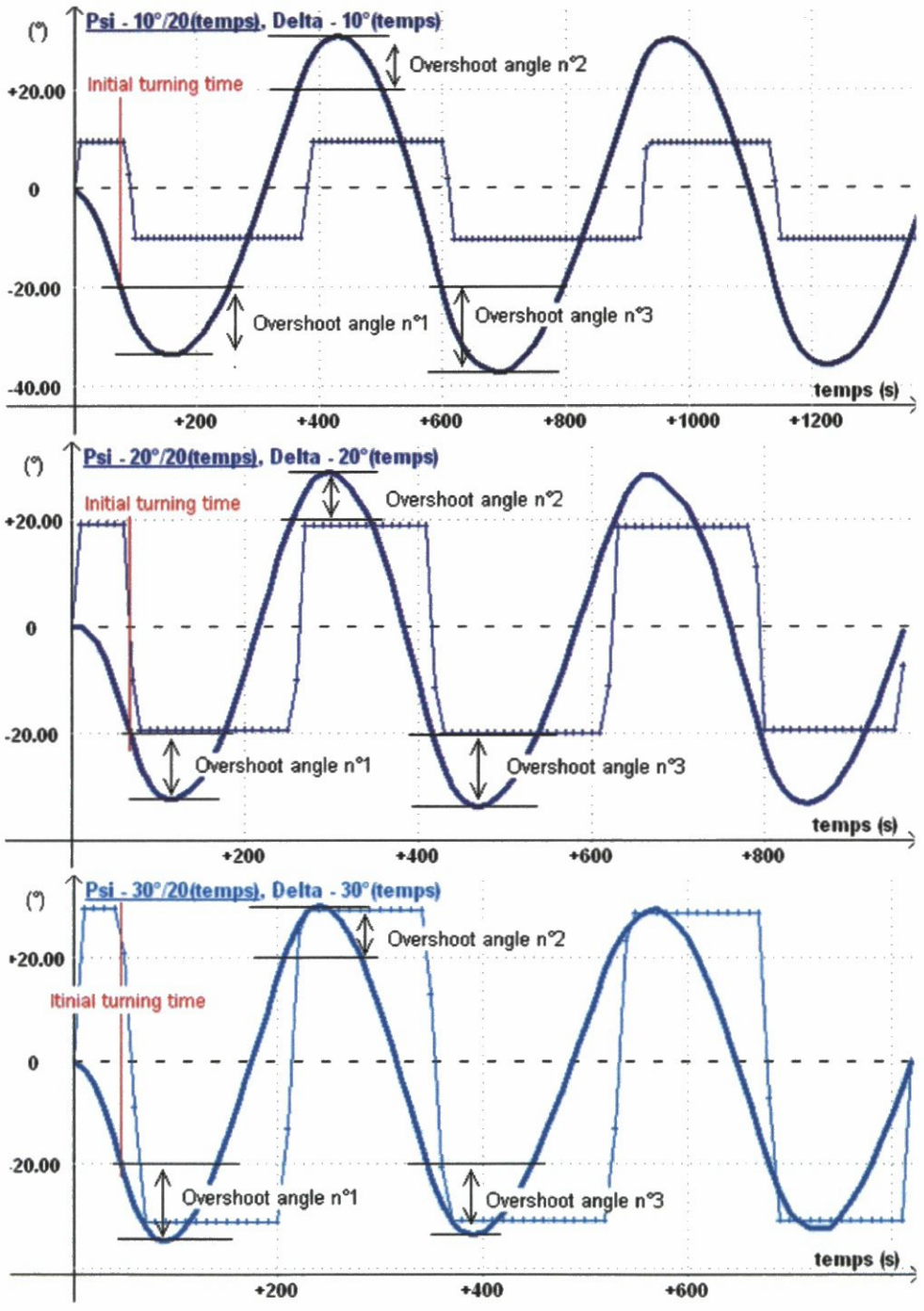

Figure 41: Ship's heading and rudder angle during zigzag manoeuvres of the *British Bombardier* in calm water (10°/20°, 20°/20°, 30°/20°) at 85 rpm - Full-scale manoeuvring trial (taken from [6])

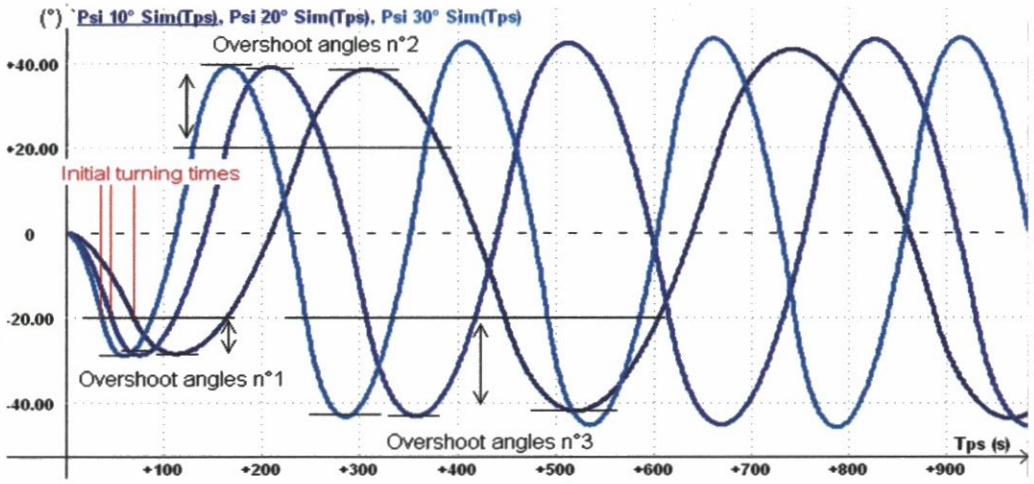

Figure 42: Ship's heading during zigzag manoeuvres of the *British Bombardier* in calm water (10°/20°, 20°/20°, 30°/20°) at 100 rpm - *Simulat* predictions

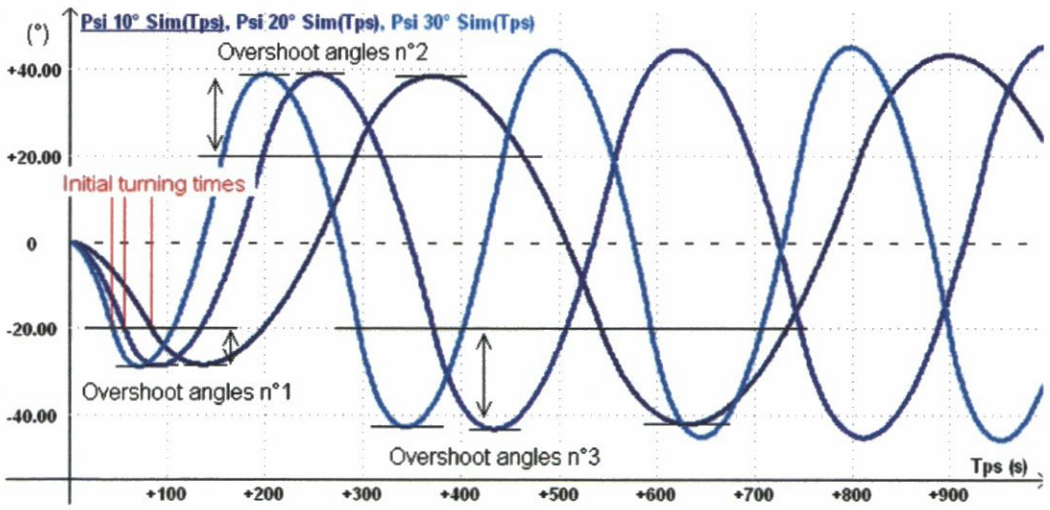

Figure 43: Ship's heading during zigzag manoeuvres of the *British Bombardier* in calm water (10°/20°, 20°/20°, 30°/20°) at 85 rpm - *Simulat* predictions

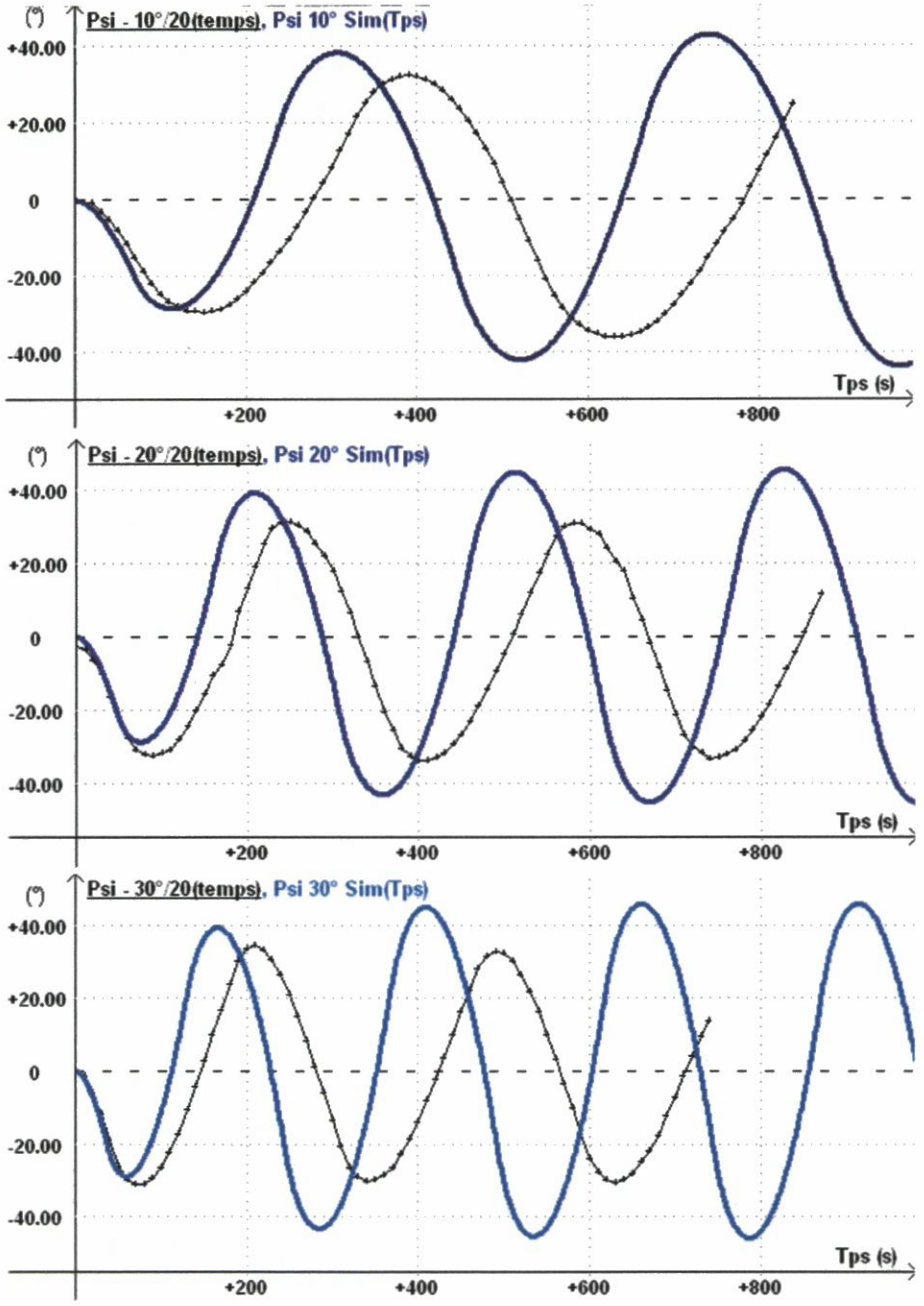

Figure 44: Ship's heading during zigzag manoeuvres of the *British Bombardier* in calm water (10°/20°, 20°/20°, 30°/20°) at 100 rpm - *Simulat* predictions (Psi °- Sim) and full-scale manoeuvring trials (Psi °/20°) (taken from [6])

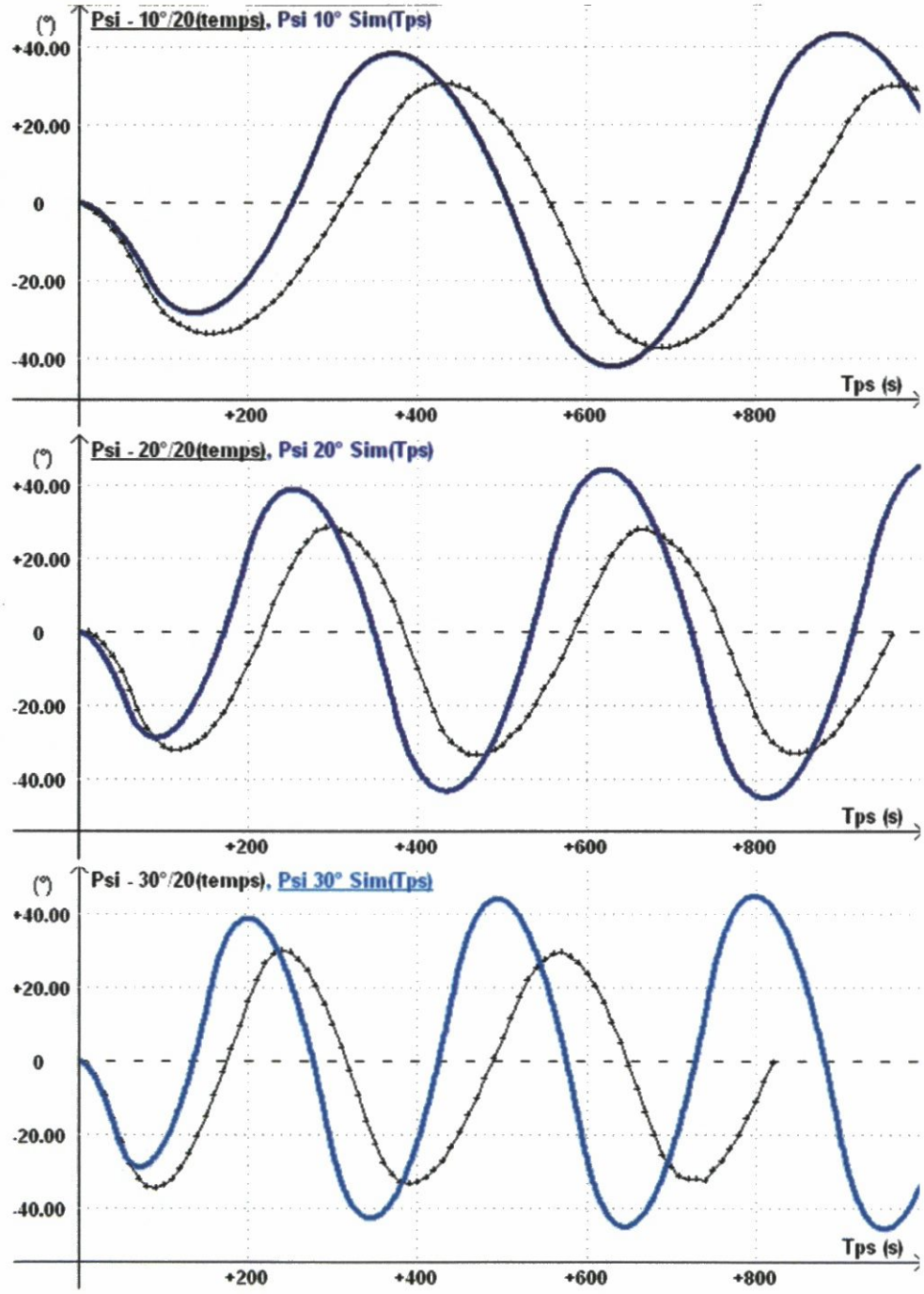

Figure 45: Ship's heading during zigzag manoeuvres of the *British Bombardier* in calm water (10°/20°, 20°/20°, 30°/20°) at 85 rpm - *Simulat* predictions (Psi °- Sim) and full-scale manoeuvring trials (Psi °/20°) (taken from [6])

Chapter 5 : Investigation of the influence of waves on ship manoeuvrability

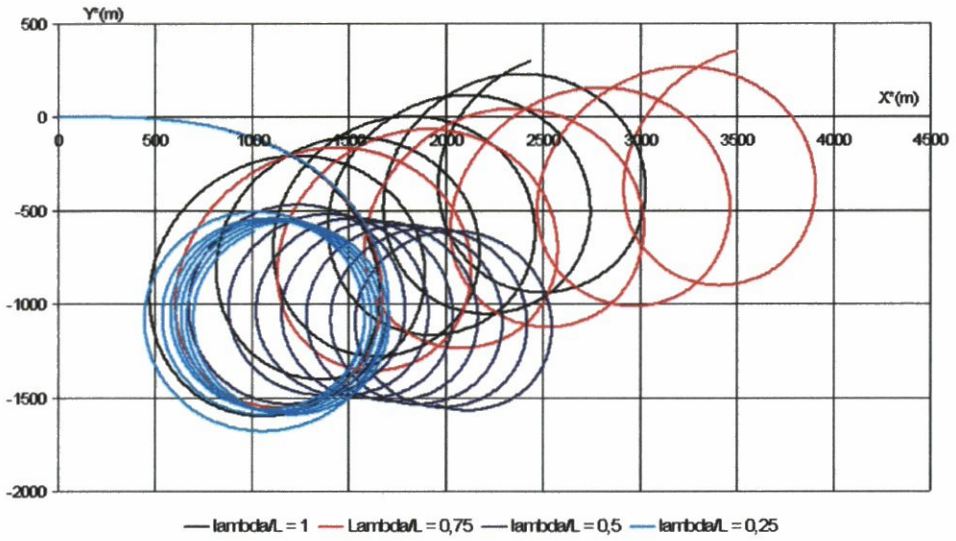

Figure 46: Circle manoeuvres of the *British Bombardier* in following waves (1m, $\lambda/L = 1, 0.75, 0.5, 0.25$), roll motion excluded, 5° rudder angle - *Simulat* prediction

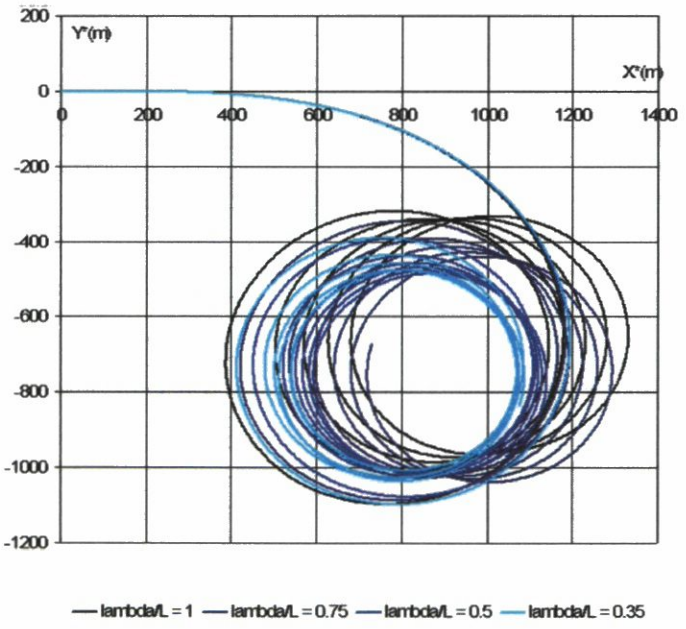

Figure 47: Circle manoeuvres of the *British Bombardier* in following waves (1m, $\lambda/L = 1, 0.75, 0.5, 0.35$), roll motion excluded, 10° rudder angle - *Simulat* prediction

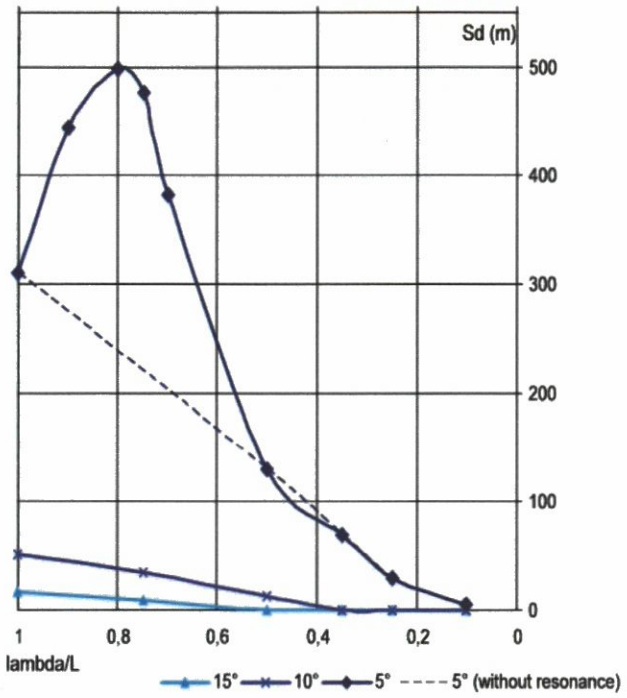

Figure 48: Drifting distance as function of the wavelength (for different rudder angles), during circle manoeuvres in following seas for the *British Bombardier*, as predicted by *Simulat*

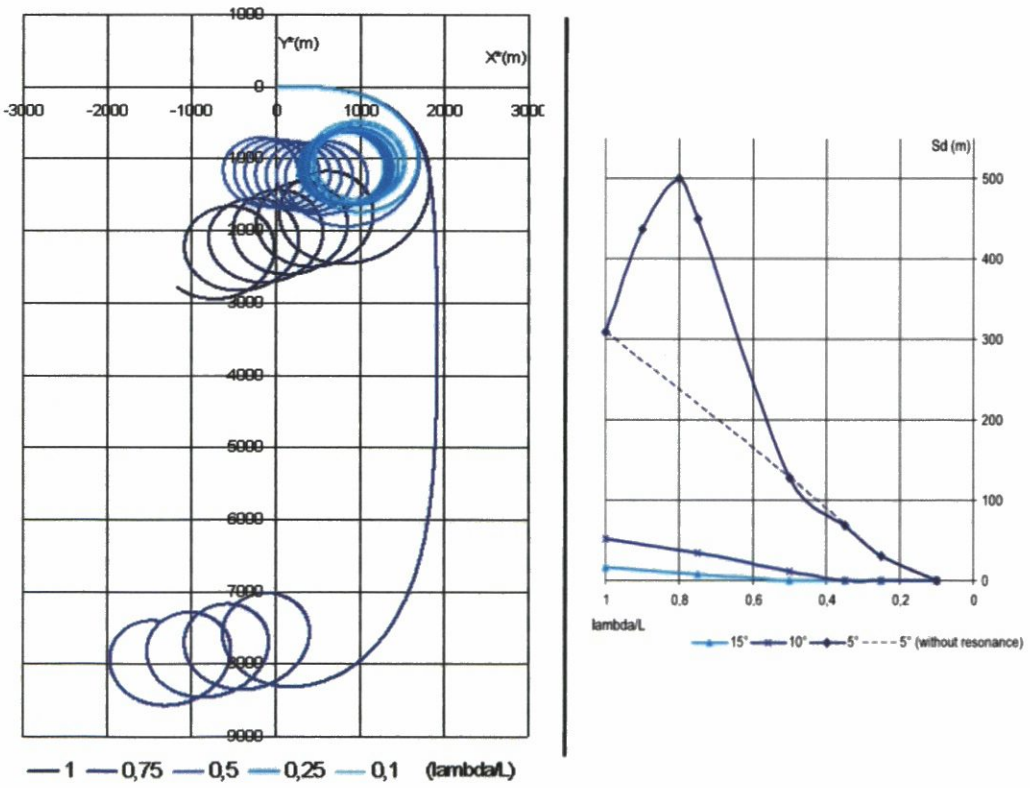

Figure 49: Circle manoeuvres of the *British Bombardier* in head waves (1m, $\lambda/L = 1, 0.75, 0.5, 0.35$), roll motion excluded, 5° rudder angle - *Simulat* prediction (left) and Drifting distance as function of the wavelength (for different rudder angles), during circle manoeuvres in head seas for the *British Bombardier*, as predicted by *Simulat* (right)

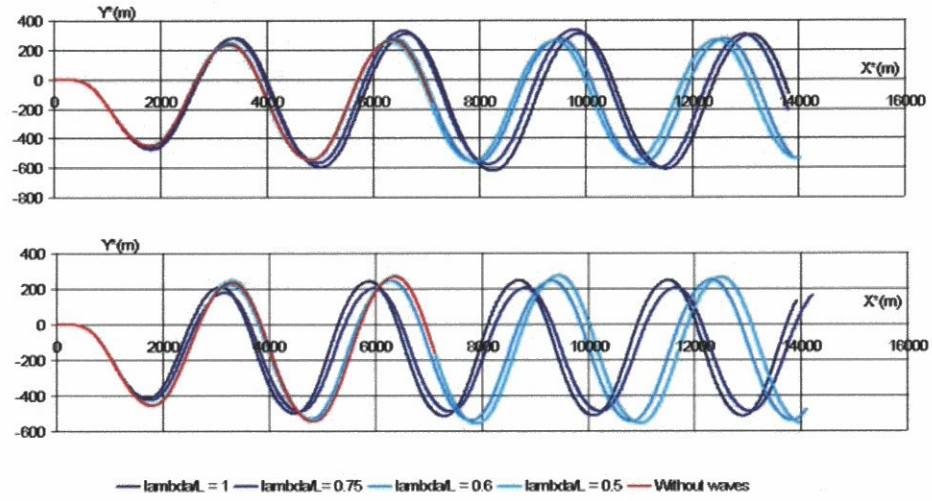

Figure 50: 10°/20° zigzag manoeuvres of the *British Bombardier* in calm water, following seas (up) and head seas (down)(1m, different wave lengths), as predicted by *Simulat*.

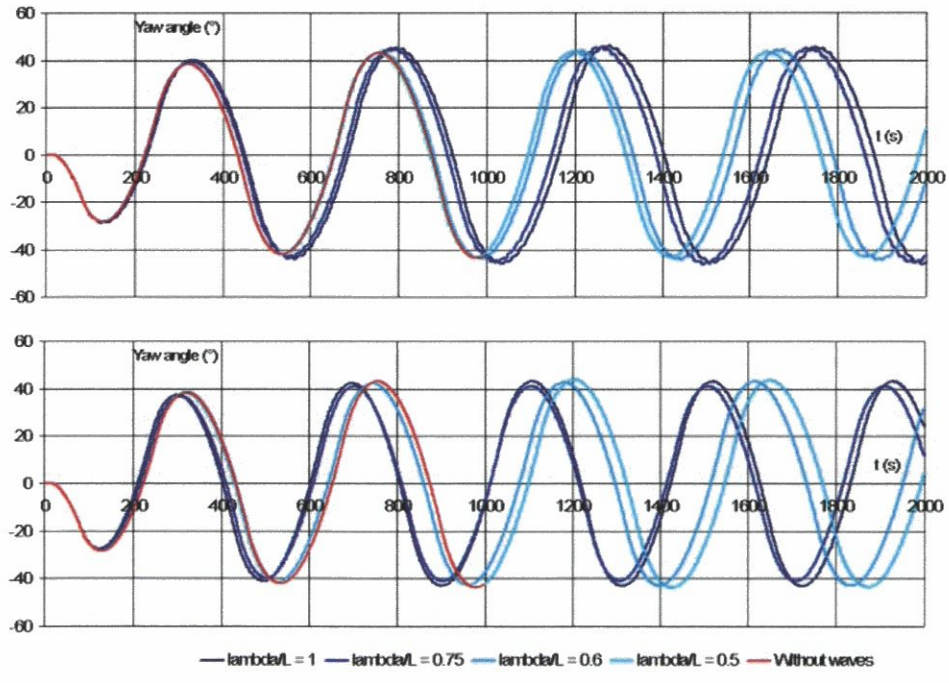

Figure 51: Yaw angle (°) during 10°/20° zigzag manoeuvres of the *British Bombardier* in calm water, following seas (up) and head seas (down)(1m, different wave lengths), as predicted by *Simulat*.

Chapter 6 : Further Investigations

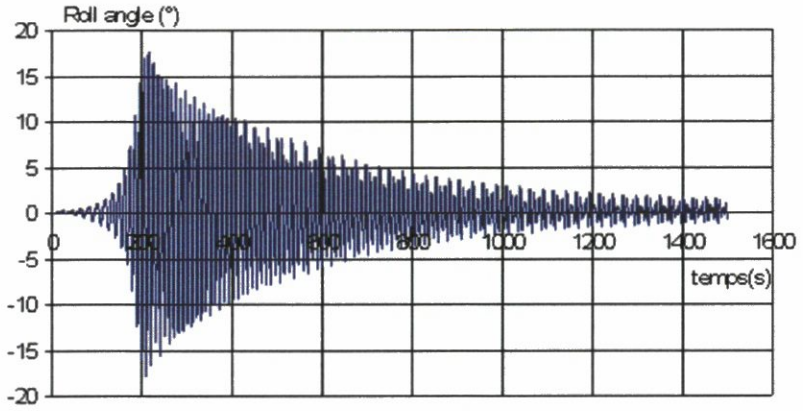

Figure 52: Roll response of a *Mariner* ship during a 5° rudder angle circle manoeuvre in waves (1m, $\lambda/L = 1$) - *Simulat* prediction

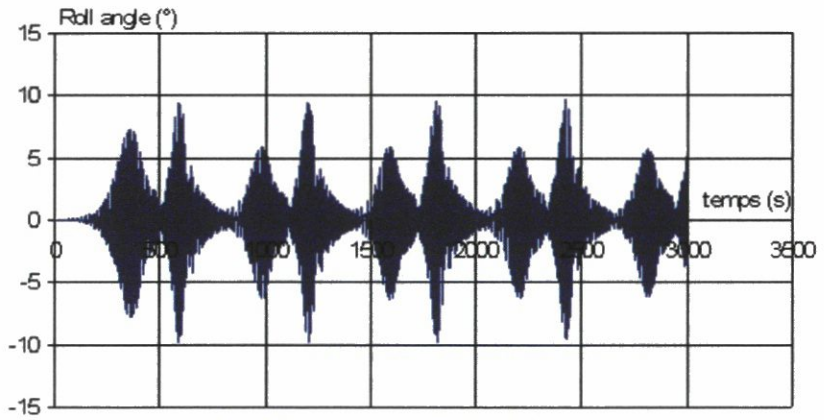

Figure 53: Roll response of the *British Bombardier* tanker during a 5° rudder angle circle manoeuvre in waves (1m, $\lambda/L = 1$) - *Simulat* prediction

Nomenclature

$A_{\xi\eta\zeta}$	Equilibrium axis system
A_{ij}	Added mass coefficients , with i, j between 1 and 6
B_{ij}	Damping coefficients , with i, j between 1 and 6
C_{ij}	Restoring moment coefficients , with i, j between 1 and 6
C_{xyz}	Body fixed axis system with origin at center of mass C
F_n	Froude number $= \overline{U}/\sqrt{Lg}$
g	Acceleration due to gravity $= 9,81ms^{-2}$
(**i**,**j**,**k**)	Unit vectors defined in the C_{xyz} body axis system
$\mathcal{I}$	Inertial moments matrix
I_{xx}, I_{yy}, I_{zz}	Roll, pitch and yaw inertias, referenced to the C_{xyz} body fixed axis system (kgm^2)
I_{xz}, I_{zx}	Cross products of inertia, referenced to the C_{xyz} body fixed axis system (kgm^2)
(K,M,N),$(\Delta K, \Delta M, \Delta N)$	Components of the global moment acting on the ship, referenced to the C_{xyz} body fixed axis system (Nm)- Δ used for perturbations
$k_i(\tau)$	Roll moment impulse response function, where i is a motion velocity, referenced to the C_{xyz} body fixed axis system
(K_0, M_0, N_0)	External moment on ship, referenced to the C_{xyz} body fixed axis system (Nm)
K_i	Roll slow motion derivative, where i is a velocity or acceleration, referenced to the C_{xyz} body fixed axis system
$\widetilde{K_i}$	Roll oscillatory derivative, where i is a velocity or acceleration, referenced to the C_{xyz} body fixed axis system
k_{xx}, k_{zz}	gyration radius, used for the inertial moments (m)
$(K_\alpha, M_\alpha, N_\alpha)$	Wave excitation moment, referenced to the C_{xyz} body fixed axis system (Nm)
K_ϕ	Roll moment hydrostatic derivative
L	Ship length (m)
m	Ship mass (kg)
$m_i(\tau)$	Pitch moment impulse response function, where i is a motion velocity, referenced to the C_{xyz} body fixed axis system
M_i	Pitch slow motion derivative, where i is a velocity or acceleration, referenced to the C_{xyz} body fixed axis system
$\widetilde{M_i}$	Pitch oscillatory derivative, where i is a velocity or acceleration, referenced to the C_{xyz} body fixed axis system
M_{z*}, M_θ	Pitch moment hydrostatic derivatives
$n_i(\tau)$	Yaw moment impulse response function, where i is a motion velocity, referenced to the C_{xyz} body fixed axis system

N_i	Yaw slow motion derivative, where i is a velocity or acceleration, referenced to the C_{xyz} body fixed axis system
$\widetilde{N}_i$	Yaw oscillatory derivative, where i is a velocity or acceleration, referenced to the C_{xyz} body fixed axis system
N_δ	Yaw moment rudder derivative with respect to rudder angle, referenced to the C_{xyz} body fixed axis system (Nm)
$OX_OY_OZ_O$	Earth fixed (or spatial) axis system
(p,q,r), (P,Q,R)	Angular velocity of ship, referenced to the C_{xyz} body fixed axis system (lower case used to denote small quantities) $(rads^{-1})$
R	Turning radius in circle manoeuvres (m)
t	Time (s)
(u,v,w), (U,V,W)	Velocity of ship, referenced to the C_{xyz} body fixed axis system (lower case used to denote small quantities) (ms^{-1})
$\overline{U}$	Steady forward speed of ship (ms^{-1})
(X,Y,Z),$(\Delta X, \Delta Y, \Delta Z)$	Components of the global force acting on the ship, referenced to the C_{xyz} body fixed axis system (N)- Δ used for perturbations
(x*,y*,z*), (X*,Y*,Z*)	Position of ship center of mass C relative to origin of earth fixed frame (lower case used to denote small quantities)(m)
$x_i(\tau)$	Surge force impulse response function, where i is a motion velocity, referenced to the C_{xyz} body fixed axis system
(X_0, Y_0, Z_0)	External force on ship, referenced to the C_{xyz} body fixed axis system (N)
X_i	Surge slow motion derivative, where i is a velocity or acceleration, referenced to the C_{xyz} body fixed axis system
$\widetilde{X}_i$	Surge oscillatory derivative, where i is a velocity or acceleration, referenced to the C_{xyz} body fixed axis system
$(X_\alpha, Y_\alpha, Z_\alpha)$	Wave excitation force, referenced to the C_{xyz} body fixed axis system (N)
$y_i(\tau)$	Sway force impulse response function, where i is a motion velocity, referenced to the C_{xyz} body fixed axis system
Y_i	Sway slow motion derivative, where i is a velocity or acceleration, referenced to the C_{xyz} body fixed axis system
$\widetilde{Y}_i$	Sway oscillatory derivative, where i is a velocity or acceleration, referenced to the C_{xyz} body fixed axis system
Y_δ	Sway force rudder derivative with respect to rudder angle, referenced to the C_{xyz} body fixed axis system (N)
$z_i(\tau)$	Heave force impulse response function, where i is a motion velocity, referenced to the C_{xyz} body fixed axis system
Z_i	Heave slow motion derivative, where i is a velocity or acceleration, referenced to the C_{xyz} body fixed axis system
$\widetilde{Z}_i$	Heave oscillatory derivative, where i is a velocity or acceleration, referenced to the C_{xyz} body fixed axis system
Z_{z*}, Z_θ	Heave force hydrostatic derivatives
α_0	Incident wave amplitude (m)
α	Wave height at time t (m)
δ	Rudder angle (rad)
Δ	Ships displacement (m^3)

Θ, θ	Euler pitch angle (lower case used to denote small quantity)
$\eta_{1,2,3}$	Small translations, referenced to the $A_{\xi\eta\zeta}$ equilibrium axis system (m)
$\eta_{4,5,6}$	Small rotations, referenced to the $A_{\xi\eta\zeta}$ equilibrium axis system (rad)
λ	Wave length (m)
ρ	Salt water density $(1025 kgm^{-3})$
τ	Time variable used in convolution integrals (s)
Φ, ϕ	Euler roll angle (lower case used to denote small quantity)
χ_0	Prescribed heading relative to waves
Ψ, ψ	Euler yaw angle (lower case used to denote small quantity)
ω	Incident wave frequency $(rads^{-1})$
ω_e	Wave encounter frequency or oscillation frequency $(rads^{-1})$
$\dot{x}, ...$	Temporal derivatives
$\ddot{x}, ...$	Temporal double derivatives

Non-dimensionalisation

$$\omega'_e = \omega_e\sqrt{L/g} \qquad \Delta' = \frac{\Delta}{\rho L^3/2} \qquad I'_{zz} = \frac{I_{zz}}{\rho L^5/2}$$

$$Y'_\delta = \frac{Y_\delta}{\rho L^2 \overline{U}^2/2} \qquad N'_\delta = \frac{N_\delta}{\rho L^3 \overline{U}^2/2}$$

$$Y'_v = \frac{Y_v}{\rho L^2 \overline{U}/2} \qquad Y'_r = \frac{Y_r}{\rho L^3 \overline{U}/2} \qquad N'_v = \frac{N_v}{\rho L^3 \overline{U}/2} \qquad N'_r = \frac{N_r}{\rho L^4 \overline{U}/2}$$

$$Y'_{\dot{v}} = \frac{Y_{\dot{v}}}{\rho L^3/2} \qquad Y'_{\dot{r}} = \frac{Y_{\dot{r}}}{\rho L^4/2} \qquad N'_{\dot{v}} = \frac{N_{\dot{v}}}{\rho L^4/2} \qquad N'_{\dot{r}} = \frac{N_{\dot{r}}}{\rho L^4/2}$$

Bibliography

[1] P.A. Bailey, W.G.Price, and P.Temarel. A unified mathematical model describing the manoeuvring of a ship travelling in a seaway. *Transactions of The Royal Institution of Naval Architects*, 1997.

[2] R.E.D. Bishop and A.G.Parkinson. Directional stability and control of rigid marine vehicles. *University College of London*, Report 3/70, 1970.

[3] D.A. Hudson. User manual for program suite THARBM, three-dimensional analysis of rigid body motions. *School of Engineering Sciences, Ship Science, University of Southampton*, 2000.

[4] IMO. Explanatory notes to the standards for ship manoeuvrability. *MSC/Circ.1053*, 16 dec 2002.

[5] IMO. Standards for ship manoeuvrability. *Resolution MSC.137(76)*, 4 dec 2002.

[6] J.M.J. Journee and D.Clarke. Experimental manoeuvring data of tanker British Bombardier. *Report n°1429, Delft University of Technology, Ship Hydromechanics Laboratory*, To be published, 2005.

[7] G. Van Leeuwen and C.C. Glansdorp. Experimental determination of linear and non-linear lateral hydrodynamic derivatives of a Mariner type ship model. *Report of Shipbuilding Laboratory, prepared for the manoeuvrability commitee of the ITTC 1966 145, Delft University of Technology*, 1966.

[8] E. Lewis. *Principles of Naval Architecture*, volume III. SNAME, 1989.

[9] P.A.Bailey. *Manoeuvring of a ship in a seaway.* PhD thesis, University of Southampton - School of Engineering Sciences, Ship Science, October 1999.

[10] P.A.Bailey, D.A.Hudson, W.G.Price, and P.Temarel. Time simulation of manoeuvring and seakeeping assessments using a unified mathematical model. *Transactions of The Royal Institution of Naval Architects*, 2001.